

1-1-2010

Synthesis And Characterization Of Metal Complexes Containing Tetrazolate, Poly(tetrazolyl)borate, And Aryl Pentazole Ligands As High Energy Density Materials

Dongmei Lu
Wayne State University

Follow this and additional works at: http://digitalcommons.wayne.edu/oa_dissertations

 Part of the [Inorganic Chemistry Commons](#)

Recommended Citation

Lu, Dongmei, "Synthesis And Characterization Of Metal Complexes Containing Tetrazolate, Poly(tetrazolyl)borate, And Aryl Pentazole Ligands As High Energy Density Materials" (2010). *Wayne State University Dissertations*. Paper 68.

This Open Access Dissertation is brought to you for free and open access by DigitalCommons@WayneState. It has been accepted for inclusion in Wayne State University Dissertations by an authorized administrator of DigitalCommons@WayneState.

**SYNTHESIS AND CHARACTERIZATION OF METAL COMPLEXES CONTAINING
TETRAZOLATE, POLY(TETRAZOLYL)BORATE, AND ARYL PENTAZOLE
LIGANDS AS HIGH ENERGY DENSITY MATERIALS**

by

DONGMEI LU

DISSERTATION

Submitted to the Graduate School

of Wayne State University,

Detroit, Michigan

in partial fulfillment of the requirements

for the degree of

DOCTOR OF PHILOSOPHY

2010

MAJOR: CHEMISTRY (Inorganic)

Approved by:

Advisor

Date

DEDICATION

To my parents

ACKNOWLEDGMENTS

I would like to express my sincere gratitude to my advisor, Professor Charles H. Winter, for his guidance and support through the years at Wayne State University. I am grateful to my committee members, Professor Stephanie L. Brock, Professor Jin K. Cha, and Professor Mark Ming-Cheng Cheng, for reviewing my thesis and giving valuable comments and suggestions.

I would like to thank Dr. Mary Jane Heeg for determining all the crystal structures, and Dr. Bashar Ksebati for his help with the NMR experiments. I would also like to thank the Winter group former and present members for their useful discussions on my research and friendship. Particularly, I am thankful to Dr. Oussama El-Kadri for helping me learn the glove box and Schlenk line techniques when I first started working in the lab, Dr. Mahesh Karunarathne for sharing his useful crystallization techniques with me, and Dr. Monika K. Wiedmann for translating German literature to English and proof reading my writing while she was around.

I would also like to thank my parents, brother, and sister for their continuous love and encouragement. My heartiest thanks go to my husband, Chao Wu, for his love, consideration, and helpful discussions on chemistry during my Ph.D. study.

Last but not least, I am also thankful to many others who have given me help and support at Wayne State. All of these help and support have made my studies possible.

TABLE OF CONTENTS

Dedication.....	ii
Acknowledgements.....	iii
List of Tables	vi
List of Figures	vii
List of Charts.....	ix
Chapter 1 – Introduction.....	1
Chapter 2 – Synthesis and Characterization of Heavier Alkaline Earth Metal Tetrazolate Complexes: Potential Energetic Materials and Colorants for Pyrotechnic Compositions.....	28
Chapter 3 – Synthesis and Characterization of Potassium Bis(tetrazolyl)borate Complexes and Their 18-Crown-6 Adducts: Unexpected Boron-Nitrogen Bond Isomerism and Associated Enforcement of κ^3 -N,N',H-Ligand Chelation	40
Chapter 4 – Synthesis and Characterization of Heavier Alkaline Earth Metal Bis(5-methyltetrazolyl)borate Complexes: Transfer of the Bis(tetrazolyl)borate Ligands to Divalent Metal Ions.....	76
Chapter 5 – Synthesis and Characterization of Sodium Cyano(tetrazolyl)borate Complexes: Attempted Reactions for the Preparation of Tris(tetrazolyl)borate Ligands with Borohydride Derivatives Other Than KBH_4	100

Chapter 6 – Attempted Synthesis of Rhenium(I)	
Aryl Pentazole Complexes	124
Chapter 7 – Conclusion.....	150
Reference	154
Abstract.....	166
Autobiographical Statement.....	168

LIST OF TABLES

Table 1.	Crystal data and data collection parameters for 63 and 64	49
Table 2.	Crystal data and data collection parameters for 66-69	50
Table 3.	Selected bond lengths (Å) and angles (°) for 63	55
Table 4.	Selected bond lengths (Å) and angles (°) for 64	57
Table 5.	Selected bond lengths (Å) and angles (°) for 66	59
Table 6.	Selected bond lengths (Å) and angles (°) for 67	61
Table 7.	Selected bond lengths (Å) and angles (°) for 68	63
Table 8.	Selected bond lengths (Å) and angles (°) for 69	65
Table 9.	Crystal data and data collection parameters for 71-73	82
Table 10.	Selected bond lengths (Å) and angles (°) for 71	87
Table 11.	Selected bond lengths (Å) and angles (°) for 72	89
Table 12.	Selected bond lengths (Å) and angles (°) for 73	92
Table 13.	Crystal data and data collection parameters for 74-77	105
Table 14.	Selected bond lengths (Å) and angles (°) for 74	110
Table 15.	Selected bond lengths (Å) and angles (°) for 75	112
Table 16.	Selected bond lengths (Å) and angles (°) for 76	114
Table 17.	Selected bond lengths (Å) and angles (°) for 77	116
Table 18.	Crystal data and data collection parameters for 78, 84, and 89	129
Table 19.	Selected bond lengths (Å) and angles (°) for 78	133
Table 20.	Selected bond lengths (Å) and angles (°) for 84	135
Table 21.	Selected bond lengths (Å) and angles (°) for 89	137

LIST OF FIGURES

Figure 1.	TGA traces for 57 , 58 , and 60 from 20 to 700 °C at 5 °C/min.....	31
Figure 2.	TGA traces for 59 , 61 , and 62 from 50 to 700 °C at 5 °C/min.....	32
Figure 3.	TGA traces for 39 , 63 , and 64 from 20 to 500 °C at 5 °C/min.....	46
Figure 4.	TGA traces for 66-69 from 50 to 700 °C at 5 °C/min	47
Figure 5.	Perspective view of 63 with thermal ellipsoids at the 50% probability level	54
Figure 6.	Perspective view of 64 with thermal ellipsoids at the 50% probability level	56
Figure 7.	Perspective view of 66 with thermal ellipsoids at the 50% probability level	58
Figure 8.	Perspective view of 67 with thermal ellipsoids at the 50% probability level	60
Figure 9.	Perspective view of 68 with thermal ellipsoids at the 50% probability level	62
Figure 10.	Perspective view of 69 with thermal ellipsoids at the 50% probability level.	64
Figure 11.	TGA traces for 70-73 from 20 to 500 °C at 5 min/°C.	80
Figure 12.	Perspective view of 71 with thermal ellipsoids at the 50% probability level	86
Figure 13.	Perspective view of 72 with thermal ellipsoids at the 50% probability level.	88
Figure 14.	Perspective view of the inorganic skeleton chain of (SrO ₂) _n in 72	90
Figure 15.	Perspective view of 73 with thermal ellipsoids at the 50% probability level.	91
Figure 16.	TGA traces for 74 and 76 from 50 to 500 °C at 5 min/°C.	103

Figure 17. Perspective view of 74 with thermal ellipsoids at the 50% probability level.	109
Figure 18. Perspective view of 75 with thermal ellipsoids at the 50% probability level	111
Figure 19. Perspective view of 76 with thermal ellipsoids at the 50% probability level.	113
Figure 20. Perspective view of 77 with thermal ellipsoids at the 50% probability level.	115
Figure 21. Hydrogen bonding interaction in the molecular packing of 77	117
Figure 22. Perspective view of 78 with thermal ellipsoids at the 50% probability level	132
Figure 23. Perspective view of 84 with thermal ellipsoids at the 50% probability level.	134
Figure 24. Perspective view of 89 with thermal ellipsoids at the 50% probability level.	136

LIST OF CHARTS

Chart 1.	Examples of Secondary Explosives	2
Chart 2.	Examples of Primary Explosives.....	3
Chart 3.	Equivalents of N ₂ per Negative Charge for Various Nitrogen Ligands	24

CHAPTER 1

Introduction

1.1 High Energy Density Materials

High Energy Density Materials (HEDMs) are a class of materials that can undergo very fast exothermic decomposition to liberate large amounts of gases and energy.¹ Generally, energetic materials can be formulated by either physically mixing solid oxidizers with fuels (such as black powder, $\text{NH}_4\text{ClO}_4/\text{Al}$, etc), or by making monomolecular compounds that combine oxidizer components and fuel components (such as TNT, RDX, etc, Chart 1). These materials have found wide applications not only in military aspects but also in civil applications. For example, they are used in fireworks, automobile air bags, and rocket or missile fuels. They also work as various types of explosives. Explosives that are very vulnerable to initiation by shock, friction, spark, or laser beam are categorized as primary explosives and are mostly used in initiating devices, whereas those less sensitive ones are secondary explosives and can only release energy when initiated by ignitors. However, secondary explosives are more powerful in consideration of performance with detonation velocities of 5500-9000 m/s compared to 3500-5500 m/s for primary explosives.² Thus, secondary explosives usually play a role as the main charge and have much wider applications than primary explosives.

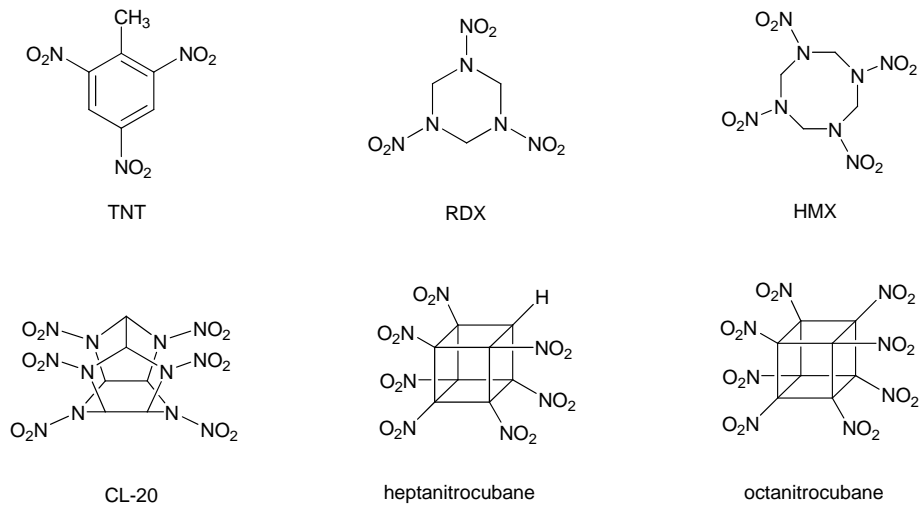


Chart 1. Examples of Secondary Explosives

Lead azide and lead styphnate were developed in the early 1900's as alternative primary explosive replacements for mercury fulminate (Chart 2), which was invented as early as in 1628.³ Lead azide and lead styphnate are superior to mercury fulminate in explosive performance and length of shelf life. However, they fail to solve the toxicity issue associated with elemental mercury because lead can also cause harmful impact to the environment and human health. The organic compound diazodinitrophenol (Chart 2) can be used as an initiating explosive, but it is darkened rapidly due to decomposition in sunlight.^{3b} Primary explosives containing only C, H, and N atoms such as tetrazene (Chart 2) are usually difficult to synthesize. Tetrazene has poor thermal stability and degrades in boiling water.⁴

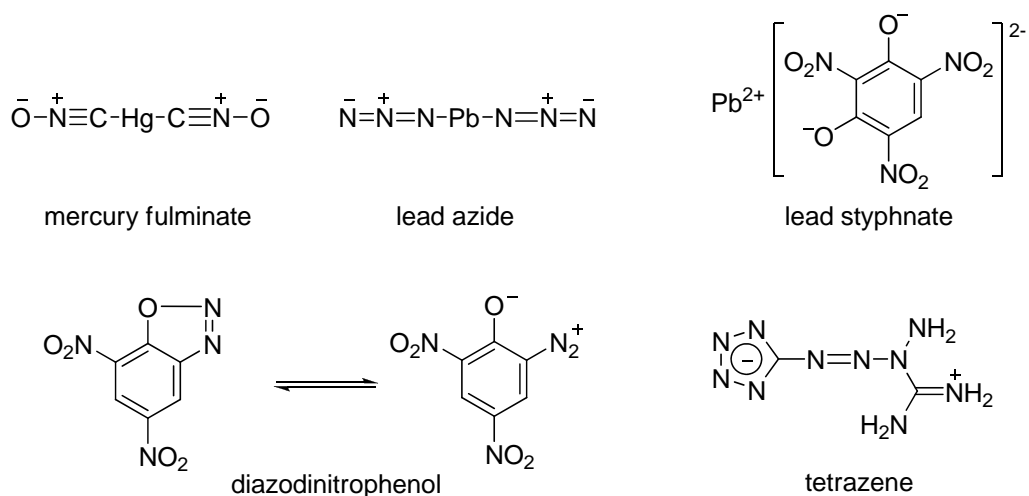


Chart 2. Examples of Primary Explosives

Traditional secondary explosives, such as trinitrotoluene (TNT), Royal Demolition eXplosive (RDX), and High Melting eXplosive (HMX), as depicted in Chart 1, derive most of their energy from the combustion of their carbon backbone.⁵ The energy densities of TNT, RDX, and HMX are only moderate, whereas modern nitro compounds, such as CL-20, heptanitrocubane, and octanitrocubane (Chart 1) are secondary explosives with enhanced energy densities due to their huge ring strain. One of the drawbacks of these nitro-group containing compounds is that they are either toxic per se, or their decomposition products are poisonous.

As described above, development of new energetic materials with improved properties is essential to meet all the requirements of both industrial and military applications. To facilitate environmental compatibility, the new energetic materials should avoid the use of heavy metal elements and organonitro groups. It is desirable to achieve higher energy

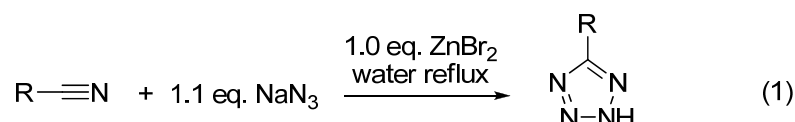
densities, better explosive performances, and at the same time, reduce the unwanted effects to maximum extent by inventing materials that have enough sensitivity for initiation, but not too much to handle and transport.⁶ Additionally, it is very important for the materials to be insensitive to moisture, light, and temperature (stable up to at least 200 °C) so that they can be stored safely for extended periods.^{3,7} Recently, nitrogen-rich compounds derived from tetrazoles or other heterocycles are of great interest in the development of “green” HEDMs in that the decomposition of these materials will result in the generation of large volumes of nitrogen gas. In contrast to traditional energetic materials which derive most of the energy from oxidation of their carbon backbone, the energy of high nitrogen energetic materials is derived from high positive heats of formation attributable to the large number of inherent N-N bonds.⁸

1.2 Tetrazoles

Tetrazoles are five-membered heterocycles with four nitrogen atoms and one carbon atom. This class of compounds has found a broad range of applications in coordination chemistry, drug design, and material sciences.⁹ For example, they can serve as ligands with versatile coordination modes in metal complexes owing to the multiple nitrogen donors;^{9b} they are used as lipophilic spacers and bioisosteres of carboxylic acid;¹⁰ and they have found use in propellants, explosives, and information recording systems.¹¹

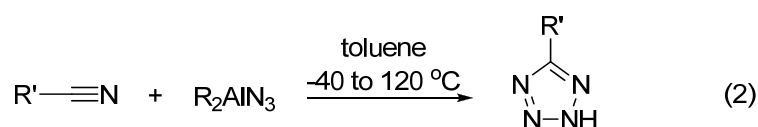
The synthesis of tetrazoles was first reported by Braun and Keller in 1932 through the reaction of organic nitriles with hydrazoic acid (HN₃).¹² Since HN₃ is highly toxic, volatile,

and explosive, this synthetic pathway did not provide a practical method for the preparation of tetrazoles. Modifications of the synthesis were explored by addition of azide salts to nitriles, however, the earlier reports were either not capable of solving the problem caused by HN_3 formed *in situ* under acidic conditions due to the use of strong Lewis acids, or they required the use of expensive and toxic metals.¹³ In 2001, Demko and Sharpless described an improved and safe procedure which afforded the tetrazoles in good yields by treatment of the specific nitriles with sodium azide in water catalyzed by zinc salts (eq 1).¹⁴

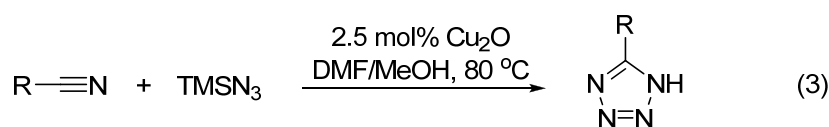


Inspired by Sharpless's pioneering work, Myznikov and coworkers explored microwave activated catalytic reaction of sodium azide with nitriles by ZnCl_2 .¹⁵ Rostamizadeh and coworkers reported the ZnCl_2 catalyzed synthesis of tetrazoles under solvent free conditions.¹⁶ Several catalytic systems for the preparation of tetrazoles were established based on zinc containing catalysts, including nanocrystalline ZnO ,¹⁷ zinc hydroxyapatite,¹⁸ and Zn/Al hydrotalcite.¹⁹ Furthermore, CdCl_2 was reported as an efficient catalyst for the [3+2] cycloaddition of NaN_3 with nitriles in DMF under mild conditions.²⁰ Other catalysts, such as tungstates (MWO_4),²¹ antimony trioxide,²² and silica-supported ferric chloride²³ or sodium hydrogen sulfate²⁴ were also investigated for the transformation of organic nitriles to the corresponding tetrazoles through reactions with NaN_3 . Roh and coworkers reported microwave irradiated reaction of nitriles with NaN_3 in the presence of

triethylamine hydrochloride in nitrobenzene.²⁵ Recently, Aureggi and Sedelmeier communicated a 1,3-dipolar cycloaddition of organoaluminum azide with nitriles for the synthesis of 5-substituted tetrazoles (eq 2).²⁶ The dialkylaluminum azide was easily prepared by the reaction of dialkylaluminum chloride with NaN_3 in toluene.



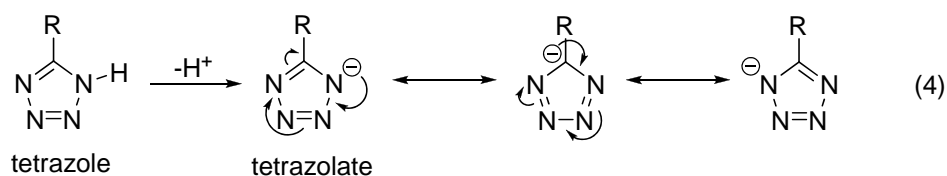
In 2004, Pizzo and coworkers reported the synthesis of tetrazoles by adding trimethylsilyl azide (TMSN_3) to organic nitriles with 10 mol % tetrabutylammonium fluoride (TBAF) as catalyst.²⁷ More recently, Yamamoto and coworkers efficiently synthesized 5-substituted 1H-tetrazoles through the copper-catalyzed [3+2] cycloaddition of nitriles and TMSN_3 (eq 3).²⁸ Bonnamour and Bolm demonstrated a synthetic method for the reaction of organic nitriles with TMSN_3 in dimethylformamide (DMF)/water solvent system using $\text{Fe}(\text{OAc})_2$ catalyst.²⁹



1.3 Metal Tetrazolate Complexes

Metal tetrazolates are usually prepared by treatment of metal bases (hydroxide, bicarbonate, or carbonate) with the specific tetrazole in aqueous or alcoholic solutions.³⁰ They have attracted attention for application as energetic materials because of their high nitrogen contents, good thermal stabilities, and insensitivities toward mechanical impact,

friction, and electrostatic discharge.^{30,31} The stability and insensitivity are attributable to the aromaticity of the five-membered heterocycle (eq 4), and these properties make metal tetrazolates good candidates as prospective secondary explosives or propellants. Nonetheless, recent reports have suggested that certain metal tetrazolates containing an electron withdrawing group (e.g., $-\text{NO}_2$, $-\text{N}_3$) on the ring core carbon atom are extremely shock and friction sensitive, and have potential in use as primary explosives.³²



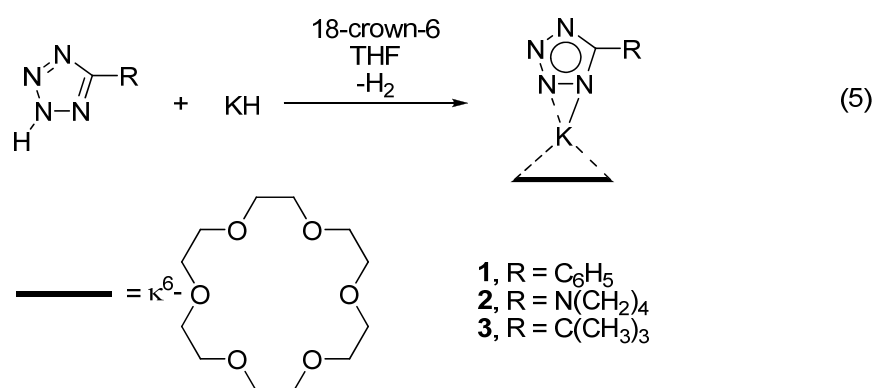
Additionally, various tetrazole ligands have been used to construct metal organic framework (MOF) solids because of their versatile coordination modes and bridging abilities.³³ Metal derivatives of tetrazoles have also been explored for applications that include optical and dielectric materials.³⁴ Herein, metal tetrazolate complexes are described based on different type of metals, including alkali, alkaline earth, transition, and lanthanide elements. Metal complexes containing various tetrazolate ligands will be presented and their energetic properties will be compared.

1.3.1 Alkali Metal Tetrazolate Complexes

To date, alkali metal complexes containing tetrazolate ligands are the most extensively studied among metal tetrazolates. These tetrazolates often possess high solid state densities and high thermal degradation temperatures. The sensitivities of alkali metal

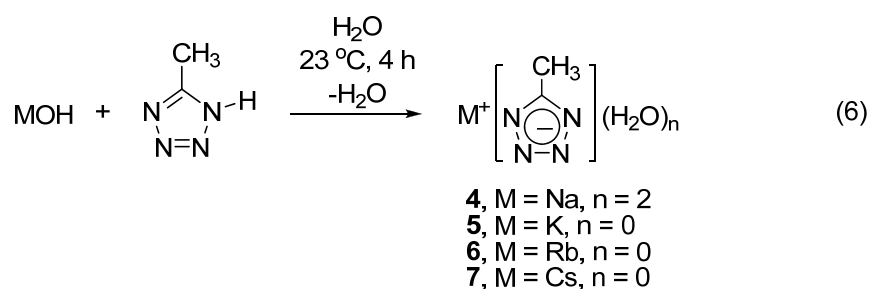
tetrazolates mostly depend on the nature of the ligands, ascribed to different functional groups of the tetrazole ring.

Recently, Winter and coworkers reported preparation, structure, and theoretical studies of a series of potassium tetrazolate 18-crown-6 complexes (**1-3**, eq 5).³⁵ Complexes **1-3** contain terminal η^2 -tetrazolate ligands and κ^6 -18-crown-6 ligands, and they were synthesized to serve as models for energetic materials. To access complexes with higher nitrogen contents, the 18-crown-6 ligands need to be removed from the complexes because they do not contain any nitrogen atoms. Removal of the 18-crown-6 ligands will leave only the tetrazolate nitrogen atoms to satisfy the bonding requirements of the metal centers, and if tetrazolate ligands with minimum number of carbon and hydrogen atoms are employed, the nitrogen content will be further increased.



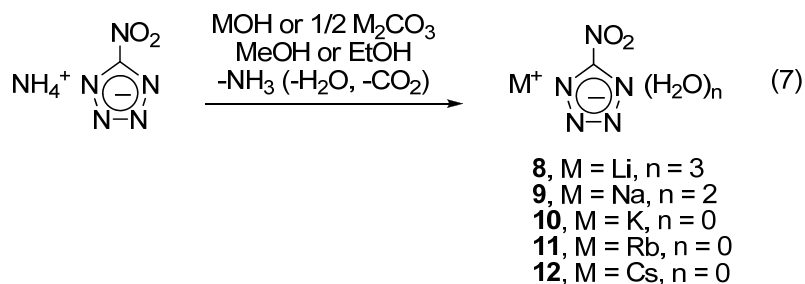
In a more recent report, Winter and coworkers described a range of heavier group 1 methyl tetrazolate complexes.³⁶ Treatment of group 1 metal hydroxides with methyl tetrazole in aqueous solutions afforded the corresponding metal tetrazolates (eq 6). The

X-ray crystal structures of **5-7** revealed that the nitrogen atoms of methyl tetrazolate ligands are very efficiently bonded to the metal ions so that no water ligands could be included in the coordination sphere. Thus the molecules are closely packed and the complexes exhibit very high solid state densities. Since the detonation pressure of a material is directly proportional to the square of its density,³⁷ achievement of high densities in energetic materials is highly desired. Alkali metal complexes containing 5-H-tetrazolate,^{30b} aminotetrazolate,^{30a} 1-methyl-5-nitriminotetrazolate,³⁸ and 5,5'-hydrazinebistetrazolate³⁹ ligands were reported by other laboratories. Along with complexes **4-7**, these metal tetrazolates were reported being insensitive toward impact and friction.



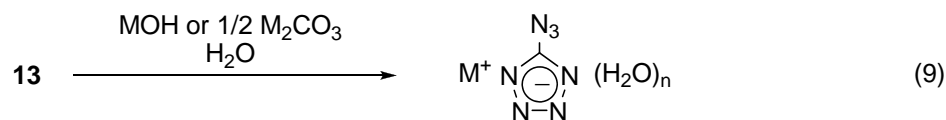
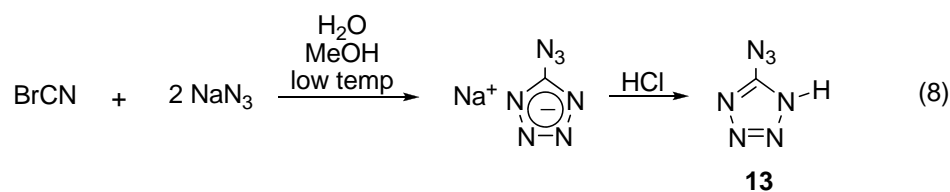
As for sensitive alkali metal complexes, Klapötke and coworkers reported a series of 5-nitrotetrazolates.^{32a} They were synthesized by two different methods. The first method involves the metathesis of copper (II) 5-nitrotetrazolate 5-nitrotetrazole with the specific metal hydroxide in aqueous solutions. This method is problematic in terms of handling because the copper complex of 5-nitrotetrazolate is extremely sensitive. The second method is more practical and can be realized by treatment of ammonium 5-nitrotetrazolate with metal hydroxide or carbonate in alcoholic solutions to afford the desired group 1 metal

5-nitrotetrazolates and the byproducts (ammonia, water, and/or carbon dioxide) (eq 7).



Complexes **8-12** are all impact sensitive and explode when small samples of the compounds are placed in a flame. Complexes **8** and **9** incorporate crystal water molecules and have impact sensitivities comparable to secondary explosives. In contrast, complexes **10-12** form anhydrous compounds and are candidates of primary explosives with very high sensitivities toward shock and friction.

Klapötke and coworkers also reported the synthesis and X-ray crystal structures of a series of alkali metal 5-azidotetrazolate complexes.^{32c} In order to prepare these complexes, 5-azidotetrazole was first synthesized by treatment of cyanogen bromide with sodium azide followed by acidic workup (eq 8), and then the tetrazole was used to react with metal bases to yield the corresponding 5-azidotetrazolate complexes (eq 9). Complexes **14-18** are all extremely sensitive, and **17** could not be isolated as a solid material because the reaction mixture detonated during the experiment, even under conditions without any disturbance in the dark. Complexes **16** and **18** crystallized with no water ligands and **18** exploded even in concentrated aqueous solutions.



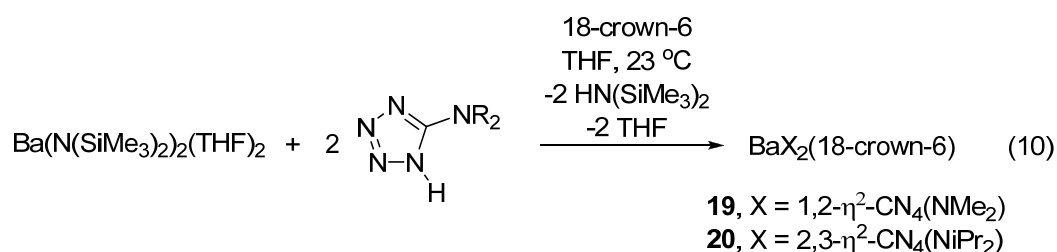
- 14**, M = Li, n = 1
15, M = Na, n = 1
16, M = K, n = 0
17, M = Rb, n = n/a
18, M = Cs, n = 0

Moreover, alkali metal complexes of the 5,5'-azobis(tetrazolate) ligand were reported to have thermal decomposition temperatures of 237-335 °C with the lithium complex being the most stable toward thermal degradation and the cesium analog the least stable.⁴⁰ All of the complexes crystallized as dimers with various amounts of water molecules either coordinated with the metal ions or stabilized by hydrogen bonds in the solid state. Once the water molecules are lost, the complexes become extremely sensitive toward impact and friction as evidenced by many explosions occurred during dehydration of the complexes under dynamic vacuum. Alkali metal 5-(5-nitrotetrazol-2-ylmethyl)tetrazolates were reported to be shock and friction sensitive and have decomposition temperatures of 168-192 °C. They are hydrated in the solid state and deflagrated when placed in a flame.⁴¹

1.3.2 Alkaline Earth Metal Tetrazolate Complexes

Reports on the synthesis and characterization of alkaline earth metal tetrazolates are not as well documented as the alkali metal tetrazolates, and many of them are patents. Winter and coworkers reported the synthesis, structural characterization, and molecular

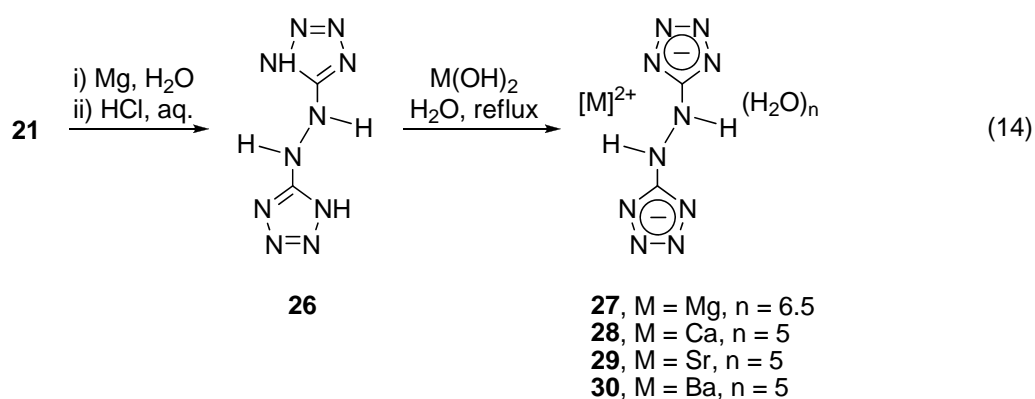
orbital calculations of two barium tetrazolate 18-crown-6 complexes (eq 10).⁴² They were also prepared to serve as models for energetic materials. Removal of the 18-crown-6 ligands will result in the formation of tetrazolate complexes with higher nitrogen contents, which are more favorable for being used as HEDMs.



Klapötke and coworkers prepared the alkaline earth metal 5-nitrotetrazolates by treatment of ammonium 5-nitrotetrazolate with a metal hydroxide or carbonate in aqueous or alcoholic solutions.^{32b} These complexes crystallized with water ligands, decomposed in the range of 180-235 °C, and resulted in loud explosions in the flame test. In comparison with the alkali metal 5-nitrotetrazolates, the hydrated group 2 metal analogs are less sensitive toward impact and friction with the sensitivities increasing in the order Mg < Ca < Sr < Ba. The sensitivities of these complexes increase dramatically when the hydrate is lost. It is reported that a sample of the strontium complex lost its crystallization water and exploded spontaneously under ambient conditions initiated by the sunlight. Also, an explosion occurred during the preparation of the barium complex caused by the formation of an insoluble solid in the reaction mixture initiated by the magnetic stir bar.

Alkaline earth metal complexes of the 5,5'-azobis(tetrazolate) ligand were also

Klapötke and coworkers reported 5,5'-hydrazinebis(tetrazolate) complexes of alkaline earth metals.^{39,43} These complexes could be synthesized by treatment of the specific metal hydroxide with neutral 5,5'-hydrazinebis(tetrazole) formed by reduction of sodium 5,5'-azobis(tetrazolate) (**21**) with magnesium powder and subsequent acid work-up (eq 14). Crystallization water molecules were found in the solid state structures of **27-30**. Complexes **27-30** showed high thermal stabilities with decomposition temperatures of 220-276 °C, and they exhibit low sensitivities to shock and friction. However, they burned vigorously in a flame when losing the hydrate and give off the characteristic flame colors of the metal ions.

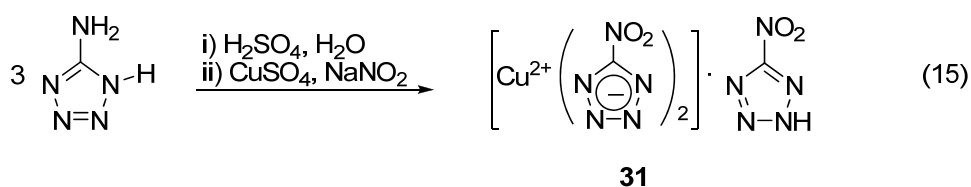


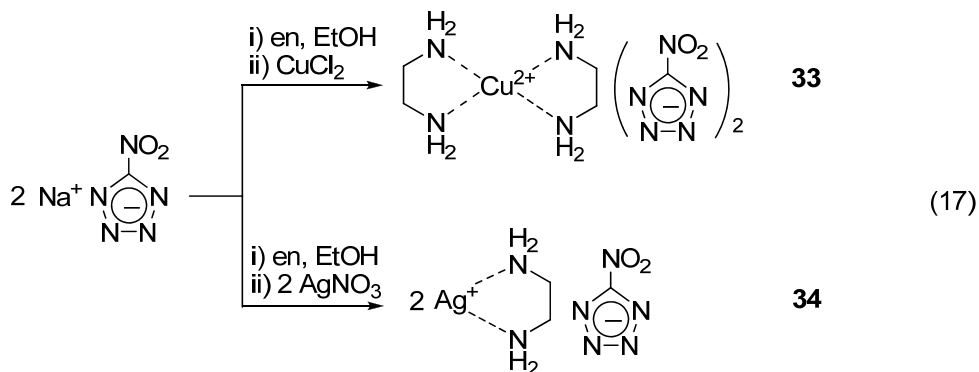
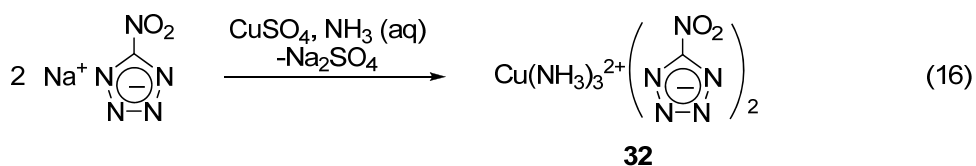
In other reports, calcium 5-azidotetrazolate was described to be very sensitive toward impact, but it has a higher stability than the alkali metal analogs.^{32c} A series of strontium nitriminotetrazolate complexes was proposed as potential color generators for pyrotechnic mixtures.⁴⁴ A strontium complex containing the 5-H-tetrazolate ligand was reported in the literature.^{30b}

1.3.3 Transition and Lanthanide Metal Tetrazolate Complexes

In recent years, transition metal complexes containing tetrazolate ligands have also been studied for use as energetic materials. Copper and silver are environmentally benign metals and nitrogen-rich complexes of them were the most widely investigated. Tetrazole-based complexes of other transition metal elements, including zinc, chromium, manganese, cobalt, and iron were also reported.

Copper(II) 5-nitrotetrazolate 5-nitrotetrazole (**31**) was prepared by the diazotization of 5-aminotetrazole with excess nitrite in the presence of copper(II) cations in an acidic aqueous solution (eq 15).⁴¹ 5-Nitrotetrazolatetriamminecopper(II) (**32**) was synthesized by treatment of sodium 5-nitrotetrazolate with copper(II) sulfate in ammonia solution (eq 16).⁴⁵ Both **31** and **32** are thermally stable up to 230 °C, but their high impact and friction sensitivities make them unsuitable as starting materials for preparation of other metal 5-nitrotetrazolate complexes. Treatment of sodium 5-nitrotetrazolate with CuCl₂ or AgNO₃ in the presence of excess ethylenediamine (en) in ethanol afforded the copper(II) and silver(I) complex ethylenediamine adducts **33** and **34**, which were considered as safe 5-nitrotetrazolate anion transfer agents with reduced shock and friction sensitivities (eq 17).⁴⁵





Bis(tetrazolyl)amine copper(II) complexes were synthesized in aqueous ammonia solutions by the direct combination of cupric chloride and bis(tetrazolyl)amine monohydrate.⁴⁶ These complexes crystallized with ammine ligands, ammonium ions, or water of crystallization. However, they are neither sensitive toward friction nor impact whether they contain hydrate or not. Copper(II) complexes of 1-methyl-5-nitriminotetrazolate, 2-methyl-5-nitriminotetrazolate, and 5-nitriminotetrazolate were synthesized by the reaction of copper (II) cations with the corresponding tetrazole in aqueous or ammonia solutions.⁴⁷ The complexes which incorporate water or ammine ligands exhibited lower impact and friction sensitivities, while those without neutral ligands behaved like primary explosives.

Shreeve and coworkers reported copper and cadmium complexes of 5,5'-azobis(tetrazolate) ligands.⁴⁸ These complexes were easily synthesized by metathesis

including energetic materials, metal organic frameworks, optical, and dielectric materials.

5,5'-Azobis(tetrazolate) complexes of the complete series of lanthanide metal elements were synthesized and characterized.⁵⁴ No energetic properties of these complexes were reported, even though they are hypothetically energetic materials. The complexes crystallized with water ligands and they have been suggested to have potential application in electronic organic light emitting diodes (OLEDs). In addition, lanthanide metal complexes containing 5,5'-bitetrazolate and 1,3-bis(tetrazol-5-yl)triazenate were reported with detailed structural descriptions.⁵⁵

1.3.4 Comparison of Metal Tetrazolate Complexes with Metal-Free Salts Containing Tetrazole Derivatized Ions

In addition to metal tetrazolate complexes, a range of metal-free nitrogen-rich salts based on tetrazoles were also comprehensively studied. These salts were also explored as potential energetic materials due to their high energy contents. They can be briefly categorized to three major types, including salts consist of tetrazolium cations and energetic oxidizing anions,^{6b,56} salts made from non-heterocyclic nitrogen-rich cations with tetrazolate anions,^{6a,32c,57} and triazolium or tetrazolium tetrazolates.^{57b-d,58}

Tetrazolium salts of oxidizing anions were usually synthesized by the direct reaction of tetrazoles with the specific concentrated acid. Tetrazolate salts of non-heterocyclic cations were prepared by treatment of neutral tetrazoles with Lewis bases, such as ammonia, hydrazine hydrate, or guanidine bicarbonate. Tetrazolium tetrazolate salts can be obtained

by reaction of two tetrazoles with different acidities. The less acidic tetrazole will be protonated and form the tetrazolium ion, while the more acidic one will be deprotonated to the tetrazolate ion. The last two types of salts can also be readily synthesized through two metathesis reactions, *i.e.* metathesis of sulfate salts of the cations with the barium tetrazolates, and metathesis of halide salts of the cations with the silver tetrazolates.

Nitrogen-rich salts containing only C, H, and N elements are particularly useful as potential gas generating agents, and they are also candidates for gun or rocket propellants since their combustion will result in low flame temperatures with increased specific impulses.⁵⁹ However, these metal-free salts are generally less sensitive than the corresponding metal complexes when paired with the same tetrazolate ions. For example, the anhydrous dihydrazinium 5,5'-azobis(tetrazolate) salt was reported as almost insensitive toward shock initiation, and can be ground forcefully in a mortar without observable detonation.⁶⁰ By contrast, anhydrous alkali, alkaline earth, and transition metal 5,5'-azobis(tetrazolate) complexes were reported to be extremely sensitive toward impact and friction. It was reported that copper(II) 5,5'-azobis(tetrazolate) was readily initiated when touched by a plastic spatula.⁴⁸

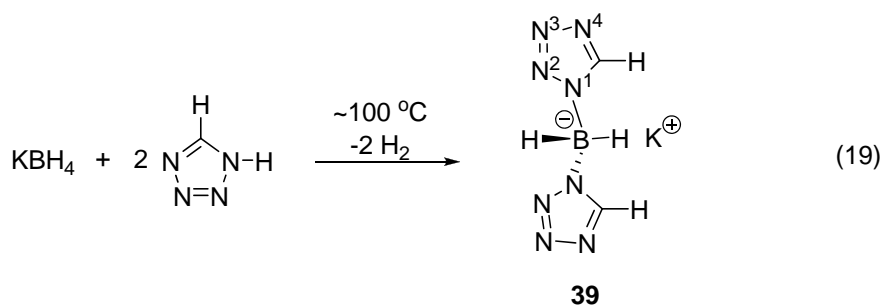
1.4 Metal Complexes Containing Poly(tetrazolyl)borate Ligands

Poly(pyrazolyl)borate ligands have found wide applications as auxiliary ligands in coordination, organometallic, and bioinorganic chemistry.⁶¹ Various substituted poly(pyrazolyl)borate ligands have been previously employed in a number of main group and

transition metal complexes.⁶² However, only a few reports have described complexes containing bis(tetrazolyl)borate ligands, whereas tris- and tetrakis(tetrazolyl)borate ligands remain unknown. So far, only bis(5-H-tetrazolyl)borate, bis(5-aminotetrazolyl)borate, and bis(thioxotetrazolyl)borate ligands have been reported.

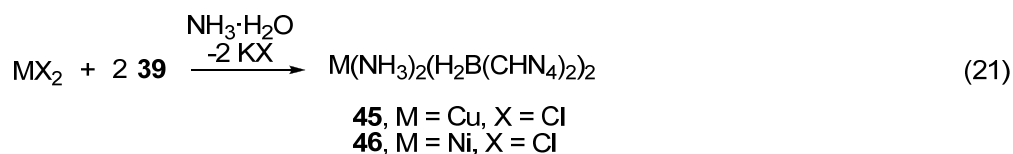
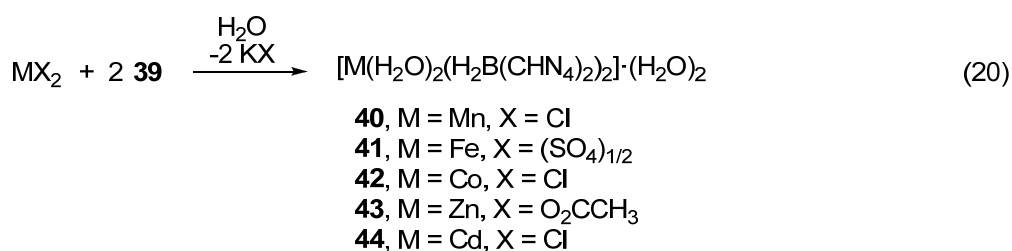
1.4.1 Potassium and Transition Metal Bis(5-H-tetrazolyl)borates

In 1993, Janiak and Esser communicated the synthesis and structure of bis(5-H-tetrazolyl)borate ligand in the form of its potassium complex.⁶³ Potassium bis(5-H-tetrazolyl)borate (**39**) was prepared by heating a solid mixture of KBH_4 and 1H-tetrazole to $\sim 100^\circ\text{C}$ (eq 19). The X-ray crystal structure of **39** revealed that the boron-nitrogen bonds of the ligands are to the C-H neighboring nitrogen atoms (eq 19, N^1) of the tetrazolyl groups. Tris- or tetrakis(tetrazolyl)borate ligands could not be obtained through a similar method using 1:3 or 1:4 ratio of KBH_4 and tetrazole even at higher temperatures.



Later, Janiak and coworkers reported a range of transition metal complexes containing bis(5-H-tetrazolyl)borate ligands.⁶⁴ These complexes were obtained by slow diffusion of the water solutions of the reactants, **39** and the specific inorganic transition metal

salts, respectively (eq 20).^{64a,64c} The isolation of the copper and nickel complexes required the use of ammonia solution, and these complexes crystallized with ammine ligands (eq 21),^{64a,b} instead of water ligands for the other analogous transition metal complexes (40-44).



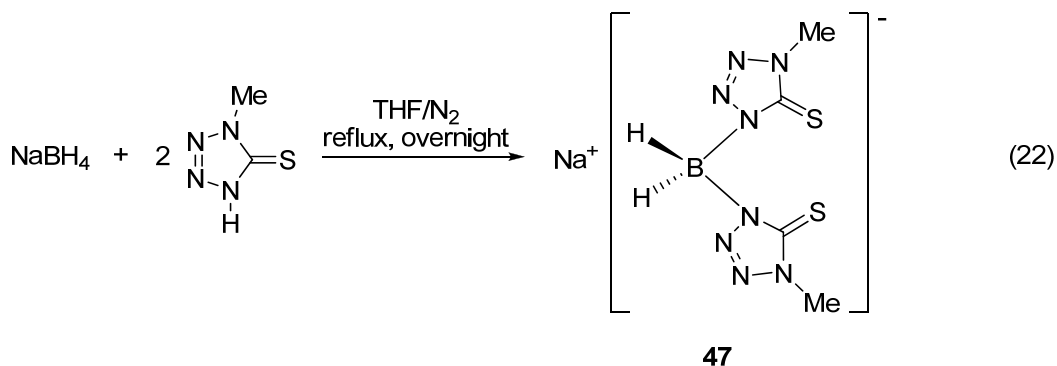
In **40-46**, the bis(5-H-tetrazolyl)borate ligand solely adopted the bridging coordination mode and the complexes crystallized as two dimensional coordination polymers. Crystal structures of **40-46** showed that only the C-H neighboring nitrogen atoms (eq 19, N⁴) are coordinated to the metal ions because they have higher basicity than the other nitrogen atoms as predicted by AM1 calculations.^{64c} In **40-44**, the uncoordinated nitrogen atoms are involved in hydrogen bond formation with the incorporated water molecules. The extensive hydrogen bonding interactions can affect the crystal packing and help to stabilize the crystal phases.⁶⁵ These transition metal complexes were reported to be sensitive to heat and temperature. Several explosive decompositions were observed at temperatures above 190 °C during heating samples of **40-44** in air or in an argon atmosphere.^{64a}

1.4.2 Metal Complexes of Other Bis(tetrazolyl)borate Ligands

Very recently, Groshens reported the synthesis of bis(5-aminotetrazolyl)borate ligand following Janiak's method by treatment of NaBH_4 or KBH_4 with 5-aminotetrazole.⁶⁶ Copper and zinc complexes of the bis(5-aminotetrazolyl)borate ligand were also prepared and characterized by X-ray crystal structures. The complexes exhibit one dimensional coordination polymeric structures in the solid states. In the copper derivative, the bis(tetrazolyl)borate ligands are bridged asymmetrically between two metal centers through N^4 and $\text{N}^{3'}$ atoms, while in the zinc analog, the ligands are bridged symmetrically through N^4 and $\text{N}^{4'}$ atoms (see numbering scheme in eq 19). These complexes were reported being sensitive to impact and they decomposed exothermically upon heating. Once initiated, they underwent rapid decomposition and yielded heat, a large volume of gas, and some ash.

Cao and coworkers prepared sodium bis(thioxotetrazolyl)borate (**47**) by treatment of NaBH_4 with 1-methyl-5-thiotetrazole (eq 22).⁶⁷ Metathesis of **47** with CoCl_2 and NiCl_2 in methanol solutions afforded the corresponding cobalt and nickel complexes, respectively. In these two complexes, the bis(tetrazolyl)borate ligands are chelated to the metal ions through the sulfur atoms of the thio- groups, while none of the nitrogen donors on the tetrazolyl rings participate in the coordination. Agostic $\text{M}\cdots\text{H-B}$ interactions between the metal ions and one of the boron-bound hydrogen atoms were reported. These complexes were proposed to be useful in bioinorganic chemistry and could serve as models in determining of the structure and kinetics of the active sites of metalloenzymes such as liver

alcohol dehydrogenase.⁶⁸



1.4.3 Comparison of Poly(tetrazolyl)borate and Azolate Ligands

In principle, the tetrazolate ligand can release 2 equivalents of N₂ per negative charge, while tetrazolate ligands containing nitrogen-based substituents on the core carbon atom can evolve larger amounts of N₂ and other gases per negative charge (Chart 3). The pentazolate ion can evolve 2.5 N₂/negative charge, and as depicted in Chart 3, the bis(tetrazolyl)borate, tris(tetrazolyl)borate, and tetrakis(tetrazolyl)borate ligands can liberate 4, 6, and 8 equivalents of N₂ per negative charge, respectively. Due to their high nitrogen content, poly(tetrazolyl)borate ligands may serve as more energetic replacements for tetrazolate ligands, and metal complexes of these ligands may constitute a new class of energetic materials. Additionally, since boron nitride is very stable thermodynamically, the inclusion of boron centers in **51-53** may contribute to the formation of highly endothermic complexes containing larger amounts of energy.

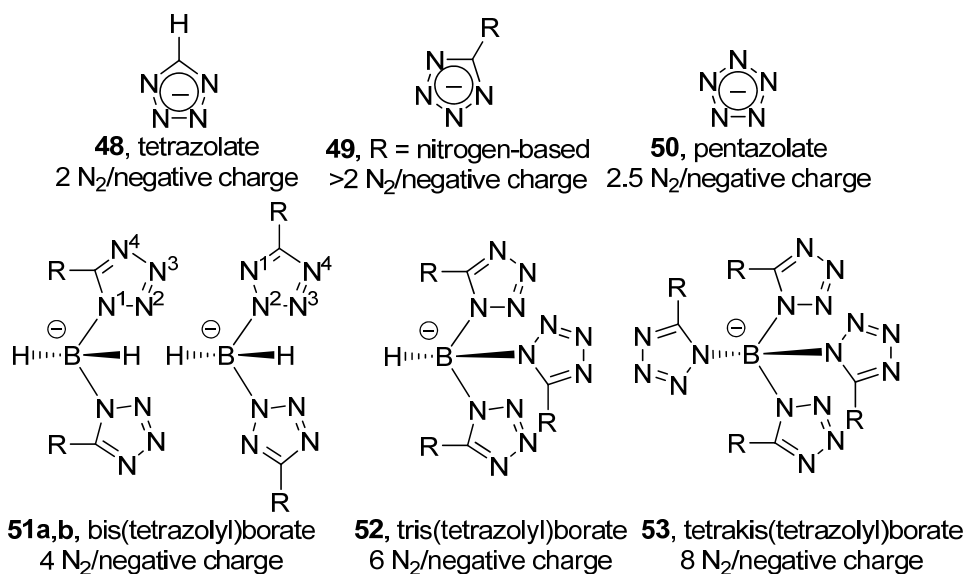
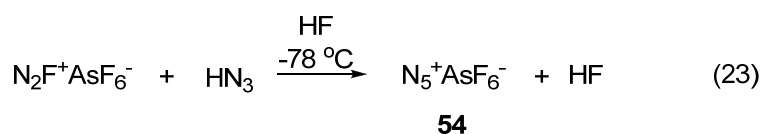


Chart 3. Equivalents of N₂ per Negative Charge for Various Nitrogen Ligands

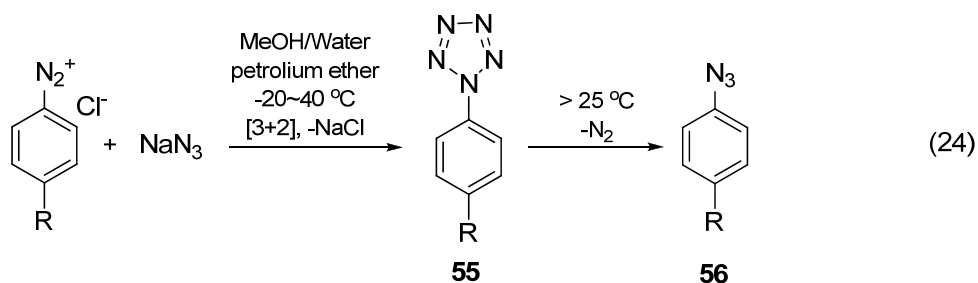
1.5 Polynitrogen Species

Polynitrogen compounds (N_x) are also potential candidates for HEDMs.⁶⁹ However, the number of known N_x is very limited, and most of the efforts in the research of polynitrogen compounds have been made through theoretical studies. This is due to the highly unstable nature of N_x, which can cause experimental difficulties in the synthesis and handling of these compounds.⁷⁰ Nonetheless, the pursuit of new members of the N_x family has never stopped and considerable laboratory work has been carried out in this area. In 1999, Christie and coworkers reported the preparation of the N₅⁺ cation by the direct reaction of N₂F⁺AsF₆⁻ and HN₃ (eq 23).^{70a}



Even though **54** is not very stable at ambient temperature, it can be stored safely at $-78\text{ }^{\circ}\text{C}$ for weeks. Therefore, **54** represents the third readily accessible homonuclear polynitrogen species besides molecular nitrogen, N_2 , and the azide ion, N_3^- .⁷¹ This remarkable breakthrough has led to an increased interest in polynitrogen compounds, especially pentazole and its derivatives.^{70b}

Crystalline aryl pentazoles were first synthesized in 1956 by Huisgen and Ugi, through the reaction of aryl diazonium chloride with sodium azide in a biphasic combination of aqueous methanol and petroleum ether at -40 to $-20\text{ }^{\circ}\text{C}$.^{9a,72} Their constitution was supported by solution UV spectra, and some of them were later characterized by X-ray crystallography.⁷³ Kinetic studies showed that the aryl pentazoles readily lose N_2 molecules to form aryl azides (eq 24).^{9a,72b}



The stability of **55** is strongly affected by the substituents on the 4-position of the phenyl ring. Electron-donating groups, such as $-\text{OMe}$ and $-\text{NMe}_2$, increase the stability toward loss of N_2 , whereas electron-withdrawing groups, such as $-\text{NO}_2$ and $-\text{Cl}$, decrease the stability toward loss of N_2 .^{9a,72b} However, even the most stable aryl pentazoles decompose slowly at room temperature, so special attention and safety precautions are required.⁷⁴

Isolation of the pentazolate anion, N_5^- , was attempted by Huisgen and Ugi through ozonization of 4-dimethylaminophenylpentazole in CD_2Cl_2 at $-60\text{ }^\circ\text{C}$, and reduction of phenylpentazole with sodium in liquid NH_3 , but in both cases destruction of the N_5 ring was observed.⁷⁴ Later, Radziszewski and coworkers performed a more controlled ozonolysis of ^{15}N labeled 4-oxophenylpentazole in CD_2Cl_2 at $-78\text{ }^\circ\text{C}$ and monitored with ^{15}N NMR, but the absence of signals for a possible pentazole moiety indicated that no N_5^- formed.⁷⁵

Recently, N_5^- was detected in the gas phase by electrospray ionization mass spectrometry (ESI-MS) with samples of 4-methoxyphenylpentazole or 4-dimethylaminophenylpentazole in polar solvents,^{70b} and by laser desorption ionization (LDI) time-of-flight (TOF) mass spectrometry with solid 4-dimethylaminophenylpentazole.⁷¹ The generation of pentazole, HN_5 , from treatment of 4-methoxyphenylpentazole with ceric ammonium nitrate (CAN) was described in 2003, and was supported by ^{15}N NMR spectroscopy.⁷⁶ However, this work was questioned two years later by the fact that the ^{15}N NMR resonance attributed to the N_5^- anion was actually from the nitrate ion.⁷⁷ So far, there are no examples of aryl pentazoles in which one or more nitrogen atoms of the pentazole ring are coordinated to a metal ion.

1.6 Thesis Problem

There is great current interest in the development of novel HEDMs that can serve as suitable replacements for the existing energetic materials.⁷⁸ The commonly used detonators have either toxicity issues associated with heavy metal, or too much sensitivity that can result

in accidents. For example, anhydrous lead styphnate is extremely sensitive and can be readily initiated by the electrostatic charge of the human body.¹ Moreover, primary explosives derived from neutral organic compounds tend to have low thermal stabilities which are not desirable in terms of achieving extended shelf life. Contamination of the battle field and the manufacturing sites caused by widely used secondary explosives, such as TNT, RDX, and HMX, is also of considerable concern. It is reported that HMX is the main polynitro-organic pollutant in soil, and the contaminated soil can affect the reproduction of earthworms and slow down the microbial processes.⁷ Besides, TNT is considered a possible carcinogen by the US Environmental Protection Agency.⁷⁹

The objective of this thesis is to synthesize new high nitrogen metal complexes for application as potential energetic materials. In particular, preparation of metal complexes containing nitrogen-rich tetrazolate, poly(tetrazolyl)borate, and aryl pentazole ligands is investigated. The goal is to prepare compounds that incorporate large amounts of stored chemical energy and have reduced shock sensitivity so that they can exothermically decompose in a controllable fashion to form molecular nitrogen, a thermodynamically stable metal oxide or nitride, and large amounts of heat. Once obtained, the new complexes are characterized by spectral, analytical, and X-ray crystallographic methods. Additionally, the nitrogen-rich complexes are subjected to thermogravimetric analysis (TGA) to explore their thermal behavior. Preliminary safety tests are also performed with small samples of the complexes to determine their sensitivities toward shock, friction, and electrostatic discharge.

CHAPTER 2

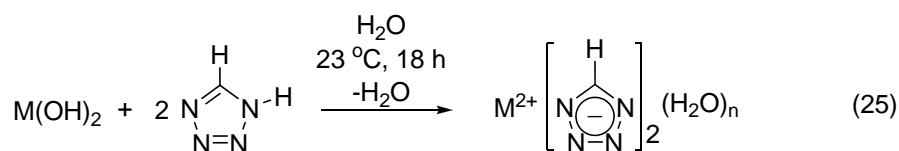
Synthesis and Characterization of Heavier Alkaline Earth Metal Tetrazolate Complexes: Potential Energetic Materials and Colorants for Pyrotechnic Compositions

2.1 Introduction

Among the assorted tetrazoles, 1H-tetrazole is the simplest derivative with a high nitrogen content of 80% and positive heat of formation of 237 kJ/mol.⁸⁰ 1H-tetrazole itself is explosive due to its endothermic nature; however, the relatively low density (1.53 g/cm³) and decomposition temperature (188 °C) limit its application as an energetic material.^{30b} Deprotonation affords the anionic 5-H-tetrazolate ion which has enhanced stability achieved by the cyclic delocalization of the ring electrons. Following the recent research on barium tetrazolate 18-crown-6 complexes reported by our group,⁴² we sought to eliminate the 18-crown-6 ligands and employ 5-H-tetrazolate as the ligand to access higher nitrogen contents. This chapter describes the synthesis, characterization, and energetic properties of heavier group 2 metal complexes of 5-H-tetrazolate. The objective was to synthesize compounds that might serve as propellant, secondary or primary energetic materials. In addition, since alkaline earth metals or their compounds are used to create colors in fireworks, we expect the new complexes described in this chapter should also have potential applications as color generators in pyrotechnic formulations.

2.2 Results

2.2.1 Synthetic Aspects. The heavier alkaline earth metal tetrazolate complexes $\text{Ca}(\text{HCN}_4)_2(\text{H}_2\text{O})_6$ (**57**), $\text{Sr}(\text{HCN}_4)_2(\text{H}_2\text{O})_5$ (**58**), and $\text{Ba}(\text{HCN}_4)_2$ (**60**) were prepared in 88-92% yields by treatment of 1H-tetrazole with $\text{Ca}(\text{OH})_2$, $\text{Sr}(\text{OH})_2(\text{H}_2\text{O})_8$, and $\text{Ba}(\text{OH})_2(\text{H}_2\text{O})_8$, respectively, in water at ambient temperature (eq 25). Complexes **57** and **58** were isolated as colorless powders and analyzed as described below to contain aqua ligands, in addition to the tetrazolate ligands. Crystals of **57** and **58** were obtained from slow evaporation of aqueous solutions. By contrast, **60** was isolated as the solvent free complex. A concentrated aqueous solution of **60** was allowed to evaporate slowly under ambient conditions to afford colorless crystals of $\text{Ba}_2(\text{HCN}_4)_4(\text{H}_2\text{O})_7$ (**59**). Dehydration of pulverized **57** and **58** under dynamic vacuum (0.05 Torr) at 111 °C afforded the anhydrous $\text{Ca}(\text{HCN}_4)_2$ (**61**) and $\text{Sr}(\text{HCN}_4)_2$ (**62**), respectively. Compounds **57-62** are soluble in water, slightly soluble in alcohols, and insoluble in common organic solvents. Since **57-62** are insoluble in tetrahydrofuran (THF), whereas 1H-tetrazole is fairly soluble, a slight excess of tetrazole was used to ensure the completely consumption of the metal bases and the products were purified by subsequent washing with copious amount of THF.



57, M = Ca, n = 6, 88%
58, M = Sr, n = 5, 89%
59, M = Ba, n = 3.5
60, M = Ba, n = 0, 92%

Complexes **57-62** were characterized by ^1H and $^{13}\text{C}\{^1\text{H}\}$ NMR spectroscopy, infrared spectroscopy, and C, H, N elemental analyses. In D_2O at ambient temperature, the protons attached to the ring core carbon atoms in **57-62** exhibited singlet resonances between δ 8.39 and δ 8.41 in the ^1H NMR spectra, while the ring carbon atoms appeared at 150.20-150.23 ppm in the $^{13}\text{C}\{^1\text{H}\}$ NMR spectra. The infrared spectra of **57-62** displayed stretching frequencies of $3109\text{-}3168\text{ cm}^{-1}$ for the C-H bonds, and other absorptions in the region of $700\text{-}1300\text{ cm}^{-1}$ for the tetrazolate ring stretching and bending vibrations. For **57-59**, the infrared spectra exhibited additional broad absorptions at $\sim 3400\text{ cm}^{-1}$ ascribed to the symmetric and asymmetric stretches of water ligands, and water O-H bond bending absorptions at $\sim 1640\text{ cm}^{-1}$. C, H, N elemental analyses for **57-62** were consistent with the formulations.

2.2.2 Thermal and Energetic Properties. Compounds **57-62** did not melt up to $400\text{ }^\circ\text{C}$, but decomposed before melting as indicated by the color change in the samples during the melting point experiments. TGA measurements were carried out under a nitrogen atmosphere with a heating rate of $5\text{ }^\circ\text{C}/\text{min}$ in order to investigate the thermal behavior of these complexes. As shown in Figure 1, **57**, **58**, and **60** first lost their water ligands and then underwent thermal degradations with onset temperatures at $325\text{-}350\text{ }^\circ\text{C}$. The decomposition processes were completed by $400\text{ }^\circ\text{C}$. Complex **57** underwent a two step weight loss of 36.8% by $230\text{ }^\circ\text{C}$ correlated to 6 water molecules, **58** lost 27.8% weight by $100\text{ }^\circ\text{C}$ associated with 5 water molecules, and **60** lost 18.4% weight by $70\text{ }^\circ\text{C}$ which

corresponds to 3.5 water molecules. For the anhydrous compounds **59**, **61**, and **62**, the TGA curves indicated that the ring destruction processes also started at 325-350 °C and finished at ~400 °C (Figure 2). The TGA trace of **61** showed a weight loss of 7.5% by 250 °C associated with less than one molecule of water per formula unit before the thermal decomposition of the tetrazolate ring, and that might be a result of moisture absorption from the air while preparing the sample.

Figure 1. TGA traces for **57**, **58**, and **60** from 20 to 700 °C at 5 °C/min.

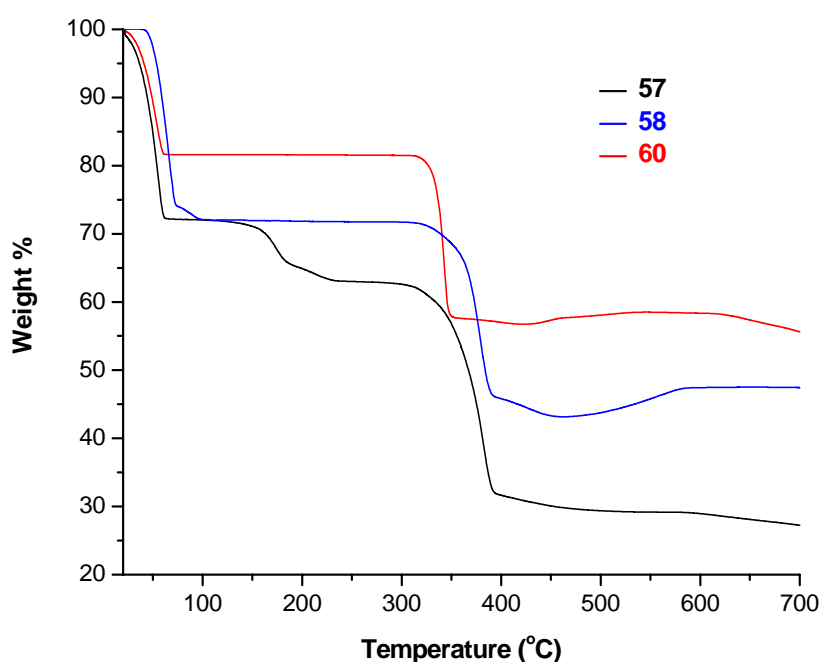
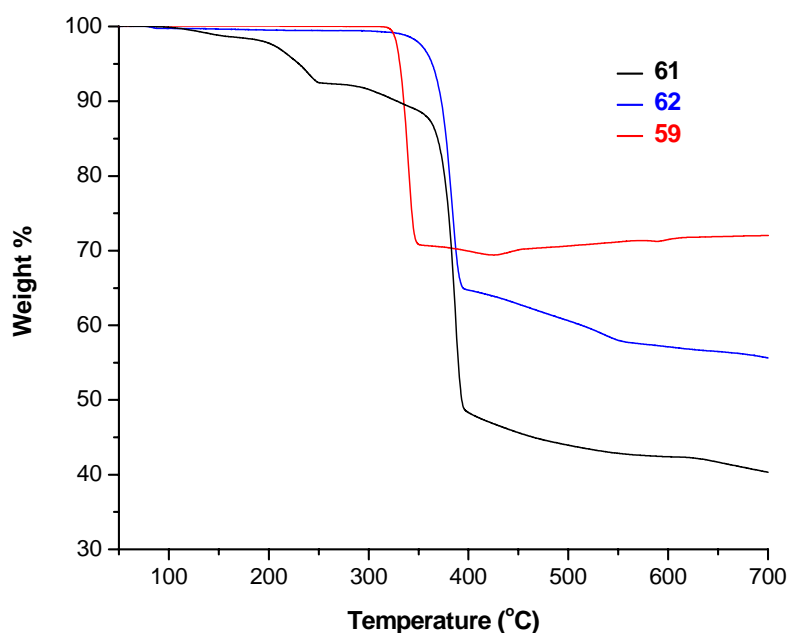


Figure 2. TGA traces for **59**, **61**, and **62** from 50 to 700 °C at 5 °C/min.



Small samples (~5 mg) of **57-62** were placed on an aluminum anvil and struck hard with a hammer. No detonations were observed under this procedure. Complexes **57-62** did not detonate when scratched with a spatula on a piece of sand paper. When using a Tesla coil to apply electrostatic discharge to **57-62**, there was no explosion or detonation. Small samples (~5 mg) of **57-62** were placed on a spatula and put in contact with a Bunsen burner flame. When the strontium complexes **58** and **62** were burned side by side, a significant difference in the flame color was detected. The hydrated **58** gave off bright red orange color, while the anhydrous **62** showed a yellow orange color. For the barium complexes, the hydrated **59** burned with a bright green color, whereas the anhydrous **60**

emitted a pale green color. Both of the anhydrous and hydrated calcium complexes **57** and **61** created similar orange red colors upon burning. In addition, the crystalline samples of **57-59** ignited a little slower than the corresponding powdery samples of **61**, **62**, and **60**, respectively. The barium complexes **59** and **60** snapped upon burning.

2.3 Discussion

This work has demonstrated the fact that deprotonation of 1H-tetrazole significantly increases the stability of the 5-membered heterocycle. Complexes **57-62** were prepared by the protonolysis of 1H-tetrazole with the specific metal hydroxides and they have thermal decomposition temperatures higher than 325 °C, which is much higher than that of the parent tetrazole at 188 °C. In addition, complexes **57-62** exhibit insensitivities toward shock, friction, and electrostatic discharge, whereas 1H-tetrazole is shock and friction sensitive. For **57-62**, the protons in the tetrazolate ligands exhibit upfield shift resonances between δ 8.39 and δ 8.41 in the ^1H NMR spectra, while the carbon atoms of the tetrazolate ligands show downfield shift resonances of 150.20-150.23 ppm in the $^{13}\text{C}\{^1\text{H}\}$ NMR spectra compared with the proton (δ 8.99) and carbon (143.1 ppm) resonances of 1H-tetrazole in D_2O . The similarity in NMR resonances of **57-62** suggests that these complexes possess very similar solution structures that most likely involve solvated, separated metal and tetrazolate ions. While we were working on this project, **58** was reported with X-ray crystal structural characterization by Klapötke and coworkers.^{30b}

According to the TGA analyses, the water ligands of **57**, **58**, and **60** were lost by 230,

100, and 70 °C, respectively. Based on this observation, it is obvious that the coordination strength of the oxygen atoms in the water ligands to the metal ions decrease in the order $\text{Ca}^{2+} > \text{Sr}^{2+} > \text{Ba}^{2+}$. This is most probably caused by the difference in Lewis acidity of the metal ions depending on the charge to size ratio. The calcium ion has the highest charge to size ratio and thus it is most acidic in the series, therefore, the water ligands are more strongly bound to the calcium ion than the strontium and barium ions. The dehydration temperatures should also be affected by hydrogen bonding in the solid states of the complexes. Since the calcium complex **57** has more water ligands per formula unit than the strontium and barium analogs (**58** and **60**), more water ligands will be available for forming hydrogen bonds in **57** and making it more stable toward dehydration. Furthermore, the inclusion of water ligands and subsequent hydrogen bonding interaction help to stabilize the compounds, as supported by the fact that the anhydrous complexes **60**, **61**, and **62** were initiated faster by a flame than the corresponding hydrated analogs **59**, **57**, and **58**, respectively. The calcium complexes **59** and **61** showed orange red colors when burned, and no difference in the flame colors could be observed between the hydrated and anhydrous samples. However, the hydrated strontium complex **58** burned and gave off a red orange color, while the strontium tetrazolate **62** burned with a yellow orange color. Moreover, the hydrated barium complex **59** exhibited a more intense green color than the anhydrous barium complex **60**. These differences originate from the formation of the light emitting species SrOH for the red color and BaOH for the green color in the gas phase for the hydrated complexes **58** and **59**, respectively, while the

corresponding anhydrous **62** and **60** do not contain available water molecules to generate SrOH or BaOH.⁸¹ The calcium and strontium complexes **57**, **58**, **61**, and **62** did not make any noise when 5 mg samples were burned. However, the barium complexes **59** and **60** made a small popping sound when a 5 mg sample was burned. These experiments suggest that **57**, **58**, **61**, and **62** are not likely to serve as primary energetic materials, although they may still contain considerable energy. Complexes **59** and **60** are energetic compounds that may behave as primary energetic materials.

2.4 Conclusions

Tetrazolate complexes of calcium, strontium and barium have been prepared and characterized by spectral and analytical techniques. TGA analyses demonstrate that **57-62** are thermally stable up to 325 °C. Preliminary safety tests show that the calcium and strontium complexes are insensitive toward classical stimuli, but they are possible “green” propellants or secondary energetic materials, while the barium complexes are sensitive to thermal shock and may behave as primary energetic materials. Complexes **57-62** present the specific flame colors of the metal ions upon burning. With high physical and thermal stabilities, these heavier alkaline earth metal tetrazolates are good candidates for colorants in pyrotechnic mixtures.

2.5 Experimental Section

General Considerations. In order to avoid the formation of metal carbonates, the syntheses of **57**, **58**, and **60** were conducted under an argon atmosphere using Schlenk line

techniques. Once isolated, they were handled under ambient conditions as the products are air stable. Compounds **61** and **62** were treated in an argon atmosphere to avoid absorption of moisture from ambient air. A 3 wt. % solution of 1H-tetrazole in acetonitrile was purchased from Aldrich Chemical Company. The acetonitrile was removed under reduced pressure, and the 1H-tetrazole was used as a solid. Ca(OH)_2 , $\text{Sr(OH)}_2 \cdot 8\text{H}_2\text{O}$, and $\text{Ba(OH)}_2 \cdot 8\text{H}_2\text{O}$ were purchased from Fisher Chemicals and used without further purification. ^1H and $^{13}\text{C}\{^1\text{H}\}$ NMR spectra were obtained at 500 and 125 MHz Varian instrument, respectively, in deuterium oxide. Infrared spectra were obtained using Nujol as the medium. Elemental analyses were performed by Midwest Microlab, Indianapolis, IN. It was necessary to add V_2O_5 as a combustion enhancing agent to obtain acceptable carbon values. Melting points were obtained on a Thermo Scientific Mel-Temp 3.0 melting point apparatus and are uncorrected. TGA experiments were conducted on a Perkin-Elmer Pyris 1 TGA system from 20 to 700 °C for **57-59**, and 50-700 °C for **60-62** using nitrogen as the flow gas with a heating rate of 5 °C/min.

General procedure for the preparation of 57-62. A 100-mL Schlenk flask was charged with the metal hydroxide, a stir bar, and degassed, distilled water (10 mL). 1H-tetrazole solution in water was prepared by dissolving solid 1H-tetrazole in degassed, distilled water (30 mL). To the stirred aqueous cloudy mixture of metal hydroxide, the 1H-tetrazole aqueous solution (2.2 molar equiv.) was slowly added, and the resultant mixture was stirred for 18 h at ambient temperature. The reaction mixture was then filtered through

a 2-cm pad of Celite on a coarse glass frit. Removal of the volatile components under reduced pressure followed by washing with 2×30 mL of THF afforded **57**, **58**, and **60** as colorless solids. Crystals of **57-59** were obtained by slow evaporation from aqueous solutions and were used for elemental analyses. Compounds **61** and **62** were prepared by vacuum drying pulverized **57** and **58** in a drying pistol under refluxing toluene for ~24 h, respectively, until no water absorptions were observed in the infrared spectra taken in fluorolube.

Bis(5-H-tetrazolate)hexaaquacalcium (57). Prepared from calcium hydroxide (0.148 g, 2.00 mmol) and 1H-tetrazole (0.308 g, 4.40 mmol) to afford **57** in 88% yield as a colorless solid. Mp > 400 °C (decompose at ~325 °C); IR (Nujol, cm^{-1}): $\tilde{\nu} = 3338$ (vs), 3109 (s), 1646 (s), 1311 (w), 1290 (s), 1219 (m), 1201 (s), 1155 (s), 1145 (s), 1128 (s), 1107 (m), 1084 (m), 1042 (m), 1024 (s), 1002 (s), 911 (m), 865 (m), 842 (w), 701(m), 695 (s); ^1H NMR (D_2O , 23 °C): $\delta = 8.39$ (s, 1H, HCN_4); $^{13}\text{C}\{^1\text{H}\}$ NMR (D_2O , 23 °C): $\delta = 150.23$ (s, HCN_4); elemental analysis calculated for $\text{C}_2\text{H}_{14}\text{N}_8\text{CaO}_6$ (%): C 8.39, H 4.93, N 39.14; found: C 8.16, H 4.85, N 39.38.

Bis(5-H-tetrazolate)pentaaquastrontium (58). Prepared from strontium hydroxide octahydrate (0.532 g, 2.00 mmol) and 1H-tetrazole (0.308 g, 4.40 mmol) to afford **58** in 89% yield as a colorless solid. Mp > 400 °C (decompose at ~325 °C); IR (Nujol, cm^{-1}): $\tilde{\nu} = 3436$ (vs), 3168 (s), 1634 (s), 1290 (s), 1201 (s), 1186 (m), 1164 (s), 1154 (m), 1142 (s), 1133 (m), 1103 (m), 1085 (m), 1018 (s), 1008 (s), 905 (s), 878 (m), 845 (w), 703 (s); ^1H NMR (D_2O ,

23 °C): $\delta = 8.42$ (s, 1H, HCN_4); $^{13}\text{C}\{^1\text{H}\}$ NMR (D_2O , 23 °C): $\delta = 150.23$ (s, HCN_4); elemental analysis calculated for $\text{C}_2\text{H}_{12}\text{N}_8\text{O}_5\text{Sr}$ (%): C 7.61, H 3.83, N 35.48; found: C 7.79, H 3.80, N 35.65.

Tetrakis(5-H-tetrazolate)heptaaquadibarium (59). Prepared from slow evaporation of an aqueous solution of **60** and obtained as colorless crystals. Mp > 400 °C (decompose at ~325 °C); IR (Nujol, cm^{-1}): $\tilde{\nu} = 3393$ (vs), 3155 (s), 1633 (s), 1298 (s), 1286 (s), 1193 (s), 1156 (s), 1137 (s), 1127 (s), 1100 (m), 1088 (m), 1017 (m), 1022 (s), 1004 (s), 882 (s), 872 (s), 698 (s); ^1H NMR (D_2O , 23 °C): $\delta = 8.39$ (s, 1H, HCN_4); $^{13}\text{C}\{^1\text{H}\}$ NMR (D_2O , 23 °C): $\delta = 150.20$ (s, HCN_4); elemental analysis calculated for $\text{C}_4\text{H}_{18}\text{N}_{16}\text{Ba}_2\text{O}_7$ (%): C 7.10, H 2.68, N 33.11; found: C 7.20, N 2.69, N 33.37.

Barium bis(5-H-tetrazolate) (60). Prepared from barium hydroxide octahydrate (0.631 g, 2.00 mmol) and 1H-tetrazole (0.308 g, 4.40 mmol) to afford **60** in 92% yield as a colorless solid. Mp > 400 °C (decompose at ~325 °C); IR (Nujol, cm^{-1}): $\tilde{\nu} = 3149$ (s), 1304 (w), 1285 (m), 1192 (s), 1158 (s), 1151 (s), 1135 (s), 1094 (m), 1017 (s), 1005 (s), 968 (w), 895 (s), 769 (w), 700 (s); ^1H NMR (D_2O , 23 °C): $\delta = 8.42$ (s, 1H, HCN_4); $^{13}\text{C}\{^1\text{H}\}$ NMR (D_2O , 23 °C): $\delta = 150.19$ (s, HCN_4); elemental analysis calculated for $\text{C}_2\text{H}_2\text{N}_8\text{Ba}$ (%): C 8.72, H 0.73, N 40.69; found: C 8.53, H 0.77, N 40.47.

Calcium bis(5-H-tetrazolate) (61). Prepared by drying small samples (~100 mg total weight in three small vials) of **57** and obtained as a colorless powder. Mp > 400 °C (decompose at ~350 °C); IR (Nujol, cm^{-1}): $\tilde{\nu} = 3113$ (s), 1298 (s), 1226 (w), 1201 (s), 1158 (s),

1138 (s), 1097 (m), 1033 (s), 1015 (s), 963 (m), 901 (s), 873 (m), 811 (m), 770 (w), 695 (s); ^1H NMR (D_2O , 23 °C): $\delta = 8.41$ (s, 1H, HCN_4); $^{13}\text{C}\{^1\text{H}\}$ NMR (D_2O , 23 °C): $\delta = 150.23$ (s, HCN_4); elemental analysis calculated for $\text{C}_2\text{H}_2\text{N}_8\text{Ca}$ (%): C 13.48, H 1.13, N 62.89; found: C 13.29, H 1.37, N 60.84.

Strontium bis(5-H-tetrazolate) (62). Prepared by drying small samples (~100 mg total weight in three small vials) of **58** and obtained as a colorless powder. Mp > 400 °C (decompose at ~350 °C); IR (Nujol, cm^{-1}): $\tilde{\nu} = 3168$ (s), 1290 (s), 1261 (w), 1201 (s), 1164 (s), 1155 (m), 1141 (m), 1103 (m), 1018 (s), 1008 (s), 972 (w), 905 (s), 799 (m), 704 (s); ^1H NMR (D_2O , 23 °C): $\delta = 8.41$ (s, 1H, HCN_4); $^{13}\text{C}\{^1\text{H}\}$ NMR (D_2O , 23 °C): $\delta = 150.13$ (s, HCN_4); elemental analysis calculated for $\text{C}_2\text{H}_2\text{N}_8\text{Sr}$ (%): C 10.64, H 0.89, N 49.64; found: C 10.42, H 1.06, N 48.54.

CHAPTER 3

Synthesis and Characterization of Potassium Bis(tetrazolyl)borate Complexes and Their 18-Crown-6 Adducts: Unexpected Boron-Nitrogen Bond Isomerism and Associated Enforcement of κ^3 -N,N',H-Ligand Chelation

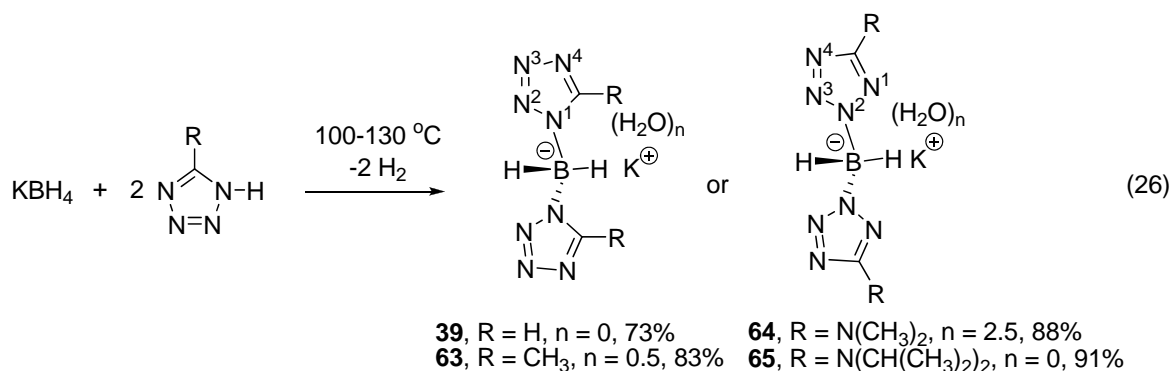
3.1 Introduction

As mentioned in Chapter 1, considerable attention has been paid to find nitrogen-rich ligands derived from tetrazoles. In order to increase the nitrogen contents, nitrogen-based substituents such as amino and nitro groups have been introduced to the tetrazolate ring.^{30a,32a,b} Tetrazolate ligands derived from bis(tetrazole), bis(tetrazolyl)amine, hydrazinebis(tetrazole), and azo(bistetrazole) have also been studied.^{40,43,82} These ligands can be regarded as substituted tetrazolates of the general structure **49** as depicted in Chart 3 in Chapter 1. Currently, there are few other classes of high nitrogen content anionic ligands available. Therefore, discovery of new classes of nitrogen-rich ligands is especially desirable for the formulation of energetic metal complexes. This chapter describes the preparation of bis(tetrazolyl)borate ligands in the form of their potassium complexes $K(BH_2(RCN_4)_2)(H_2O)_n$, and their coordination to the $[(18\text{-crown-}6)]^+$ fragment $K(BH_2(RCN_4)_2)(18\text{-crown-}6)$, where $R = H, Me, NMe_2, \text{ and } NiPr_2$. Formulation and properties of the new complexes were investigated. Moreover, isomeric B-N positions in the bis(tetrazolyl)borate ligands were identified depending on the size of substituents on the

ring core carbon atoms. In the solid state, one dimensional polymeric structures were found in $K(BH_2(RCN_4)_2)(18\text{-crown-}6)$, where $R = H$ and Me , and the bis(tetrazolyl)borate ligands bridge between the potassium ions. By contrast, monomeric structures were determined in $K(BH_2(RCN_4)_2)(18\text{-crown-}6)$, where $R = NMe_2$ and $NiPr_2$, and the ligands chelate to the potassium centers.

3.2 Results

3.2.1 Synthetic Aspects. Potassium bis(5-H-tetrazolyl)borate $K(BH_2(HCN_4)_2)$ (**39**) was prepared following literature procedures.⁶³ The other potassium bis(tetrazolyl)borate complexes $K(BH_2(MeCN_4)_2)(H_2O)_{0.5}$ (**63**), $K(BH_2(Me_2NCN_4)_2)(H_2O)_{2.5}$ (**64**), and $K(BH_2(iPr_2NCN_4)_2)$ (**65**) were synthesized in a similar fashion by heating a solid mixture of KBH_4 with two equivalents of the specific tetrazole to 100-130 °C (eq 26). Complexes **63** and **64** picked up water from ambient air after isolation as evidenced by infrared spectroscopy. Despite many attempts with 3:1 or 4:1 tetrazole to KBH_4 stoichiometry, it was not possible to prepare complexes containing tris(tetrazolyl)borate or tetrakis(tetrazolyl)borate ligands by this thermolysis route, and only **39** and **63-65** were isolated. This observation is similar to the findings by Janiak.⁶³

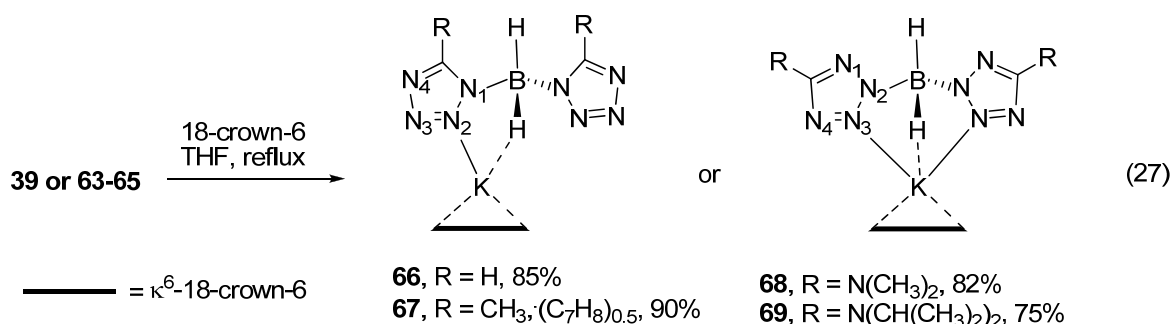


In the preparation of **39** and **63**, a slight excess of the tetrazoles was employed to ensure the complete consumption of the potassium borohydride. Since **39** and **63** are insoluble in THF, whereas 1H-tetrazole and 5-methyl-1H-tetrazole are very soluble in this solvent, the unreacted tetrazoles can be removed by subsequent washing the crude products with THF. Complexes **39**, **63**, and **64** are soluble in water and methanol. Complex **65** is moderately soluble in THF, but is insoluble in water and hexane. Complexes **63** and **64** were crystallized by slow evaporation of methanol/water solutions. Complex **65** was precipitated as a microcrystalline solid by adding excess hexane to a THF solution, but it was unsuitable for X-ray crystal structural determination and not pure enough to get a C, H, N elemental analysis with less than 0.4% error. The structures and compositions of **39** and **63-65** were established by NMR and IR spectroscopy; **63** and **64** were also characterized by X-ray crystal structural determinations. The hydrogen atoms on the ring core carbon atom, and the methyl and dimethylamino groups in **39**, **63**, and **64** appeared as singlets in the ¹H NMR spectra. In addition, the boron-bound hydrogen atoms in **39**, **63**, and **64** exhibited broad resonances at δ 3.58-3.71. By contrast, no resonances of the BH₂ group in **65** could

be seen in the ^1H NMR spectrum, and the diisopropyl groups exhibited a septet and a doublet at δ 3.91 and δ 1.15, respectively. In the $^{13}\text{C}\{^1\text{H}\}$ spectra of **39** and **63-65**, the ring core carbon atoms resonated between 148.17 and 169.89 ppm. The methyl groups in **63** and dimethylamino groups in **64** appeared at 8.79 and 38.92 ppm, respectively. The tertiary and primary carbon atoms on the diisopropyl groups in **65** exhibited resonances at 47.47 and 20.52 ppm, respectively. The ^{11}B NMR spectra for **39**, **63**, and **64** consisted broad singlets in the range of -9.38 to -13.76 ppm, relative to $\text{BF}_3 \cdot \text{Et}_2\text{O}$ as the external standard. In the infrared spectra of **39** and **63-65**, the B-H stretching absorptions appeared between 2473 and 2410 cm^{-1} .

The 18-crown-6 adducts of the potassium complexes $\text{K}(\text{BH}_2(\text{HCN}_4)_2)(18\text{-crown-6})$ (**66**), $\text{K}(\text{BH}_2(\text{MeCN}_4)_2)(18\text{-crown-6}) \cdot (\text{C}_7\text{H}_8)_{0.5}$ (**67**), $\text{K}(\text{BH}_2(\text{Me}_2\text{NCN}_4)_2)(18\text{-crown-6})$ (**68**), and $\text{K}(\text{BH}_2(\text{iPr}_2\text{NCN}_4)_2)(18\text{-crown-6})$ (**69**) were obtained as colorless crystalline solids by treatment of the corresponding potassium complexes (**39** and **63-65**) with one equivalent of 18-crown-6 in THF under reflux conditions (eq 27). The structures and compositions of **66-69** were established by spectroscopic and analytical methods, as well as by X-ray crystal structure determinations. Singlets were observed in ^1H NMR spectra of **66-68** for the H, Me, and NMe_2 substituents of the tetrazolyl groups, and a septet and a doublet were observed for the NiPr_2 groups in **69**. In addition, the 18-crown-6 ^1H NMR resonances in **66-69** were observed as sharp singlets, suggesting dynamic processes in solution at room temperature that lead to exchange of the diastereotopic methylene hydrogen atoms. The ^{11}B NMR

resonances for **66-69** appeared as broad singlets between -7.9 and -12.52 ppm, relative to $\text{BF}_3 \cdot \text{Et}_2\text{O}$ as the external standard. The infrared spectra of **66-69** exhibited absorptions attributable to B-H stretches between 2483 and 2409 cm^{-1} .



3.2.2 Thermal and Energetic Properties. Complexes **39**, **63**, and **64** were investigated by TGA under a nitrogen atmosphere at a heating rate of 5 $^\circ\text{C}/\text{min}$ with a temperature range of 20-500 $^\circ\text{C}$ (Figure 3); **66-69** were analyzed by TGA under similar conditions between 50 and 700 $^\circ\text{C}$ (Figure 4). The TGA of **39** showed a single weight loss event with the onset at 225 $^\circ\text{C}$ and a total weight loss of 38.3%. The weight loss for **39** is consistent with 2.6 equiv. of N_2 . Complexes **63** and **64** each showed two weight loss events, including the losses of coordinated water and the decomposition of the bis(tetrazolyl)borate ligands. The weight losses of 3.9% and 13.7% by 110 $^\circ\text{C}$ for **63** and **64**, respectively, are consistent with 0.5 and 2.5 equiv. of H_2O . Complexes **63** and **64** lost 58.6% and 56.5% weight from 275 to 500 $^\circ\text{C}$, respectively, which are associated with more than 4 equiv. of N_2 . The weight losses probably correspond to the liberation of N_2 and other gases such as CH_4 or NH_3 derived from the methyl and dimethylamino groups in **63** and **64**. The onset of thermal decomposition of

66-69 started between 210 and 220 °C, and the weight loss events appeared to involve 18-crown-6 evolution and bis(tetrazolyl)borate ligand decomposition, as judged by residual weights upon reaching 450 °C. Complex **66** exhibited a total weight loss of 71.1% which is corresponding to 2.1 equiv. of N₂ in addition to 1 equiv. of 18-crown-6. The weight losses of **68** and **69** were 80.9% and 85.5%, respectively, and they are associated with 1 equiv. of 18-crown-6 plus more than 4 equiv. of N₂. Again, these weight losses most likely consist of the release of other gases besides N₂ and 18-crown-6. Complex **67** possibly detonated at about 350 °C during the TGA analysis. For safety reasons, this analysis was not repeated and the data are presented herein as obtained. Complexes **39**, **63**, and **64** melt between 179 and 189 °C without decomposition, whereas complexes **66-69** possess lower melting points of 111-158 °C. Small samples of **39** and **63-69** (~5 mg) did not explode upon being struck hard with a hammer or upon scraping across 150 grit sand paper with a spatula. Passing sparks from a Tesla coil through ~5 mg samples of **39** and **63-69** on an aluminum plate did not lead to explosions or burning. When burned on a spatula tip in a Bunsen burner flame, ~10 mg samples **39** and **63** deflagrated with considerable gas evolution; **39** left some residue after burning. Placing ~10 mg samples of **64-69** into a Bunsen burner flame resulted in rapid burning with intense light and little smoke. These experiments suggest that **39** and **63-69** contain considerable energy, although they are unlikely to have applications as primary energetic materials because they are not shock sensitive.

Figure 3. TGA traces for **39**, **63**, and **64** from 20 to 500 °C at 5 °C/min.

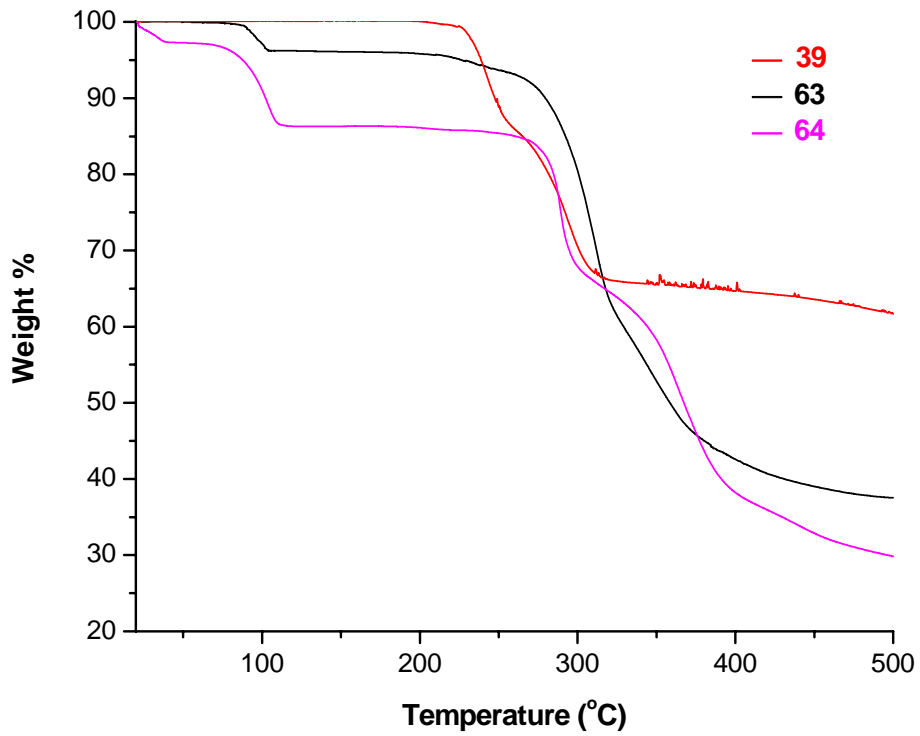
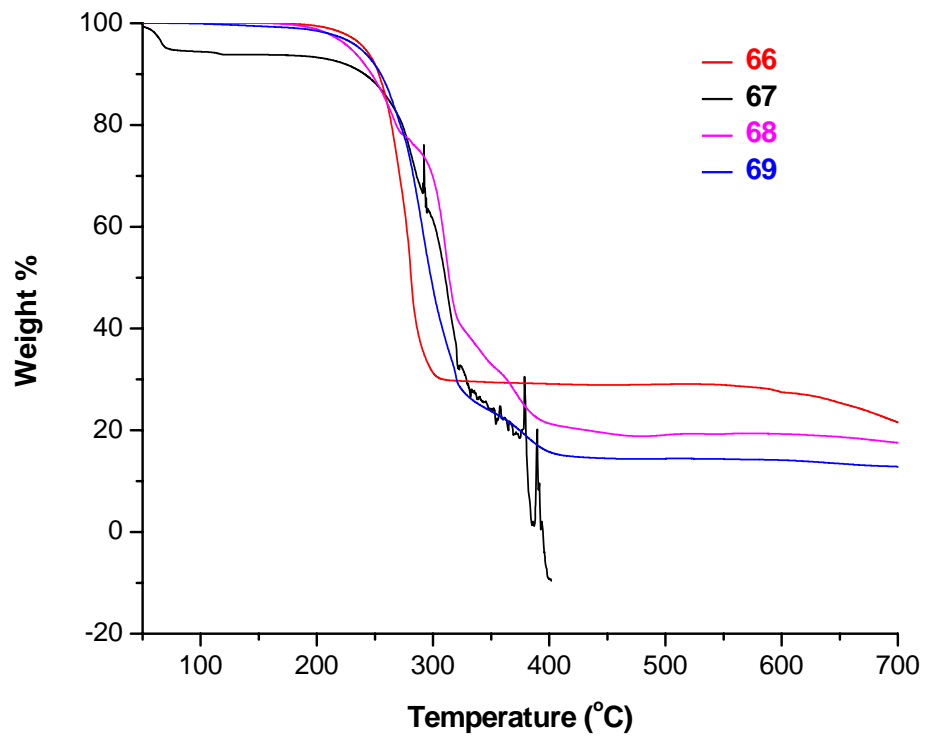


Figure 4. TGA traces for **66-69** from 50 to 700 °C at 5 °C/min.



3.2.3 Structural Aspects. The X-ray crystal structures of **63**, **64**, and **66-69** were determined to establish the geometry about the potassium centers and the bonding modes of the bis(tetrazolyl)borate ligands. Perspective views are illustrated in Figures 5-10, experimental crystallographic parameters are listed in Tables 1 and 2, and selected bond lengths and angles are given in Tables 3-8. The crystal structure of **39** has been previously reported.⁶³ Despite many attempts to grow single crystals of **65**, only microcrystalline solid were obtained, which were not suitable for X-ray diffraction studies.

Table 1. Crystal data and data collection parameters for **63** and **64**.

	63	64
Empirical formula	C ₄ H ₉ BKN ₈ O _{0.5}	C ₁₂ H ₃₈ B ₂ K ₂ N ₂₀ O ₅
FW	227.10	642.44
Space group	P2 ₁ /c	C2/c
a (Å)	10.0528(4)	15.6655(6)
b (Å)	15.8865(6)	20.5270(6)
c (Å)	13.7406(5)	19.2366(6)
β (°)	111.345(2)	94.117(2)
V (Å ³)	2043.90(13)	6169.9(4)
Z	8	8
T (K)	100(2)	100(2)
λ (Å)	0.71073	0.71073
ρ _{calc} (g cm ⁻³)	1.476	1.383
μ (mm ⁻¹)	0.502	0.367
R(<i>F</i>) (%)	0.0313	0.0453
R _w (<i>F</i>) (%)	0.0820	0.1110

$$R(F) = \frac{\sum ||F_o| - |F_c||}{\sum |F_o|}, R_w(F)^2 = \frac{[\sum w(F_o^2 - F_c^2)^2]}{\sum w(F_o^2)^2}]^{1/2} \text{ for } I > 2\sigma(I).$$

Table 2. Crystal data and data collection parameters for **66-69**.

	66	67	68	69
Empirical formula	C ₁₄ H ₂₈ N ₈ BKO ₆	C _{19.5} H ₃₆ N ₈ BKO ₆	C ₁₈ H ₃₈ N ₁₀ BKO ₆	C ₂₆ H ₅₄ N ₁₀ BKO ₆
FW	454.35	528.47	540.49	652.70
Space group	P2 ₁ /n	P1bar	P2 ₁ /n	Pbca
a (Å)	8.5551(2)	8.8464(3)	9.9554(5)	20.1745(6)
b (Å)	19.8351(6)	10.0021(4)	16.8330(8)	14.1816(4)
c (Å)	13.6130(4)	16.1443(6)	16.6956(8)	24.8676(8)
β (°)	91.5750(10)	94.052(2)	99.982(2)	90
V (Å ³)	2309.13(11)	1339.86(9)	2755.5(2)	7114.8(4)
Z	4	2	4	8
T (K)	100(2)	100(2)	100(2)	100(2)
λ (Å)	0.71073	0.71073	0.71073	0.71073
ρ _{calc} (g cm ⁻³)	1.307	1.310	1.303	1.219
μ (mm ⁻¹)	0.275	0.247	0.244	0.200
R(<i>F</i>) (%)	3.75	3.05	5.55	3.85
R _w (<i>F</i>) (%)	7.74	8.34	13.40	8.18

$$R(F) = \frac{\sum ||F_o| - |F_c||}{\sum |F_o|}, R_w(F)^2 = \frac{[\sum w(F_o^2 - F_c^2)^2]}{\sum w(F_o^2)^2}]^{1/2} \text{ for } I > 2\sigma(I).$$

A perspective view of **63** is depicted in Figure 5. Complex **63** crystallized as a three-dimensional polymer and it contains half a water ligand per formula unit. The O(1) atom of the water ligand is bridging between K(1) and K(2) ions. The K-O bond distances are 2.6886(8) and 2.8451(8) Å for K(1)-O(1) and K(2)-O(1), respectively, and the K(1)-O(1)-K(2) angle is 104.09 (2)°. The K-N bond lengths range from 2.8045(8) to 2.9657(8) Å. Each bis(5-methyltetrazolyl)borate ligand consists of two equivalent tetrazolyl groups that are connected to the boron atom through the N¹ atoms (eq 26). The hydrogen atoms attached to O(1) atom form hydrogen bonds with adjacent N(8) and N(15) atoms. In the O-H...N hydrogen bonds, the O-H bond distances are 0.860 and 0.930 Å; the H...N distances are 1.934 and 2.318 Å; the O...N separations are 2.790 and 3.164 Å; and O-H-N angles are 172.54 and 151.16°, respectively. The shortest distance between the potassium ion and a boron-bound hydrogen atom is 3.09 Å, and the associated K-B distance is 3.68 Å.

A perspective view of **64** is shown in Figure 6. It is also polymeric and **64** contains two and half water ligands per formula unit. The K-O bond distances are in the range of 2.6629(11) to 3.3337(13) Å, and the K-O-K angles are between 52.91(3) and 178.07(4)°. Each bis(5-dimethylaminotetrazolyl)borate ligand in **64** is composed of two equal tetrazolyl rings and the B-N bonds are formed through the N² atoms (eq 26). The K-N bond distances are between 2.8418(12) and 3.4417(12) Å. The water ligands form O-H...O hydrogen bonds between each other, as well as O-H...N hydrogen bonds with the adjacent nitrogen

atoms of the tetrazolyl groups. In the O-H \cdots O hydrogen bonds, the O-H bond lengths are 0.787-0.810 Å; the H \cdots O distances are 1.793-2.008 Å; the O \cdots O separations are 2.727-2.769 Å; and O-H-O angles are 156.24-160.01°. In the O-H \cdots N hydrogen bonds, the O-H bond distance are 0.770-0.859 Å; the H \cdots N distances are 1.893-2.674 Å; the O \cdots N separations range between 2.742 and 3.411 Å; and the O-H-N angles are 133.64-177.13°. The K-H distance from the potassium ion to the nearest boron-bound hydrogen atom is 3.11 Å, and the K-B distance is 3.96 Å.

Complex **66** exists as a one-dimensional polymer that forms through bridging of N(2) and N(4) between potassium ions (Figure 7). The K-N distances are 3.040(1) and 2.928(1) Å, respectively. The nitrogen atoms of the other tetrazolyl group are not coordinated to the K ion. The B-N bonds in **66** are to N(1) and N(5), which correspond to the N¹ atoms of the tetrazolyl groups (eq 27). One of the boron-bound hydrogen atoms is directed toward the potassium ion, with K-H and K-B distances of 3.17(2) and 3.875(2) Å, respectively. Thus, the bis(5-H-tetrazolyl)borate ligand in **66** adopts a κ^2 -N(2),H-coordination mode to each potassium ion, and further has a μ_2 -N(2),N(4)-bridging coordination mode between potassium ions. The K-O bond distances range between 2.803(1) and 2.955(1) Å.

In analogy to **66**, the molecular structure of **67** exists as a one dimensional polymer that is formed through K-N bonds to N(1) and N(5) of the bis(5-methyltetrazolyl)borate ligands as illustrated in Figure 8. The K-N bond lengths are 2.9496(9) and 2.8876(10) Å. Unlike **66**, both tetrazolyl rings have K-N bonds in the crystal structure of **67**. The K-B and

boron-bound K-H distances are 4.056(1) and 3.34(2) Å, respectively. The bis(5-methyltetrazolyl)borate ligand in **67** thus takes on a κ^2 -N(1),H-coordination mode to each potassium ion, and additionally adopts a μ_2 -N(1),N(5)-bridging coordination motif between two potassium ions. Similar to **66**, the B-N bonds in **67** are to N(4) and N(7) atoms, which corresponds to the N¹ atoms of the methyl tetrazolyl moieties (eq 27). The K-O bond distances in **67** are from 2.7523(8) to 2.8854(8) Å.

Complex **68** adopts a molecular structure that consists of isolated monomeric complexes, with κ^3 -N(1),N(6),H-coordination of the bis(5-dimethylaminotetrazolyl)borate ligand to the potassium ion (Figure 9). In addition, the B-N bonds in **68** are to N(4) and N(9), which correspond to the N² atoms of the dimethylaminotetrazolyl groups (eq 27). The K-N distances are 3.151(2) and 2.972(2) Å for K(1)-N(1) and K(1)-N(6), respectively. The K-B and boron-bound K-H distances are 3.464(3) and 2.87(3) Å, respectively, which are shorter than the values in **66** and **67**. The K-O distances in **68** range from 2.7912(18) to 3.0207(19) Å.

A perspective view of **69** is shown in Figure 10. It is monomeric and similar to that of **68** with κ^3 -N(2),N(7),H-coordination of the bis(5-diisopropylaminotetrazolyl)borate ligand. The K-B and boron-bound K-H distances are 3.719(2) and 3.08(2) Å, respectively. Like **68**, the B-N bonds of **69** are formed to N(3) and N(8) atoms, which match the N² atom of each diisopropylaminotetrazolyl group (eq 27). The K-N distances are 2.965(1) and 2.990(1) Å, respectively. The K-O distances in **69** range from 2.837(1) to 2.968(1) Å.

Figure 5. Perspective view of **63** with thermal ellipsoids at the 50% probability level.

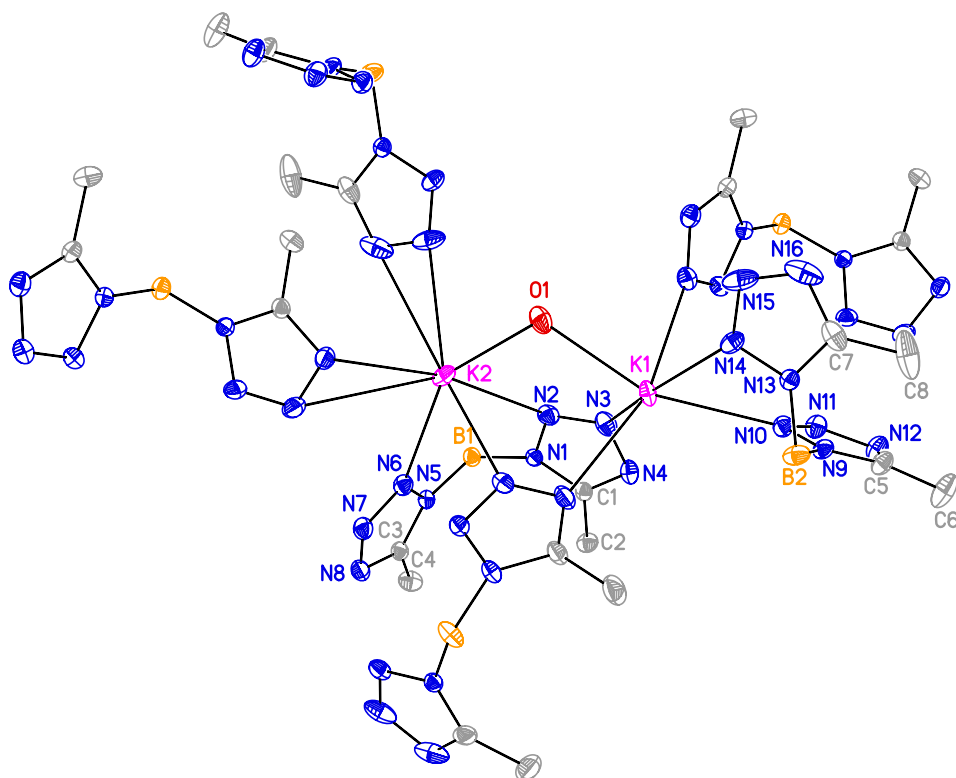


Table 3. Selected bond lengths (Å) and angles (°) for **63**.

K(1)-O(1)	2.6886(8)	K(1)-O(1)-K(2)	104.09(2)
K(2)-O(1)	2.8451(8)	O(1)-K(1)-N(3)	95.14(3)
K(1)-N(3)	2.8045(8)	O(1)-K(1)-N(14)	95.34(2)
K(1)-N(14)	2.8475(8)	N(3)-K(1)-N(14)	161.21(2)
K(1)-N(10)	2.8982(8)	O(1)-K(1)-N(10)	159.65(2)
K(1)-K(2)	4.3645(3)	N(3)-K(1)-N(10)	94.52(2)
K(2)-N(6)	2.8847(8)	N(14)-K(1)-N(10)	70.96(2)
K(2)-N(2)	2.9657(8)	O(1)-K(2)-N(6)	146.41(2)
B(1)-N(1)	1.5606(12)	O(1)-K(2)-N(2)	87.11(2)
B(1)-N(5)	1.5629(12)	N(6)-K(2)-N(2)	73.05(2)
N(1)-C(1)	1.3456(10)	N(1)-B(1)-N(5)	109.03(6)
N(1)-N(2)	1.3549(10)	N(13)-B(2)-N(9)	107.30(7)
N(2)-N(3)	1.2984(12)		
N(3)-N(4)	1.3589(12)		
N(4)-C(1)	1.3294(11)		

Figure 6. Perspective view of **64** with thermal ellipsoids at the 50% probability level.

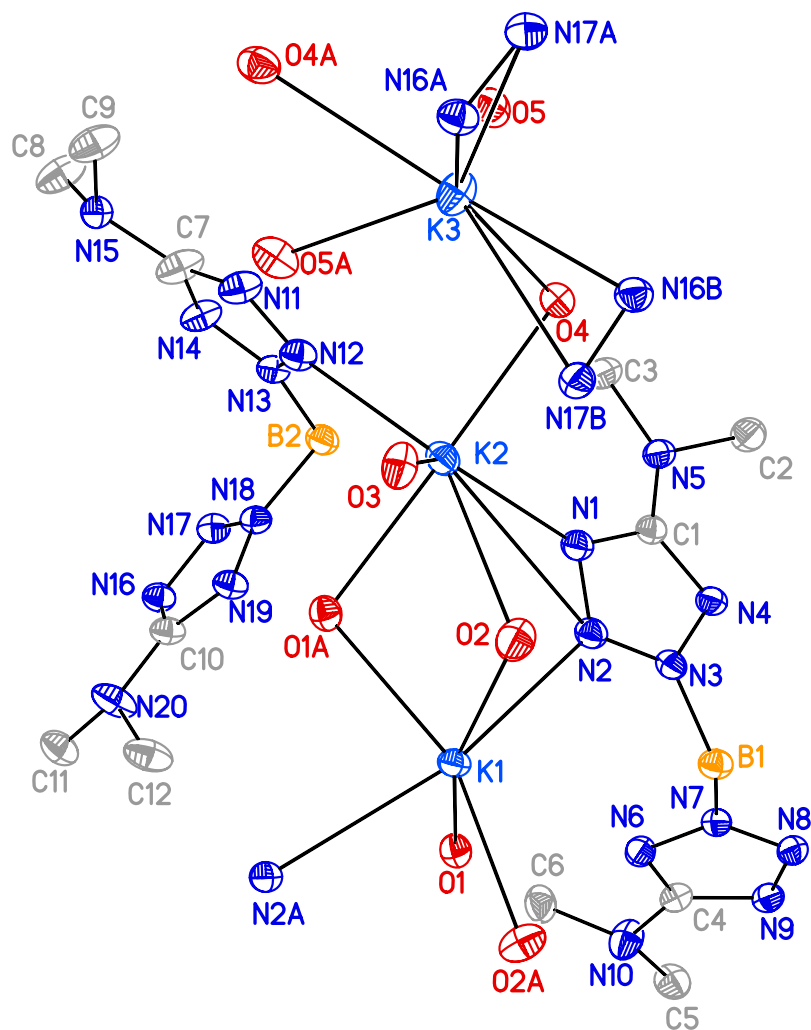


Table 4. Selected bond lengths (Å) and angles (°) for **64**.

K(1)-O(2)	2.7089(11)	O(2)-K(1)-O(1)	159.22(3)
K(1)-O(1)	2.7732(10)	O(2)-K(1)-N(2)	78.32(3)
K(2)-O(4)	2.6629(11)	O(1)-K(1)-N(2)	81.87(3)
K(2)-O(3)	2.7812(11)	O(4)-K(2)-O(3)	89.51(4)
K(2)-O(2)	3.3337(13)	O(4)-K(2)-N(1)	92.97(3)
K(3)-O(5)	2.7008(12)	O(3)-K(2)-N(1)	136.15(3)
K(3)-O(4)	2.9809(12)	O(4)-K(2)-N(12)	94.91(4)
K(1)-N(2)	2.9755(11)	O(3)-K(2)-N(12)	113.42(3)
K(2)-N(1)	2.8810(12)	N(1)-K(2)-N(12)	109.96(3)
K(2)-N(12)	2.9416(12)	O(4)-K(2)-O(2)	107.50(3)
K(2)-N(2)	3.4417(12)	O(3)-K(2)-O(2)	52.91(3)
K(1)-K(2)	4.1389(3)	N(1)-K(2)-O(2)	84.93(3)
N(3)-B(1)	1.5602(19)	N(12)-K(2)-O(2)	152.61(3)
B(1)-N(7)	1.5641(18)	O(4)-K(2)-N(2)	105.84(3)
N(1)-C(1)	1.3607(17)	O(3)-K(2)-N(2)	116.81(3)
N(4)-C(1)	1.3413(17)	N(1)-K(2)-N(2)	22.21(3)
N(1)-N(2)	1.3363(16)	N(12)-K(2)-N(2)	125.19(3)
N(2)-N(3)	1.3128(16)	O(2)-K(2)-N(2)	64.08(3)
N(3)-N(4)	1.3525(15)	K(1)-O(2)-K(2)	85.80(3)
K(2)-O(4)-K(3)	100.86(4)	N(3)-B(1)-N(7)	109.02(10)

Figure 7. Perspective view of **66** with thermal ellipsoids at the 50% probability level.

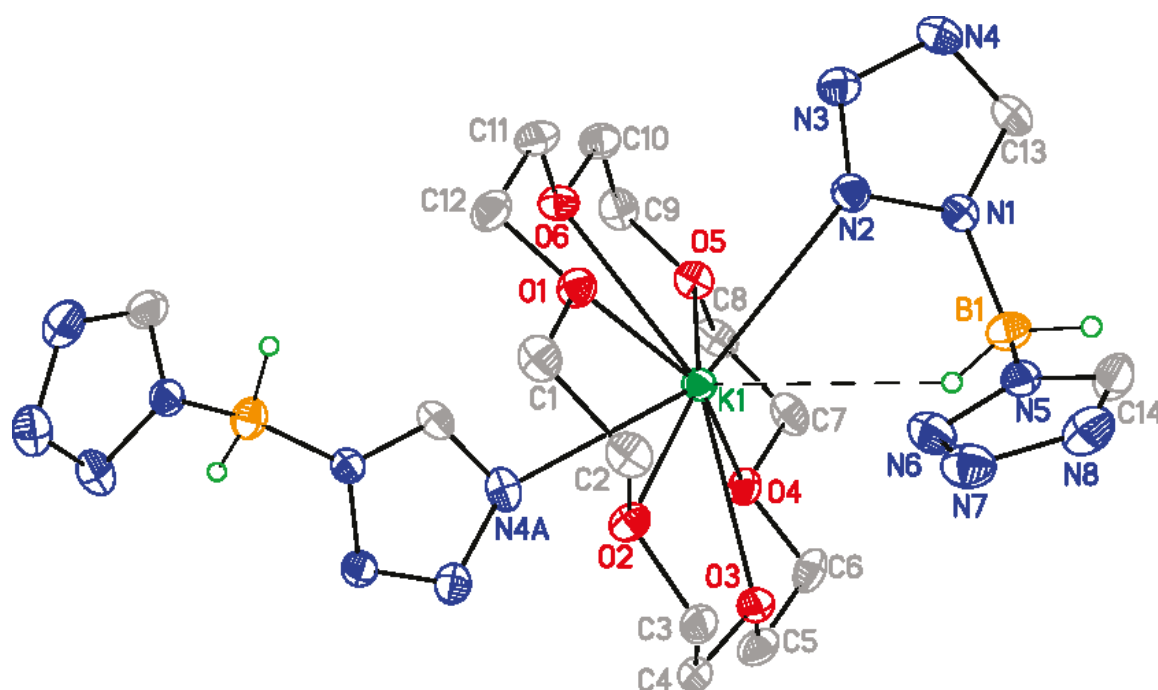


Table 5. Selected bond lengths (Å) and angles (°) for **66**.

K(1)-N(2)	3.0400(14)	N(5)-B(1)-N(1)	107.95(13)
K(1)-N(4)#1	2.9281(13)	N(1)-N(2)-K(1)	117.38(9)
K(1)-O(1)	2.8029(11)	N(3)-N(2)-K(1)	135.29(10)
K(1)-O(2)	2.8574(11)	N(2)-N(1)-B(1)	123.15(13)
K(1)-O(3)	2.8397(11)	N(6)-N(5)-B(1)	122.61(14)
K(1)-O(4)	2.9092(11)	N(4)#1-K(1)-N(2)	156.16(4)
K(1)-O(5)	2.8974(11)		
K(1)-O(6)	2.9554(12)		
N(1)-B(1)	1.568(2)		
N(5)-B(1)	1.568(2)		
K(1)-B(1)	3.875(2)		
K(1)-H	3.17(2)		

Figure 8. Perspective view of **67** with thermal ellipsoids at the 50% probability level.

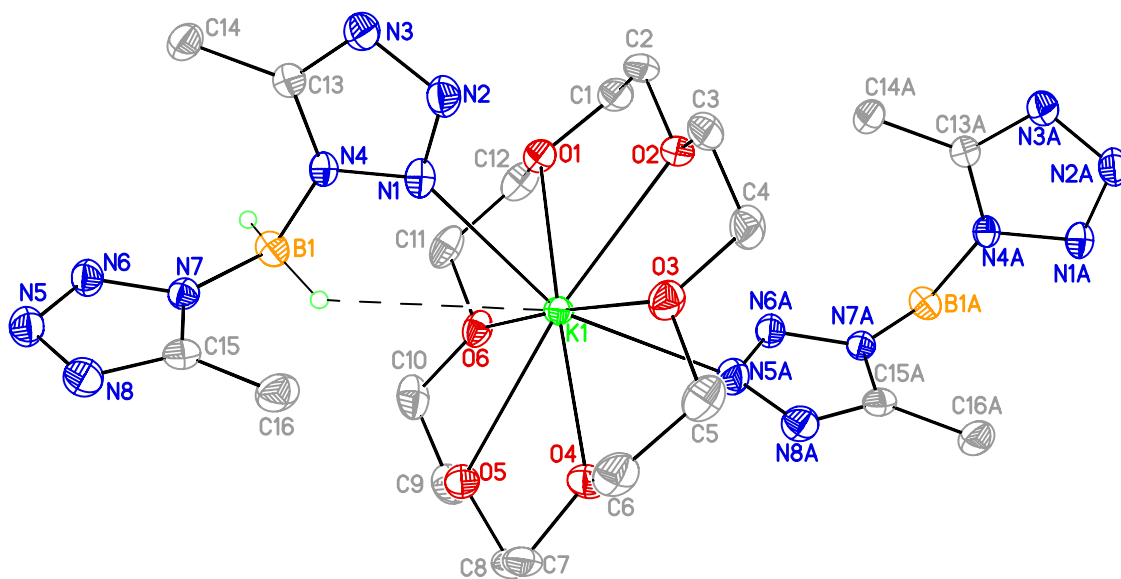


Table 6. Selected bond lengths (Å) and angles (°) for **67**.

K(1)-N(1)	2.9496(9)	N(4)-B(1)-N(7)	107.60(8)
K(1)-N(5)#1	2.8876(10)	N(4)-N(1)-K(1)	124.05(6)
K(1)-O(1)	2.7909(7)	N(2)-N(1)-K(1)	125.36(7)
K(1)-O(2)	2.7891(8)	N(1)-N(4)-B(1)	122.65(8)
K(1)-O(3)	2.8317(8)	N(6)-N(7)-B(1)	122.82(8)
K(1)-O(4)	2.7523(8)	N(5)#1-K(1)-N(1)	157.73(3)
K(1)-O(5)	2.8854(8)		
K(1)-O(6)	2.8132(8)		
N(4)-B(1)	1.5590(14)		
B(1)-N(7)	1.5583(14)		
K(1)-B(1)	4.056(1)		
K(1)-H	3.3396(2)		

Figure 9. Perspective view of **68** with thermal ellipsoids at the 50% probability level.

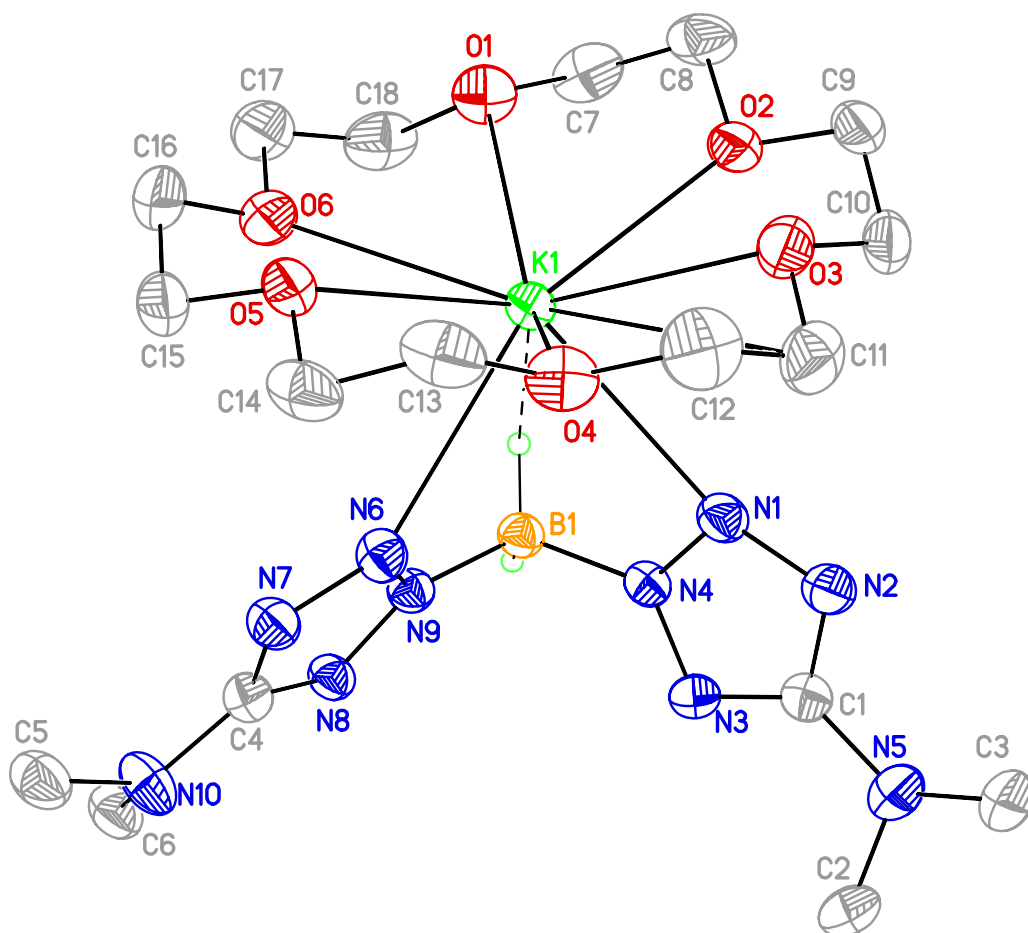


Table 7. Selected bond lengths (Å) and angles (°) for **68**.

K(1)-N(1)	3.151(2)	N(6)-K(1)-N(1)	71.94(5)
K(1)-N(6)	2.972(2)	N(4)-N(1)-K(1)	103.54(14)
K(1)-O(1)	3.0207(19)	N(2)-N(1)-K(1)	143.08(15)
K(1)-O(2)	2.9308(18)	N(9)-N(6)-K(1)	107.53(14)
K(1)-O(3)	2.8586(18)	N(7)-N(6)-K(1)	141.81(15)
K(1)-O(4)	2.7912(18)	N(1)-N(4)-B(1)	123.1(2)
K(1)-O(5)	2.9510(18)	N(6)-N(9)-B(1)	123.48(19)
K(1)-O(6)	2.9388(19)		
N(4)-B(1)	1.551(3)		
B(1)-N(9)	1.555(3)		
K(1)-B(1)	3.464(3)		
K(1)-H	2.8746(5)		

Figure 10. Perspective view of **69** with thermal ellipsoids at the 50% probability level.

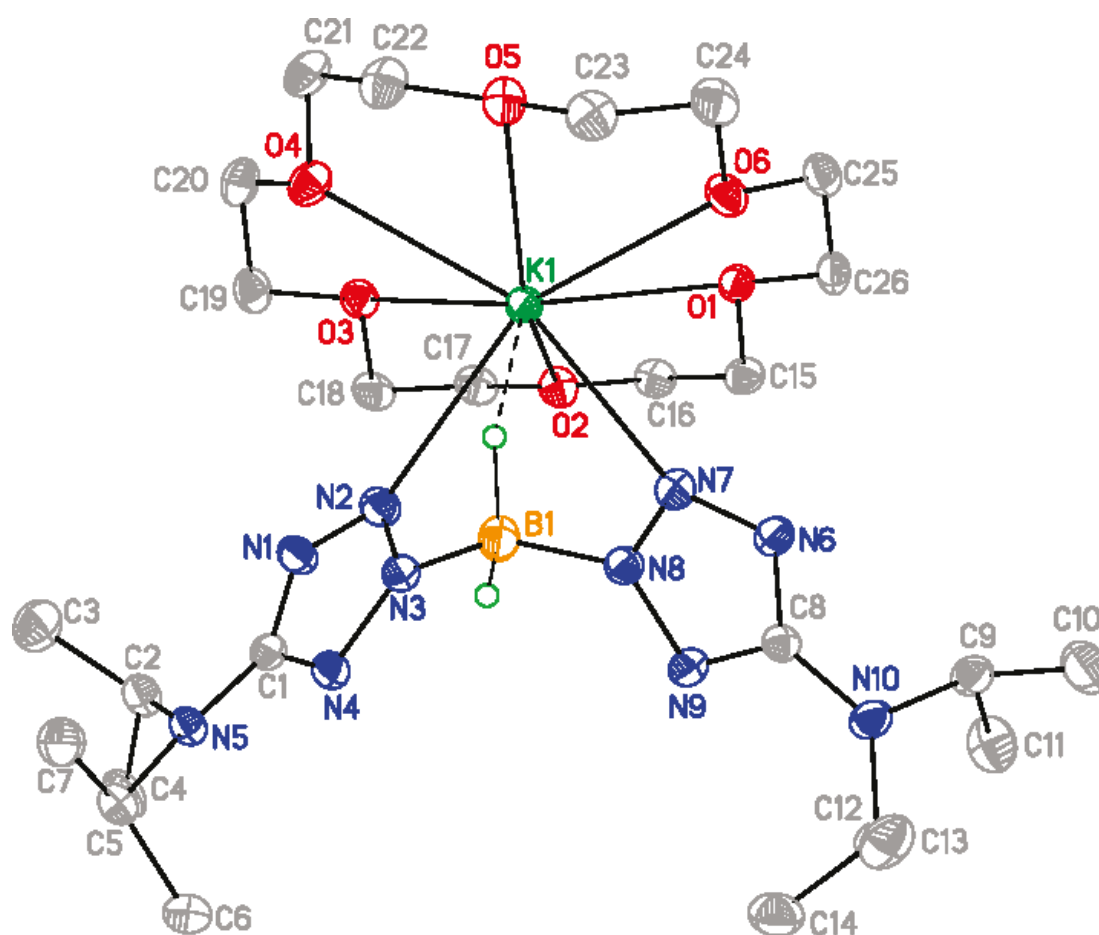


Table 8. Selected bond lengths (Å) and angles (°) for **69**.

K(1)-N(2)	2.9653(13)	N(2)-K(1)-N(7)	71.29(4)
K(1)-N(7)	2.9899(13)	N(3)-N(2)-K(1)	116.85(9)
K(1)-O(1)	2.9684(11)	N(1)-N(2)-K(1)	135.27(9)
K(1)-O(2)	2.8373(11)	N(8)-N(7)-K(1)	114.92(9)
K(1)-O(3)	2.9088(11)	N(6)-N(7)-K(1)	134.88(9)
K(1)-O(4)	2.8927(11)	N(2)-N(3)-B(1)	121.73(12)
K(1)-O(5)	2.8969(11)	N(7)-N(8)-B(1)	122.23(12)
K(1)-O(6)	2.8868(11)		
N(3)-B(1)	1.566(2)		
B(1)-N(8)	1.569(2)		
K(1)-B(1)	3.719(2)		
K(1)-H	3.08(2)		

3.3 Discussion

Numerous poly(azolyl)borate complexes derived from pyrazoles and triazoles have been synthesized and characterized by various techniques.^{61a} In comparison, poly(tetrazolyl)borate complexes have been less frequently studied. In this research, bis(tetrazolyl)borate complexes **39** and **63-69** were prepared and analyzed by spectroscopic and X-ray crystallographic methods. Complexes **39** and **63-69** exhibited broad singlet resonances between -7.9 and -13.76 ppm in the ¹¹B NMR spectra, which appeared upfield of BF₃·Et₂O and are similar to the ¹¹B NMR chemical shifts of poly(pyrazolyl)borates and poly(triazolyl)borates.⁸³ The B-H stretching frequencies between 2483 and 2409 cm⁻¹ of **39** and **63-69** in the infrared spectra are also in the same region as complexes containing bis(pyrazolyl)borate ligands.⁸⁴

In reports to date,⁶³⁻⁶⁶ the bis(5-H-tetrazolyl)borate and bis(5-aminotetrazolyl)borate ligands have exclusively served as bridging ligands between metal centers, rather than adopting the chelating κ^3 -N,N',H coordination mode that has been commonly observed in bis(pyrazolyl)borate ligands.^{61,85} The reluctance of the bis(5-H-tetrazolyl)borate ligand to coordinate to a single metal center with the κ^3 -N,N',H mode was ascribed to the higher basicity of the tetrazolyl ring nitrogen atom that is distal to the boron-bound nitrogen atom (eq 26, N⁴), compared to the nitrogen atom that is proximal to the boron-bound nitrogen atom (eq 26, N²).^{64c} As described above, the B-N bonds in **63** are to the N¹ atoms of the 5-methyltetrazolyl groups, and are consistent with previous structures of complexes

containing the bis(5-H-tetrazolyl)borate or bis(5-aminotetrazolyl)borate ligands.⁶³⁻⁶⁶ By contrast, the B-N bonds in **64** are to the N² atoms of the 5-dimethylaminotetrazolyl groups, and are different than those in **63** and the earlier reported complexes.⁶³⁻⁶⁶ The crystal structures of **63** and **64** contain water ligands, while the analogous potassium bis(5-H-tetrazolyl)borate (**39**) is anhydrous in the solid state structure.⁶³ The boron-bound K-H distances of 3.09 and 3.11 Å in **63** and **64** are longer than that of 2.89(3) Å in **39**, but they are significantly shorter than the sum of the van der Waals radii of potassium and hydrogen atoms (K, 2.75 Å; H, 1.20 Å).⁸⁶ Consequently, B-H···K interactions are present in **63** and **64**.

Similar to **63** and the previously reported complexes, the B-N bonds in **66** and **67** are to the N¹ atoms of the tetrazolyl groups. In **66**, the bis(5-H-tetrazolyl)borate ligands are bridged between two potassium ions through nitrogen atoms on the same tetrazolyl moiety, while the other tetrazolyl ring does not form bonds with the metal center. The presence of a “free” tetrazolyl group makes the structure of **66** unique among the previously investigated bis(tetrazolyl)borate complexes. Moreover, the bis(5-methyltetrazolyl)borate ligands in **67** bridge between two potassium centers through the N² and N^{3'} atoms of the two different tetrazolyl rings. This is a new coordination mode for the bis(tetrazolyl)borate ligand.⁶³⁻⁶⁶

In contrast to **63** and previous structures containing bis(tetrazolyl)borate ligands, **68** and **69** have the B-N bonds to the N² atoms of the tetrazolyl groups. The isomeric B-N bond positions in **68** and **69** probably originate from unfavorable steric interactions at the

tetrazole N^1 atoms during hydrogen evolution and B-N bond formation, compared to the more favorable situation at N^2 . The tetrazolyl ring carbon atom substituents in **68** and **69** sterically block coordination of the N^1 and N^4 atoms to the potassium ions, which leaves the N^3 positions as the only donor atoms and affords the $\kappa^3-N^3,N^{3'},H$ -coordination mode. As a result, the ligands in **68** and **69** are likely to coordinate to many different metal ions with the chelating $\kappa^3-N^3,N^{3'},H$ coordination mode. The coordination chemistry of the new isomeric bis(tetrazolyl)borate ligands should therefore resemble that of the extensively studied bis(pyrazolyl)borate and other poly(azolyl)borate ligands.

For complexes **66-69**, the K-H distances between the potassium ion and one of the boron-bound hydrogen atoms and K- N^2-N^1 or K- N^3-N^2 angles increase in the order **68** (2.87(3) Å; 103.5(1), 107.5(1)°) < **69** (3.08(2) Å; 114.92(9), 116.85(9)°) < **66** (3.17(2) Å; 117.38(9)°) < **67** (3.34(2) Å; 124.06(6)°), whereas the B-N-N angles fall between 121.7 and 123.5°. Clearly, the K-N bonds act as the “hinge” that controls the K···H interaction,⁶¹ which is probably facilitated by the ionic bonding between the potassium ion and the nitrogen atoms. The K-H distances in **66-69** are longer than those in $K(BH_4)(18\text{-crown-}6)$ (avg = 2.74(8) Å),⁸⁷ but the value in **68** is similar to that in **39** (2.89(3) Å).⁶³

Since bis(tetrazolyl)borate and tetrazolate ligands have the same charge, use of bis(tetrazolyl)borate ligands may lead to metal complexes that can be used to develop new classes of HEDMs. In this vein, a recent theoretical study has suggested that metal salts of $BH(N_3)_3^-$ should be promising HEDMs if a synthetic route becomes available.⁸⁸ Energetic

silver and azolium salts of bis(1,2,4-triazolyl)borate and tris(1,2,4-triazolyl)borate have been reported.⁸⁹ Finally, metal complexes containing the bis(3-nitro-1,2,4-triazolyl)borate ligand have been structurally characterized.⁹⁰

3.4 Conclusions

Various potassium bis(tetrazolyl)borate complexes were synthesized and characterized. A major discovery herein is the isomeric B-N bonds that form in **64**, **68**, and **69**, compared to those found in **63**, **66**, **67**, and previous reports of complexes containing bis(tetrazolyl)borate ligands.⁶³⁻⁶⁶ With small tetrazolyl core carbon atom substituents, the B-N bonds form to N¹, while larger core carbon atom groups form B-N bonds to N². The ligands with B-N bonds to N² adopt the chelating κ^3 -N,N',H-coordination mode to [K(18-Crown-6)]⁺, whereas the ligands with B-N bonds to N¹ take on bridging coordination modes. All new complexes are air stable and have thermal decomposition temperatures higher than 210 °C as evidenced by TGA. They are insensitive toward impact, friction, and spark, but deflagrate when burned in a Bunsen burner flame. These potassium bis(tetrazolyl)borate complexes can serve as starting materials to make other high nitrogen content bis(tetrazolyl)borate complexes.

3.5 Experimental Section

General Considerations. Complexes **39** and **63-69** are air stable and all reactions were performed under ambient conditions unless stated otherwise. A 3 wt. % solution of 1H-tetrazole in acetonitrile was purchased from Aldrich Chemical Company. The

acetonitrile was removed under reduced pressure, and the 1H-tetrazole was used as a solid. 5-Methyl-1H-tetrazole was purchased from Aldrich Chemical Company and was used as received. 5-Dimethylamino-1H-tetrazole and 5-diisopropylamino-1H-tetrazole were prepared according to literature procedures.¹³ ¹H, ¹³C{¹H}, and ¹¹B NMR spectra were obtained at 500, 125, and 160 MHz, respectively. Chemical shifts for ¹¹B NMR were measured in ppm using BF₃·Et₂O as the external reference. Infrared spectra were obtained using Nujol as the medium. Elemental analyses were performed by Midwest Microlab, Indianapolis, IN. It was necessary to add V₂O₅ as a combustion enhancing agent to obtain acceptable carbon values. Melting points were obtained on a Thermo Scientific Mel-Temp 3.0 melting point apparatus and are uncorrected. TGA experiments were conducted on a Perkin-Elmer Pyris 1 TGA system from 20 to 700 °C for **39**, **63**, and **64**, and 50-700 °C for **66-69** using nitrogen as the flow gas with a heating rate of 5 °C/min.

General procedure for the preparation of 39 and 63-65. A 100-mL Schlenk flask, equipped with a stir bar and reflux condenser, was charged with potassium borohydride and two equivalents of the tetrazole as a fine powder. The flask was purged with argon to avoid reaction of potassium borohydride with the moisture in ambient air. The solid mixture was then heated under stirring to 100 °C for **39** and **63**, and 130 °C for **64** and **65**, until about two equivalents of gas evolved. Crystals of **63** and **64** were obtained from slow evaporation of methanol/water solutions, while **39** and **65** were obtained as white solids.

General procedure for the preparation of 66-69. To the specific potassium

bis(tetrazolyl)borate, an equimolar quantity of 18-crown-6 was added and THF (30 mL) was then added. The resultant mixture was refluxed for 1 h and then filtered through a 2-cm pad of Celite on a coarse glass frit. The clear filtrate was concentrated to about 10 mL, and was then layered with hexane (80 mL). After slow diffusion of the two solvents, colorless crystalline solids were obtained for **66**, **68**, and **69**, and the crystals were suitable for X-ray crystallographic studies. Crystals of **67** were grown from a concentrated toluene/THF solution at -25 °C. The crystalline samples were also used for the microanalyses.

K(BH₂(HCN₄)₂) (39). Prepared from potassium borohydride (0.540 g, 10.0 mmol) and 1H-tetrazole (1.543 g, 22.00 mmol) to afford **39** in 73% yield as a colorless solid. Mp: 179-180 °C; IR (Nujol, cm⁻¹): $\tilde{\nu}$ = 3143 (s), 3133 (s), 2455 (s), 2344 (w), 2313 (w), 1792 (w), 1365 (s), 1304 (w), 1256 (w), 1245 (w), 1234 (w), 1197 (m), 1186 (s), 1166 (s), 1147 (m), 1137 (s), 1116 (s), 1044 (m), 984 (s), 898 (m), 864 (m), 744 (m), 714 (s), 671 (w), 656 (w), 641 (s), 620 (w); ¹H NMR (D₂O, 23 °C): δ = 8.79 (s, 2H, HCN₄), 3.71 (m, br, 2H, BH₂); ¹³C{¹H} NMR (D₂O, 23 °C): δ = 148.17 (s, HCN₄); ¹¹B NMR (D₂O, 23 °C): δ = -13.76 (s, br, BH₂).

K(BH₂(MeCN₄)₂)(H₂O)_{0.5} (63). Prepared from potassium borohydride (0.540 g, 10.0 mmol) and 5-methyl-1H-tetrazole (1.850 g, 22.00 mmol) to afford **63** in 83% yield as a colorless crystalline solid. Mp: 185-187 °C; IR (Nujol, cm⁻¹): $\tilde{\nu}$ = 2473 (s), 2454 (s), 2447 (s), 2286 (w), 2250 (w), 2232 (w), 2213 (w), 1507 (s), 1400 (s), 1275 (s), 1269 (m), 1251 (w), 1214 (m), 1203 (s), 1194 (s), 1161 (m), 1150 (s), 1129 (s), 1118 (s), 1106 (s), 1043 (m), 1029

(w), 1019 (m), 1003 (m), 881 (m), 868 (s), 752 (m), 708 (w), 702 (w), 694 (m), 633 (m), 624 (s), 614 (s); ^1H NMR (D_2O , 23 °C): δ = 3.59 (m, br, 2H, BH_2), 2.33 (s, 6H, CH_3CN_4); $^{13}\text{C}\{^1\text{H}\}$ NMR (D_2O , 23 °C): δ = 157.14 (s, CH_3CN_4), 8.97 (s, CH_3CN_4); ^{11}B NMR (D_2O , 23 °C): δ = -12.56 (s, br, BH_2); elemental analysis calculated for $\text{C}_4\text{H}_8\text{N}_8\text{BK}$ (%): C 22.03, H 3.70, N 51.38; found: C 22.18, H 3.71, N 51.29. Complex **63** is hygroscopic and needs to be dehydrated in a drying pistol with refluxing toluene to remove the water ligands as well as the moisture it absorbed in order to obtain acceptable elemental analysis result. The elemental analysis of a crystal sample indicated one water molecule per formula unit instead of a half. Elemental analysis calculated for $\text{C}_4\text{H}_{10}\text{N}_8\text{BKO}$ (%): C 20.35, H 4.27, N 47.46; found: C 20.05, H 4.09, N 47.57.

$\text{K}(\text{BH}_2(\text{Me}_2\text{NCN}_4)_2)(\text{H}_2\text{O})_{2.5}$ (64**).** Prepared from potassium borohydride (0.540 g, 10.0 mmol) and 5-dimethylamino-1H-tetrazole (2.263 g, 20.00 mmol) to afford **64** in 88% yield as a colorless crystalline solid. Mp: 187-189 °C; IR (Nujol, cm^{-1}): $\tilde{\nu}$ = 3403 (br), 2457 (s), 2410 (s), 2371 (w), 2351 (w), 2344 (w), 2265 (w), 1572 (s), 1399 (m), 1353 (s), 1302 (m), 1286 (m), 1254 (s), 1216 (w), 1179 (m), 1142 (s), 1113 (s), 1067 (s), 1031 (m), 1021 (s), 964 (m), 884 (w), 869 (m), 839 (s), 761 (m), 740 (m), 699 (m), 675 (w), 666 (w); ^1H NMR (D_2O , 23 °C): δ = 3.58 (m, br, 2H, BH_2), 2.70 (s, 12H, $(\text{CH}_3)_2\text{NCN}_4$); $^{13}\text{C}\{^1\text{H}\}$ NMR (D_2O , 23 °C): δ = 169.89 (s, $(\text{CH}_3)_2\text{NCN}_4$), 38.92 (s, $(\text{CH}_3)_2\text{NCN}_4$); ^{11}B NMR (D_2O , 23 °C): δ = -9.38 (s, br, BH_2); elemental analysis calculated for $\text{C}_{12}\text{H}_{38}\text{N}_{20}\text{B}_2\text{K}_2\text{O}_5$ (%): C 22.44, H 5.96, N 43.61; found: C 22.74, H 5.79, N 43.36.

K(BH₂(iPr₂NCN₄)₂) (65). Prepared from potassium borohydride (0.540 g, 10.0 mmol) and 5-diisopropylamino-1H-tetrazole (3.385 g, 20.00 mmol) to afford **65** in 64% crude yield as a colorless crystalline solid. IR (Nujol, cm⁻¹): $\tilde{\nu}$ = 2464 (s), 2438 (s), 2280 (w), 1608 (w), 1547 (s), 1513 (m), 1405 (s), 1346 (s), 1291 (m), 1200 (m), 1176 (m), 1150 (s), 1132 (s), 1097 (w), 1073 (s), 1064 (s), 1033 (s), 1027 (s), 1020 (s), 967 (w), 951 (w), 934 (w), 916 (w), 890 (w), 872 (w), 861 (w), 800 (w), 757 (m), 695 (m), 673 (w); ¹H NMR (CD₂Cl₂, 23 °C): δ = 3.91 (septet, J = 6.5 Hz, 4H, CH₃CHCH₃), 1.15 (d, J = 7.0 Hz, 24H, CH₃CHCH₃); ¹³C{¹H} NMR (CD₂Cl₂, 23 °C): δ = 167.46 (s, iPr₂NCN₄), 47.47 (s, CH₃CHCH₃), 20.52 (s, CH₃CHCH₃).

K(BH₂(HCN₄)₂)(18-crown-6) (66). Prepared from **39** (0.200 g, 1.053 mmol) and 18-crown-6 (0.278 g, 1.053 mmol) to afford **66** in 85% yield as a colorless crystalline solid. Mp: 121-123 °C; IR (Nujol, cm⁻¹): $\tilde{\nu}$ = 3133 (s), 2431 (s), 2422 (s), 2295 (w), 2254 (w), 1973 (w), 1588 (w), 1351 (s), 1284 (s), 1251 (s), 1235 (s), 1185 (s), 1170 (s), 1160 (s), 1136 (s), 1107 (s), 1030 (s), 975 (m), 960 (s), 896 (m), 886 (m), 862 (m), 838 (s), 770 (w), 743 (m), 716 (s), 682 (w), 651 (m), 634 (s); ¹H NMR (D₂O, 23 °C): δ = 8.81 (s, 2H, HCN₄), 3.52 (s, 24H, OCH₂CH₂O); ¹³C{¹H} NMR (D₂O, 23 °C): δ = 148.20 (s, HCN₄), 69.86 (s, OCH₂CH₂O); ¹¹B NMR (D₂O, 23 °C): δ = -11.23 (s, br, BH₂); elemental analysis calculated for C₁₄H₂₈N₈BK₂O₆ (%): C 37.01, H 6.21, N 24.66; found: C 37.23, H 5.98, N 24.82.

K(BH₂(MeCN₄)₂)(18-crown-6)·(C₇H₈)_{0.5} (67). Prepared from **63** (0.200 g, 0.881 mmol) and 18-crown-6 (0.233 g, 0.881 mmol) to afford **67** in 90% yield as a colorless

crystalline solid. Mp: 109-111 °C; IR (Nujol, cm^{-1}): $\tilde{\nu} = 2437$ (s), 2417 (s), 2256 (w), 1974 (w), 1602 (w), 1505 (s), 1402 (s), 1352 (s), 1286 (s), 1251 (s), 1194 (s), 1134 (s), 1105 (s), 994 (m), 961 (s), 879 (w), 866 (m), 839 (s), 746 (s), 737 (m), 726 (s), 703 (m), 624 (s); ^1H NMR (CD_3OD , 23 °C): $\delta = 7.21$ -7.08 (m, 2.5H, $\text{C}_6\text{H}_5\text{CH}_3$), 3.60 (s, 24H, $\text{OCH}_2\text{CH}_2\text{O}$), 2.55 (s, 6H, CH_3CN_4), 2.31 (s, 1.5H, $\text{C}_6\text{H}_5\text{CH}_3$); $^{13}\text{C}\{^1\text{H}\}$ NMR (CD_3OD , 23 °C): $\delta = 157.13$ (s, CH_3CN_4), 138.92 (s, *ipso*- $\text{C}_6\text{H}_5\text{CH}_3$), 129.93 (s, *o*- $\text{C}_6\text{H}_5\text{CH}_3$), 129.22 (s, *m*- $\text{C}_6\text{H}_5\text{CH}_3$), 126.30 (s, *p*- $\text{C}_6\text{H}_5\text{CH}_3$), 71.30 (s, $\text{OCH}_2\text{CH}_2\text{O}$), 21.47 (s, $\text{C}_6\text{H}_5\text{CH}_3$), 9.80 (s, CH_3CN_4); ^{11}B NMR (D_2O , 23 °C): $\delta = -12.52$ (s, br, BH_2); elemental analysis calculated for $\text{C}_{19.5}\text{H}_{36}\text{N}_8\text{BKO}_6$ (%): C 44.32, H 6.87, N 21.20; found: C 44.38, H 6.79, N 21.25.

$\text{K}(\text{BH}_2(\text{Me}_2\text{NCN}_4)_2)(18\text{-crown-6})$ (68). Prepared from **64** (0.200 g, 0.623 mmol) and 18-crown-6 (0.165 g, 0.623 mmol) to afford **68** in 82% yield as a colorless crystalline solid. Mp: 138-140 °C; IR (Nujol, cm^{-1}): $\tilde{\nu} = 2457$ (s), 2410 (s), 2266 (w), 1978 (w), 1571 (s), 1503 (w), 1400 (s), 1353 (s), 1301 (m), 1286 (m), 1254 (s), 1217 (w), 1179 (m), 1143 (s), 1112 (s), 1068 (s), 1031 (m), 1021 (s), 964 (s), 884 (w), 868 (m), 839 (s), 761 (m), 740 (m), 699 (m), 675 (w), 665 (m); ^1H NMR (D_2O , 23 °C): $\delta = 3.51$ (s, 24H, $\text{OCH}_2\text{CH}_2\text{O}$), 2.79 (s, 12H, $(\text{CH}_3)_2\text{NCN}_4$); $^{13}\text{C}\{^1\text{H}\}$ NMR (D_2O , 23 °C): $\delta = 170.00$ (s, $(\text{CH}_3)_2\text{NCN}_4$), 69.85 (s, $\text{OCH}_2\text{CH}_2\text{O}$), 39.04 (s, $(\text{CH}_3)_2\text{NCN}_4$); ^{11}B NMR (D_2O , 23 °C): $\delta = -10.24$ (s, br, BH_2); elemental analysis calculated for $\text{C}_{18}\text{H}_{38}\text{N}_{10}\text{BKO}_6$ (%): C 40.00, H 7.09, N 25.92; found: C 40.19, H 6.94, N 26.07.

$\text{K}(\text{BH}_2(\text{iPr}_2\text{NCN}_4)_2)(18\text{-crown-6})$ (69). Prepared from **65** (0.200 g, 0.515 mmol)

and 18-crown-6 (0.136 g, 0.515 mmol) to afford **69** in 75% yield as a colorless crystalline solid. Mp: 156-158 °C; IR (Nujol, cm^{-1}): $\tilde{\nu}$ = 2483 (s), 2409 (s), 2285 (w), 1978 (w), 1563 (s), 1547 (s), 1543 (s), 1539 (s), 1505 (w), 1406 (s), 1352 (s), 1287 (s), 1253 (m), 1238 (w), 1204 (s), 1189 (m), 1176 (m), 1146 (s), 1134 (s), 1111 (s), 1032 (s), 963 (s), 889 (w), 871 (w), 861 (w), 837 (s), 758 (m), 700 (m), 679 (m); ^1H NMR (CD_2Cl_2 , 23 °C): δ = 4.04 (septet, J = 6.8 Hz, 4H, CH_3CHCH_3), 3.66 (s, 24H, $\text{OCH}_2\text{CH}_2\text{O}$), 1.26 (d, J = 6.5 Hz, 24H, CH_3CHCH_3); $^{13}\text{C}\{^1\text{H}\}$ NMR (CD_2Cl_2 , 23 °C): δ = 167.41 (s, iPr_2NCN_4), 70.44 (s, $\text{OCH}_2\text{CH}_2\text{O}$), 47.20 (s, CH_3CHCH_3), 20.78 (s, CH_3CHCH_3); ^{11}B NMR (D_2O , 23 °C): δ = -7.87 (s, br, BH_2); elemental analysis calculated for $\text{C}_{26}\text{H}_{54}\text{N}_{10}\text{BKO}_6$ (%): C 47.85, H 8.34, N 21.46; found: C 48.17, H 8.11, N 21.04.

CHAPTER 4

Synthesis and Characterization of Heavier Alkaline Earth Metal

Bis(5-methyltetrazolyl)borate Complexes: Transfer of the Bis(tetrazolyl)borate Ligands to Divalent Metal Ions

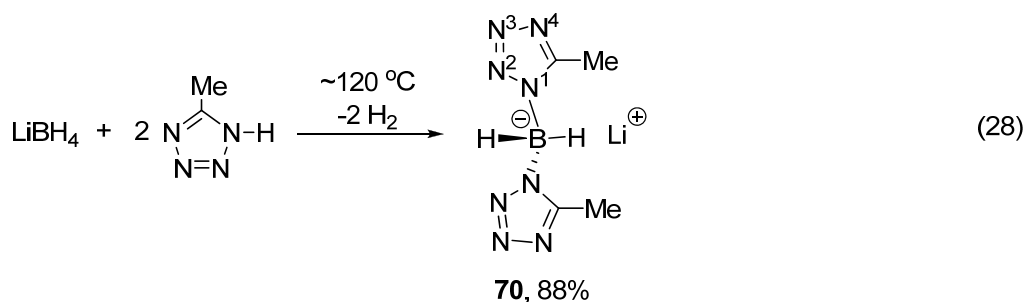
4.1 Introduction

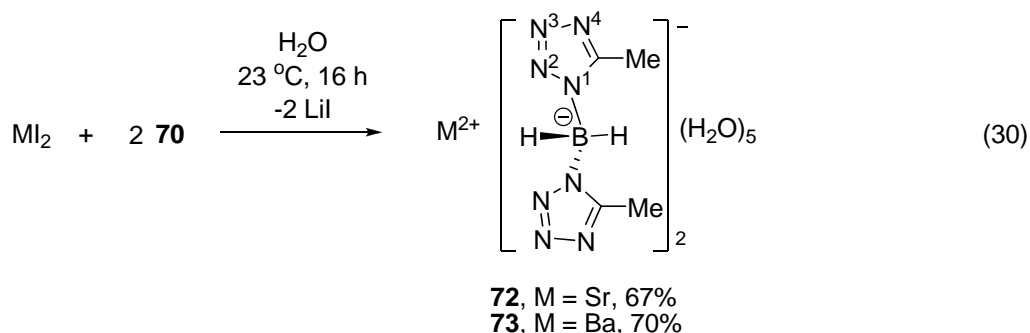
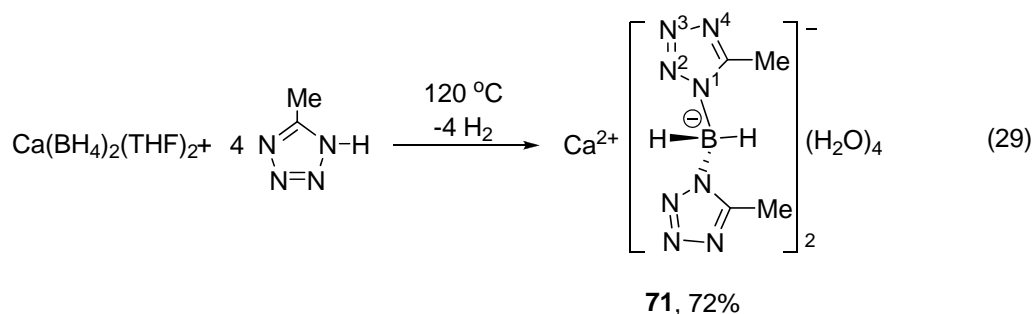
The synthesis and characterization of a series of bis(tetrazolyl)borate ligands have been recently reported by our laboratory.⁹¹ Transfer of the ligands to metal ions with multiple charges should lead to the formation of metal complexes with even higher nitrogen content. This chapter describes the synthesis and characterization of heavier group 2 metal bis(5-methyltetrazolyl)borate complexes. Attempted preparation of group 2 metal complexes containing other bis(tetrazolyl)borate ligands is also discussed briefly. The thermal and energetic properties of the new complexes suggest that the group 2 metal bis(5-methyltetrazolyl)borates are more energetic than the analogous potassium complexes.

4.2 Results

4.2.1 Synthetic Aspects. The lithium complex $\text{Li}(\text{BH}_2(\text{MeCN}_4)_2)$ (**70**) was prepared by heating a solid mixture of LiBH_4 and 2.2 equivalents 5-methyl-1H-tetrazole at 120 °C (eq 28). It was purified by washing the crude product with sufficient THF to remove the excess methyl tetrazole. The calcium complex $\text{Ca}(\text{BH}_2(\text{MeCN}_4)_2)_2(\text{H}_2\text{O})_4$ (**71**) was synthesized following similar procedures by the thermolysis of $\text{Ca}(\text{BH}_4)_2(\text{THF})_2$ with 4.4 equivalents

5-methyl-1H-tetrazole (eq 29). Complex **71** absorbed water from ambient air after isolation. The number of aqua ligands was determined based on X-ray diffractive study of a single crystal of **71** obtained as described below. Treatment of strontium and barium iodides with two equivalents of **70** afforded the corresponding complexes $M(\text{BH}_2(\text{MeCN}_4)_2)(\text{H}_2\text{O})_5$ ($M = \text{Sr}$, **72**; Ba , **73**) in 67 and 72% yields, respectively (eq 30). Since **72** and **73** are insoluble in THF, whereas the side product, lithium iodide is fairly soluble, the products could be purified by washing with copious amount of THF. Complexes **70-73** are soluble in water and methanol, but insoluble in aprotic organic solvents. The structural assignments and compositions of **70-73** were established by spectral and analytical techniques. Crystals of **70-73** were grown by slow evaporation of methanol/water solutions and they were also used for elemental analyses. Single crystal structures of **71-73** were obtained. Despite several attempts in crystallizing **70**, no high quality single crystals could be grown for X-ray diffraction studies.





The NMR spectra were obtained using D₂O as the solvent, and they were similar for **70-73**. ¹H NMR spectra showed the expected broad resonances around δ 3.50 for the BH₂ units in the bis(5-methyltetrazolyl)borate ligands, along with the singlet resonances at δ 2.30 for the methyl group hydrogen atoms. The ¹³C{¹H} NMR spectra exhibited resonances between 157.09 and 157.15 ppm for the tetrazolyl ring carbon atoms, and between 8.91 and 8.98 ppm for the methyl group carbon atoms. The ¹¹B NMR showed broad singlet resonances between -15.02 and -15.19 ppm for the BH₂ boron atoms. These resonances suggest very similar solution structures that probably involve solvated, separated metal and bis(5-methyltetrazolyl)borate ions. The infrared spectra were also similar for **70-73**, and exhibited absorptions attributable to the tetrazolyl moieties and the typical BH₂ stretching frequencies between 2460 and 2488 cm⁻¹. In addition, **71-73** showed broad absorptions at

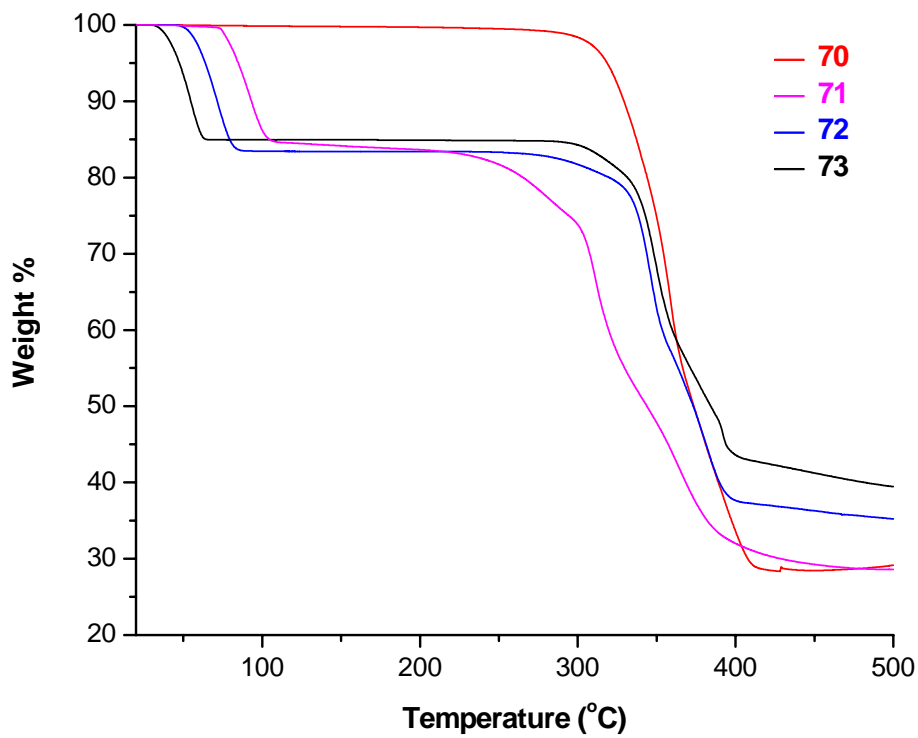
3367-3394 cm^{-1} and 1643-1667 cm^{-1} , which are assigned to the stretching and bending vibrations of the water ligands.

4.2.2 Thermal and Energetic Properties. Complexes **70-73** decomposed with color change before melting, and no melting was observed up to 400 °C. The thermal decomposition behavior of **70-73** was examined by TGA experiments under a nitrogen atmosphere between 20 and 500 °C with a heating rate of 5 °C/min (Figure 11). There was no evidence of detonation during the melting point and TGA experiments. The onset thermal decomposition of **70** started at ~315 °C and 71.5% weight was lost upon reaching 450 °C, which corresponds to ~4.3 equiv. of N_2 . Two-step weight loss events were observed for **71-73**. The first weight loss events exhibited 5.8%, 6.6%, and 5.1% weight losses by 110 °C, 90 °C, and 70 °C for **71**, **72**, and **73**, respectively. The weight losses are associated with 4, 5, and 5 equiv. of H_2O . In the second weight loss event, **71** decomposed starting at ~230 °C and lost another 54.9% of weight by 450 °C, which corresponds to ~9.2 equiv. of N_2 . The weight losses of **72** and **73** from the onsets of ~300 °C to 450 °C were 47.1% and 47.7%, respectively, and they correspond to ~9 equiv. of N_2 .

Small samples of **70-73** (~5 mg) were struck hard with a hammer on an iron anvil to check the shock sensitivity, but no detonation occurred during these processes. Sensitivity toward electrostatic discharge of **70-73** was checked by passing sparks with a Tesla coil through ~5 mg samples, and there was no detonation or deflagration observed during these procedures. Small samples of **70-73** (~10 mg) were placed on a spatula tip and burned in a

Bunsen burner flame. The complexes deflagrated with some noise and bright colored flames (Li: red, Ca: orange red, Sr: red, Ba: green). These experiments suggest that **70-73** contain significant amounts of energy and are good candidates for secondary energetic materials and propellents.

Figure 11. TGA traces for **70-73** from 20 to 500 °C at 5 min/°C.



4.2.3 Structural Aspects. X-ray crystal structure investigations were carried out for **71-73** to explore the geometries about the metal centers and the bonding modes of the bis(5-methyltetrazolyl)borate ligands. Experimental crystallographic data for **71-73** are summarized in Table 9, selected bond lengths and angles are listed in Tables 10-12, while perspective views are given in Figures 12-15.

Table 9. Crystal data and data collection parameters for **71-73**.

	71	72	73
Empirical formula	C ₈ H ₂₄ N ₁₆ B ₂ CaO ₄	C ₈ H ₂₆ N ₁₆ B ₂ O ₅ Sr	C ₈ H ₂₆ N ₁₆ B ₂ BaO ₅
FW	470.13	535.69	585.41
Space group	P2 ₁	Pbcn	Pbcn
a (Å)	6.7329(2)	16.7951(5)	16.7633(5)
b (Å)	17.7042(6)	9.3010(3)	9.5225(3)
c (Å)	9.2944(3)	29.2384(9)	29.8908(8)
β (°)	99.549(2)	90	90
V (Å ³)	1092.55(6)	4567.4(2)	4771.4(2)
Z	2	8	8
T (K)	100(2)	100(2)	100(2)
λ (Å)	0.71073	0.71073	0.71073
ρ _{calc} (g cm ⁻³)	1.429	1.558	1.630
μ (mm ⁻¹)	0.339	2.417	1.718
R(F) (%)	3.50	2.99	2.00
R _w (F) (%)	8.12	5.78	4.85

$$R(F) = \frac{\sum ||F_o| - |F_c||}{\sum |F_o|}, R_w(F)^2 = \frac{[\sum w(F_o^2 - F_c^2)^2]}{\sum w(F_o^2)^2}]^{1/2} \text{ for } I > 2\sigma(I).$$

A perspective view of **71** is shown in Figure 12. Each calcium ion is situated at the center of a distorted octahedron, and coordinated to two bis(5-methyltetrazolyl)borate ligands and four aqua ligands. The bis(5-methyltetrazolyl)borate ligands are coordinated to the calcium center in a κ^1 fashion through the N⁴ atoms, which are *trans* within the octahedron. The four oxygen atoms in the aqua ligands lie in an approximate plane containing the calcium ion. The Ca-N distances are 2.4397(16) and 2.4706(14) Å, while the N-Ca-N angle is 167.48(5)°. The N-Ca-O angles range between 82.52(5) and 102.47(5)°. The Ca-O distances are between 2.3050(12) and 2.4044(13) Å. The *cis* O-Ca-O angles are between 85.15(5) and 95.02(5)°, and the *trans* O-Ca-O angles are 171.05(5) and 177.37(5)°, respectively. In the solid state, **71** is composed of discrete molecules, linked by O-H \cdots N hydrogen bonds formed between the aqua ligand hydrogen atoms and the tetrazolyl group N², N³ and N⁴ nitrogen atoms that have no B-N or Ca-N bonds. The crystal lattice is further stabilized by O-H \cdots O hydrogen bonds formed between the aqua ligands. In the O-H \cdots N hydrogen bonds, the O-H distances are between 0.768 and 1.019 Å, the H-N distances range from 1.844 to 2.133 Å, the O \cdots N separations range between 2.760 and 2.927 Å, and the O-H-N angles are from 157.45 to 177.02°.

A perspective view of **72** is shown in Figure 13. The strontium ions are nine coordinate, and each has bonds to three terminal aqua ligands, four bridging μ_2 -aqua ligands, and two κ^1 -N³-bis(5-methyltetrazolyl)borate ligands. The Sr-O distances with the terminal water ligands range from 2.5466(9) to 2.5947(9) Å, the Sr-O distances with the bridging

water ligands are a little longer in the range of 2.7172(8)-2.7583(8) Å, while the Sr-N bonds are longer than the Sr-O bonds having distances of 2.7827(9) and 2.7889(10) Å. The two bis(5-methyltetrazolyl)borate ligands are not exactly opposite to each other, since the N(3)-Sr(1)-N(11) angle is 137.71(3)°. In the ligand, the N-B-N angle is 107.3° which is similar to that found in other complexes containing bis(5-methyltetrazolyl)borate ligands. The adjacent strontium ions are connected via bridging water molecules resulting in a one dimensional chain which is almost linear with a Sr-Sr-Sr angle of 173.898(4)°. Along the chain, two neighboring strontium ions together with the two oxygen atoms of the bridging aqua ligands form a four-membered ring binuclear [Sr₂O₂] unit with a Sr-Sr distance of 4.65710(15) Å, and the binuclear units are linked end to end with a common strontium ion leading to an inorganic skeleton chain of (SrO₂)_n as can be seen in Figure 14. The 1-D infinite chains are parallel to each other and further linked through O-H...N hydrogen bonds formed by hydrogen atoms of the aqua ligands and the nitrogen atoms which are not connected with a boron atom or a strontium ion.

Complexes **73** and **72** are isostructural and have similar bonding interactions. A perspective view of **73** is shown in Figure 15. The barium ions are nine coordinate and they have Ba-O bonds of 2.7215(9)-2.7959(9) Å with the end-on aqua ligands, Ba-O bonds of 2.8321(8)-2.8772(8) Å with the bridging aqua ligands, and Ba-N bonds of 2.9266(9) and 2.9369(10) Å with the κ¹-N³-bis(5-methyltetrazolyl)borate ligands. The N(11)-Ba(1)-N(3) angle is 137.96(3)° and the N-B-N angle in the ligands is 107.6°. The linear chain is made

from an inorganic skeleton of $(\text{BaO}_2)_n$ with a Ba-Ba distance of 4.77062(15) Å and a Ba-Ba-Ba angle of 172.817(3)°. The chains are also parallel to each other and further linked through O-H...N hydrogen bonds resulting in a three dimensional polymeric structure.

Figure 12. Perspective view of **71** with thermal ellipsoids at the 50% probability level.

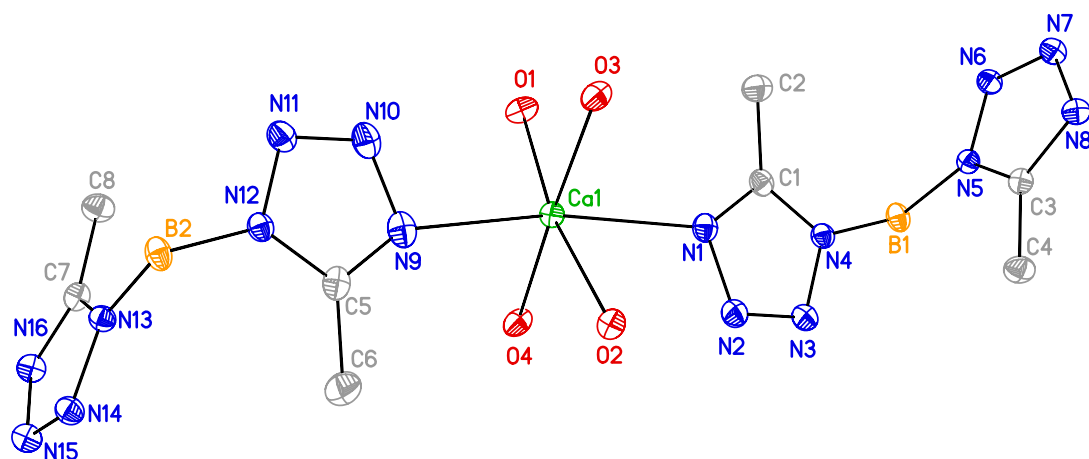


Table 10. Selected bond lengths (Å) and angles (°) for **71**.

Ca(1)-N(1)	2.4706(14)	N(4)-B(1)-N(5)	107.08(14)
Ca(1)-N(9)	2.4397(16)	N(2)-N(1)-Ca(1)	112.00(10)
Ca(1)-O(1)	2.3050(12)	C(1)-N(1)-Ca(1)	141.05(11)
Ca(1)-O(2)	2.4044(13)	N(3)-N(4)-B(1)	122.34(14)
Ca(1)-O(3)	2.3458(13)	C(1)-N(4)-B(1)	130.55(14)
Ca(1)-O(4)	2.3412(13)	N(6)-N(5)-B(1)	123.34(15)
N(4)-B(1)	1.559(2)	C(3)-N(5)-B(1)	129.20(15)
B(1)-N(5)	1.575(3)		
N(1)-C(1)	1.322(2)		
N(4)-C(1)	1.339(2)		
N(1)-N(2)	1.3672(19)		
N(2)-N(3)	1.294(2)		
N(3)-N(4)	1.3626(19)		
N(5)-C(3)	1.338(3)		
N(8)-C(3)	1.332(2)		
N(5)-N(6)	1.3468(19)		
N(6)-N(7)	1.297(2)		
N(7)-N(8)	1.354(2)		

Figure 13. Perspective view of **72** with thermal ellipsoids at the 50% probability level.

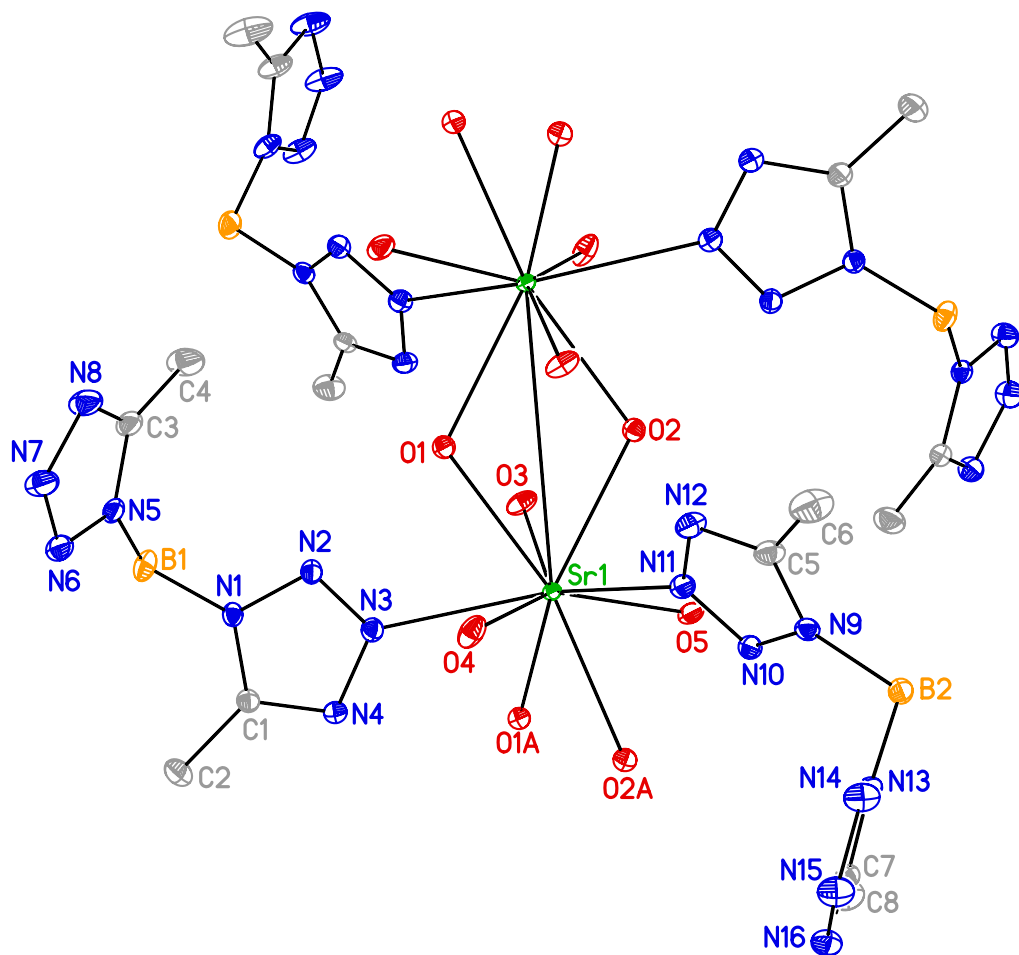


Table 11. Selected bond lengths (Å) and angles (°) for **72**.

Sr(1)-N(3)	2.7827(9)	N(5)-N(6)	1.3469(14)
Sr(1)-N(11)	2.7889(10)	N(6)-N(7)	1.2988(15)
Sr(1)-O(1)	2.7453(8)	N(7)-N(8)	1.3561(14)
Sr(1)-O(1)#1	2.7186(8)		
Sr(1)-O(2)	2.7172(8)	Sr(1)-Sr(1)#2	4.65710(15)
Sr(1)-O(2)#1	2.7583(8)	N(3)-Sr(1)-N(11)	137.71(3)
Sr(1)-O(3)	2.5466(9)	N(2)-N(3)-Sr(1)	125.33(7)
Sr(1)-O(4)	2.5659(9)	N(4)-N(3)-Sr(1)	123.76(7)
Sr(1)-O(5)	2.5947(9)	Sr(1)#2-Sr(1)-Sr(1)#1	173.898(4)
N(1)-B(1)	1.5589(17)	Sr(1)#2-O(1)-Sr(1)	116.94(3)
B(1)-N(5)	1.5621(17)	Sr(1)-O(2)-Sr(1)#2	116.54(3)
N(1)-C(1)	1.3438(14)	O(2)-Sr(1)-O(1)	63.36(2)
N(4)-C(1)	1.3285(14)	N(3)-Sr(1)-Sr(1)#2	98.20(2)
N(1)-N(2)	1.3502(13)	N(11)-Sr(1)-Sr(1)#2	83.76(2)
N(2)-N(3)	1.2965(13)	N(1)-B(1)-N(5)	107.38(10)
N(3)-N(4)	1.3622(13)	N(2)-N(1)-B(1)	121.90(9)
N(5)-C(3)	1.3453(15)	N(6)-N(5)-B(1)	121.47(10)
N(8)-C(3)	1.3266(16)		

Figure 14. Perspective view of the inorganic skeleton chain of $(\text{SrO}_2)_n$ in **72**.

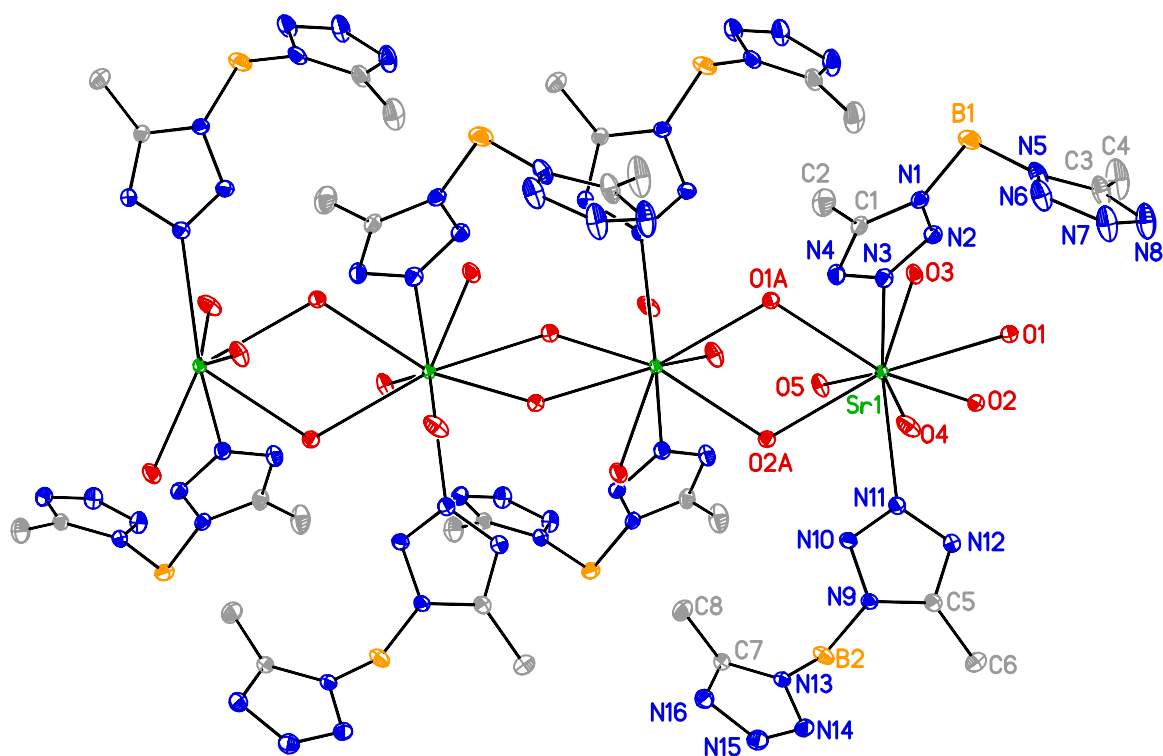


Figure 15. Perspective view of **73** with thermal ellipsoids at the 50% probability level.

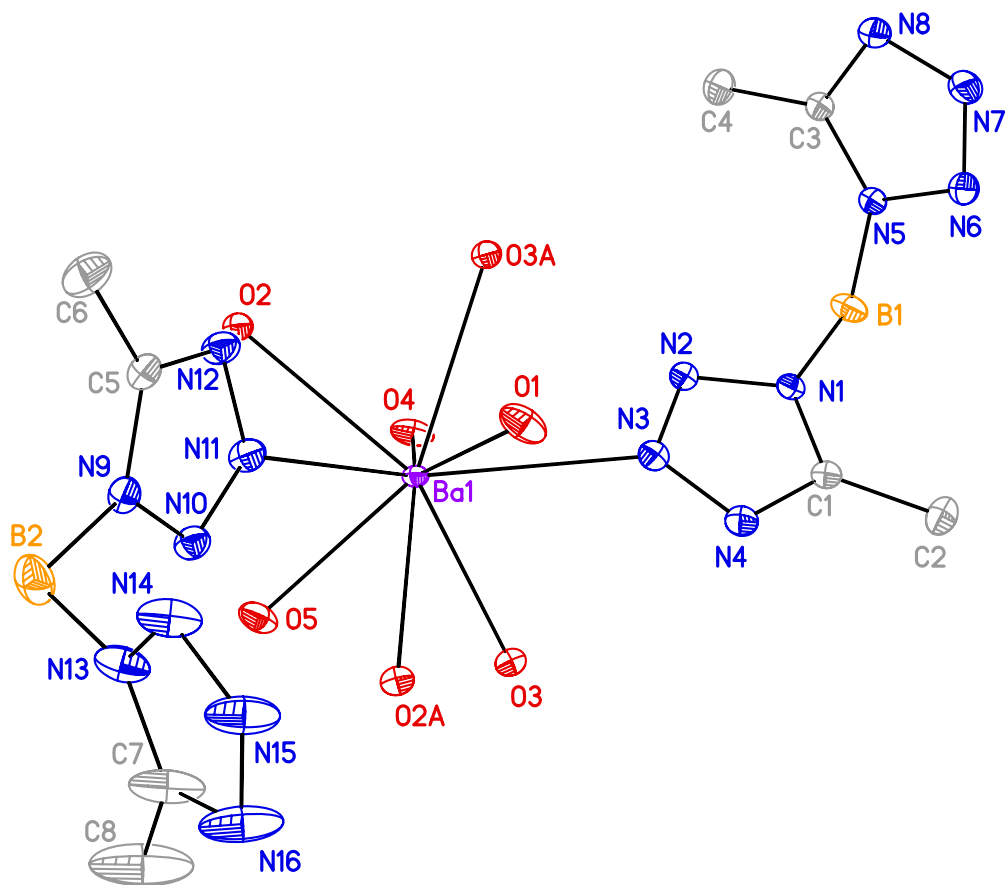


Table 12. Selected bond lengths (Å) and angles (°) for **73**.

Ba(1)-N(3)	2.9369(10)	N(5)-N(6)	1.3470(14)
Ba(1)-N(11)	2.9266(9)	N(6)-N(7)	1.2973(15)
Ba(1)-O(1)	2.7321(10)	N(7)-N(8)	1.3524(14)
Ba(1)-O(2)	2.8416(8)		
Ba(1)-O(2)#1	2.8750(8)	Ba(1)-Ba(1)#2	4.77062(15)
Ba(1)-O(3)	2.8321(8)	N(11)-Ba(1)-N(3)	137.96(3)
Ba(1)-O(3)#2	2.8772(8)	N(2)-N(3)-Ba(1)	118.18(7)
Ba(1)-O(4)	2.7959(9)	N(4)-N(3)-Ba(1)	131.27(7)
Ba(1)-O(5)	2.7215(9)	Ba(1)#2-Ba(1)-Ba(1)#1	172.817(3)
B(1)-N(1)	1.5633(16)	Ba(1)-O(2)-Ba(1)#2	113.13(3)
B(1)-N(5)	1.5649(16)	Ba(1)-O(3)-Ba(1)#1	113.35(3)
N(1)-C(1)	1.3439(14)	O(2)-Ba(1)-O(3)#2	66.68(2)
N(4)-C(1)	1.3308(15)	N(3)-Ba(1)-Ba(1)#2	98.87(2)
N(1)-N(2)	1.3495(13)	N(11)-Ba(1)-Ba(1)#2	84.552(19)
N(2)-N(3)	1.2987(13)	N(1)-B(1)-N(5)	107.60(9)
N(3)-N(4)	1.3572(14)	N(2)-N(1)-B(1)	120.92(9)
N(5)-C(3)	1.3458(14)	N(6)-N(5)-B(1)	120.67(10)
N(8)-C(3)	1.3308(15)		

4.3 Discussion

Initially, the heavier group 2 metal bis(5-methyltetrazolyl)borate complexes **71-73** were synthesized by salt metathesis of potassium bis(5-methyltetrazolyl)borate (**63**) with the specific group 2 metal chlorides. However, the desired products could not be separated from the side product KCl, because the products and KCl have similar solubilities in water and a range of other solvents. The products and KCl crystallized out at the same time from slow evaporation of methanol/water solutions. Consequently, the lithium complex **70** was used to react with the group 2 metal iodides, since **70** is soluble in THF and can be removed by washing the crude products with THF. The isolation of the strontium and barium complexes **72** and **73** was successful by this method. However, the calcium complex **71** could not be made through similar procedures because CaI_2 is not stable under ambient conditions used in the metathesis. CaI_2 decomposes slowly in the air due to the reaction with CO_2 and O_2 forming CaCO_3 and I_2 .⁹² Therefore, **71** was made by solid state thermal reaction of $\text{Ca}(\text{BH}_4)_2(\text{THF})_2$ with 5-methyltetrazole.

Other potassium bis(tetrazolyl)borate complexes **39**, **64**, and **65** were also treated with heavier group 2 metal salts to make the corresponding metal complexes. No alkaline earth metal complexes containing the bis(5-dimethylaminotetrazolyl)borate or bis(5-diisopropylaminotetrazolyl)borate ligands could be isolated after the reactions using **64** or **65** as the reactants, respectively. The metathesis of potassium bis(5-H-tetrazolyl)borate complex **39** and group 2 metal salts should proceed similarly to that using potassium

bis(5-methyltetrazolyl)borate complex **63**, since the two ligands both have small substituents on the ring core carbon atoms of the tetrazolyl groups. Since the crystallization of the group 2 metal bis(tetrazolyl)borate products is very slow and usually takes more than a month, the synthesis and characterization of group 2 bis(5-H-tetrazolyl)borate complexes were not explored in detail, but they should have similar structural features to **71-73**.

In the solid state, **71-73** adopt two different types of structures depending on the size of the metal centers. With a relatively smaller size, the calcium ions coordinate to the bis(tetrazolyl)borate ligands via the N^4 nitrogen atoms of the tetrazolyl groups, and **71** is composed of discrete molecules linked by hydrogen bonds. By contrast, the larger strontium and barium ions coordinate via the N^3 atoms of the tetrazolyl groups, and the isostructural complexes **72** and **73** consist of linear chains linked by bridging water ligands. The chains are further linked to each other by extensive hydrogen bonds.

Each bis(5-methyltetrazolyl)borate ligand has 8 nitrogen atoms and can form 4 N_2 molecules upon decomposition. The lithium complex **70** has one bis(5-methyltetrazolyl)borate ligand per formula unit, but the weight loss of **70** is associated with more than 4 equiv. of N_2 in the TGA experiments. Additionally, **71-73** have two bis(5-methyltetrazolyl)borate ligands per formula unit and should liberate 8 equiv. of N_2 , but the weight losses correspond to ~ 9 equiv. of N_2 . These TGA data suggest that some other gases must have formed during the thermal decomposition of the ligands. Since the bis(5-methyltetrazolyl)borate ligand contains methyl substituents, it is likely that the methyl

groups are transformed to CH_4 and released as a gaseous component in the decomposition products.

Complexes **70-73** did not detonate or explode in the hammer, friction, and electrostatic tests, which suggest that they are not primary energetic materials. However, **71-73** burned rapidly in the flame tests and the deflagration was more violent than that of the potassium bis(5-methyltetrazolyl)borate. The more violent deflagration is probably caused by more nitrogen atoms per molecule of the complexes resulting from two bis(5-methyltetrazolyl)borate ligands per metal ion. Violent deflagration was also experienced when burning the lithium complex **70**. Although the lithium complex contains only one ligand per metal ion, its anhydrous nature and high nitrogen content due to the lower molecular weight of lithium atom should definitely help to make the complex more energetic. The lithium, calcium, and strontium complexes give off red flame colors, while the barium complex emits green light upon burning. Therefore, **70-73** are also potential color generating agents in pyrotechnic mixtures.

4.4 Conclusions

Lithium and heavier group 2 metal bis(5-methyltetrazolyl)borate complexes **70-73** have been prepared. Complexes **71-73** were structurally characterized. Crystals of **72** and **73** contain highly ordered inorganic M-O (M = Sr, Ba) bonds. The new complexes are insensitive toward impact, friction and electrostatic discharge, but they deflagrate more violently in flame tests compared with the potassium bis(5-methyltetrazolyl)borate.

Complexes **70-73** have thermal decomposition temperatures between 230 °C and 315 °C as indicated by TGA; they have potential use as secondary energetic materials and colorants in pyrotechnic compositions.

4.5 Experimental Section

General Considerations. All starting materials and products were air stable and reactions were performed under ambient conditions unless stated otherwise. 5-Methyl-1H-tetrazole and $\text{Ca}(\text{BH}_4)(\text{THF})_2$ were purchased from Aldrich Chemical Company and used without further purification. SrI_2 was purchased from Alfa Aesar and used as received. $\text{BaI}_2(\text{THF})_3$ was prepared according to literature procedures.^{62b} ^1H and $^{13}\text{C}\{^1\text{H}\}$ NMR spectra were obtained at 500 and 125 MHz Varian instrument, respectively, in deuterium oxide. Infrared spectra were obtained using Nujol as the medium. Elemental analyses were performed by Midwest Microlab, Indianapolis, IN. It was necessary to add V_2O_5 as a combustion enhancing agent to obtain acceptable carbon values. Melting points were obtained on a Thermo Scientific Mel-Temp 3.0 melting point apparatus and are uncorrected. TGA was conducted on a Perkin-Elmer Pyris 1 TGA system between 20 and 500 °C, using nitrogen as the flow gas with a heating rate of 5 °C/min.

$\text{Li}(\text{BH}_2(\text{MeCN})_2)$ (70). A 100-mL Schlenk flask was charged with lithium borohydride (0.218 g, 10.0 mmol) and 2.2 equivalents of 5-methyl-1H-tetrazole (1.851 g, 22.00 mmol) as fine powders, a stir bar, and was equipped with a reflux condenser. The

flask was purged with argon to avoid reaction of lithium borohydride with the moisture in ambient air. The solid mixture was then heated with stirring to 120 °C, until the gas evolution ceased. The resultant white solid was washed with 2 × 30 mL portions of THF to remove the unreacted methyl tetrazole, and the desired product was collected by filtration on a sintered glass funnel. Complex **70** was thus obtained in 88% yield as a colorless solid. Mp > 400 °C (decompose at ~315 °C); IR (Nujol, cm⁻¹): $\tilde{\nu}$ = 2488 (s), 2471 (s), 2390 (w), 2366 (w), 2251 (w), 2215 (w), 1738 (w), 1576 (w), 1513 (s), 1405 (s), 1290 (s), 1258 (m), 1202 (s), 1169 (s), 1159 (s), 1137 (s), 1121 (s), 1051 (m), 1040 (m), 1012 (w), 998 (m), 883 (w), 869 (s), 799 (m), 752 (s), 702 (s), 623 (s); ¹H NMR (D₂O, 23 °C): δ = 3.49 (m, br, 2H, BH₂), 2.31 (s, 6H, CH₃CN₄); ¹³C{¹H} NMR (D₂O, 23 °C): δ = 157.14 (s, CH₃CN₄), 8.91 (s, CH₃CN₄); ¹¹B NMR (D₂O, 23 °C): δ = -15.08 (s, br, BH₂); elemental analysis calculated for C₄H₈N₈BLi (%): C 25.84, H 4.34, N 60.27; found: C 25.82, H 4.43, N 60.06.

Ca(BH₂(MeCN₄)₂)₂(H₂O)₄ (71). In a fashion similar to the preparation of **70**, treatment of Ca(BH₄)₂(THF)₂ (0.500 g, 2.34 mmol) and 4.4 equivalents of 5-methyl-1H-tetrazole (0.864 g, 10.3 mmol) afforded **71** in 85% as a colorless solid. Mp > 400 °C (decompose at ~230 °C); IR (Nujol, cm⁻¹): $\tilde{\nu}$ = 3367 (vs), 2479 (s), 2460 (s), 2326 (w), 2271 (w), 1667 (s), 1504 (s), 1291 (s), 1277 (w), 1200 (s), 1170 (m), 1142 (s), 1115 (s), 1050 (m), 1022 (w), 997 (m), 968 (w), 890 (w), 862 (w), 752 (m), 711 (s), 697 (m), 628 (s); ¹H NMR (D₂O, 23 °C): δ = 3.34 (m, br, 4H, BH₂), 2.21 (s, 12H, CH₃CN₄); ¹³C{¹H} NMR (D₂O, 23 °C): δ = 156.95 (s, CH₃CN₄), 8.90 (s, CH₃CN₄); ¹¹B NMR (D₂O, 23 °C): δ = -15.06 (s, br,

BH_2); elemental analysis calculated for $C_8H_{24}N_{16}B_2CaO_4$ (%): C 20.44, H 5.15, N 47.67; found: C 20.26, N 5.00, N 47.26.

Sr(BH₂(MeCN₄)₂)₂(H₂O)₅ (72). A 100-mL Schlenk flask was charged with strontium iodide (0.171 g, 0.500 mmol), **70** (0.186 g, 1.00 mmol), a stir bar, and distilled water (10mL). The resultant mixture was stirred for 18 h at ambient temperature. The reaction mixture was then filtered through a 2-cm pad of Celite on a coarse glass frit. Removal of the volatile components under reduced pressure followed by washing with 2 × 30 mL portions of THF afforded **72** in 67% yield as a colorless solid. Mp > 400 °C (decompose at ~300 °C); IR (Nujol, cm⁻¹): $\tilde{\nu}$ = 3368 (vs), 2481 (s), 2460 (s), 2322 (w), 2266 (w), 1643 (m), 1504 (s), 1416 (w), 1395 (s), 1305 (w), 1287(m), 1251 (w), 1209 (m), 1198 (s), 1166 (s), 1141 (s), 1113 (s), 1050 (m), 1024 (m), 999 (m), 967 (w), 892 (w), 875 (w), 861 (m), 770 (w), 751 (m), 708 (m), 697 (s), 626 (s); ¹H NMR (D₂O, 23 °C): δ = 3.47 (m, br, 4H, BH_2), 2.31 (s, 12H, CH_3CN_4); ¹³C{¹H} NMR (D₂O, 23 °C): δ = 157.14 (s, CH_3CN_4), 8.97 (s, CH_3CN_4); ¹¹B NMR (D₂O, 23 °C): δ = -15.19 (s, br, BH_2); elemental analysis calculated for $C_8H_{26}N_{16}B_2O_5Sr$ (%): C 17.94, H 4.89, N 41.84; found: C 18.02, N 4.89, N 41.82.

Ba(BH₂(MeCN₄)₂)₂(H₂O)₅ (73). In a fashion similar to the preparation of **73**, treatment of BaI₂(THF)₃ (0.304 g, 0.500 mmol) with **70** (0.186 g, 1.00 mmol) afforded **73** in 70% yield as a colorless solid. Mp > 400 °C (decompose at ~300 °C); IR (Nujol, cm⁻¹): $\tilde{\nu}$ = 3394 (vs), 2486 (s), 2463 (s), 2322 (w), 2252 (w), 1648 (s), 1507 (s), 1304 (w), 1281 (s), 1204 (s), 1164 (s), 1132 (s), 1113 (s), 1046 (w), 998 (m), 968 (w), 882 (w), 868 (m), 838 (w),

752 (m), 708 (m), 700 (s), 625 (s); ^1H NMR (D_2O , 23 °C): δ = 3.46 (m, br, 4H, BH_2), 2.30 (s, 12H, CH_3CN_4); $^{13}\text{C}\{^1\text{H}\}$ NMR (D_2O , 23 °C): δ = 157.09 (s, CH_3CN_4), 8.94 (s, CH_3CN_4); ^{11}B NMR (D_2O , 23 °C): δ = -15.02 (s, br, BH_2); elemental analysis calculated for $\text{C}_8\text{H}_{26}\text{N}_{16}\text{B}_2\text{BaO}_5$ (%): C 16.42, H 4.48, N 38.29; found: C 16.68, N 4.33, N 38.09.

CHAPTER 5

Synthesis and Characterization of Sodium Cyano(tetrazolyl)borate Complexes: Attempted Reactions for the Preparation of Tris(tetrazolyl)borate Ligands with Borohydride Derivatives Other Than KBH_4

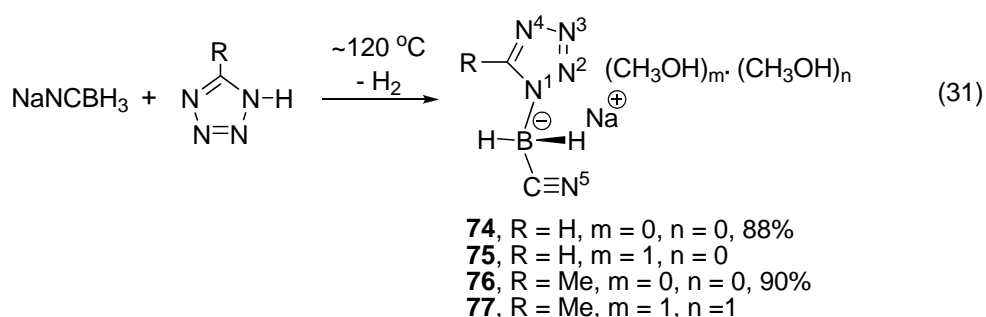
5.1 Introduction

Since the synthesis of tris(tetrazolyl)borate ligands by thermolysis of KBH_4 with a range of tetrazoles failed, some other borohydrides were used to explore the formation of this unique type of ligand. Sodium cyanoborohydride and lithium methylborohydride were treated with three equivalents of tetrazoles at high temperatures to examine whether the tris(tetrazolyl)borate ligands would form under these conditions. However, despite many attempted reactions, only one of the protons on the boron atom was replaced by one tetrazole, and no further substitution was observed. This chapter describes the preparation and characterization of a series of sodium cyano(tetrazolyl)borate complexes. Reactions of lithium methylborohydride with tetrazoles will also be discussed briefly. The sodium cyano(tetrazolyl)borate compounds are potential energetic materials due to their high nitrogen contents.

5.2 Results

5.2.1 Synthetic Aspects. Complexes **74-77** were prepared by heating a solid mixture of NaNCBH_3 and one equivalent of 1H-tetrazole (**74** and **75**) or 5-methyl-1H-tetrazole (**76** and

77) at 120 °C (equation 31), and followed by washing with sufficient Et₂O to remove any unreacted tetrazole. Complexes **74-77** are soluble in water, methanol, acetone, and THF, but are not soluble in Et₂O or hexane. Colorless crystals of **74** and **76** were obtained from concentrated methanol solutions and they do not contain methanol ligands. The crystals were suitable for X-ray diffraction studies and elemental analyses. Complexes **75** and **77** were crystallized by slow evaporation of dilute methanol solutions at ambient conditions and methanol ligands or solvates were included in these crystals. Crystals of **75** and **77** were suitable for X-ray structural determinations, but could not be used to get acceptable elemental analyses since they lose the crystallization methanol molecules within a few minutes at 23 °C after isolating from the solvents. Since **74** and **76** are the methanol-free forms of **75** and **77**, respectively, **75** and **77** were not subjected to elemental analyses.



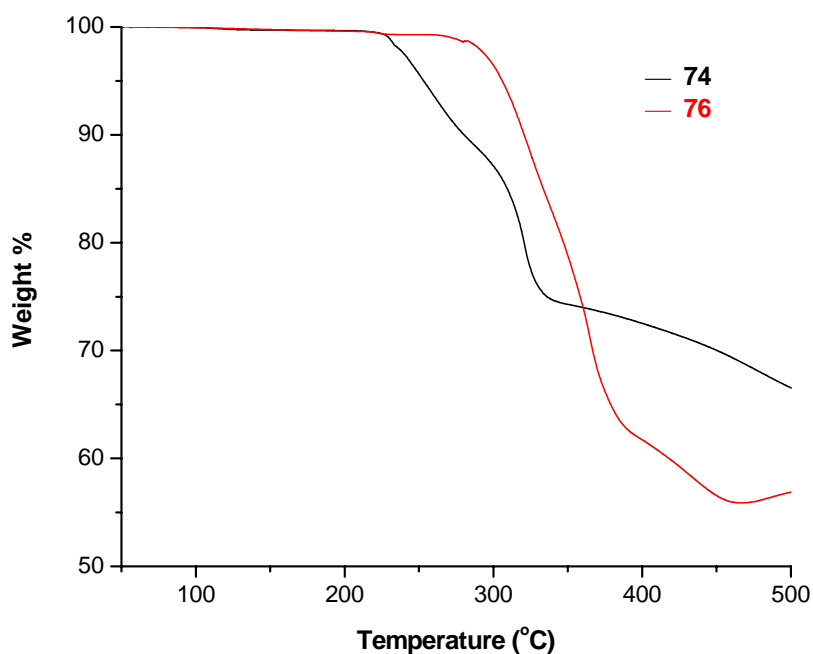
The spectroscopic properties of **75** and **77** are similar to those of **74** and **76**, respectively, except that there are some characteristics resulted from the residual crystallization methanol molecules. Therefore, the spectroscopic properties of only **74** and **76** are described herein. All of the NMR spectra were obtained using D₂O as the solvent. ¹H NMR spectra showed the expected broad quartets at δ 2.47 and 2.35 for the BH₂ groups in

the cyano(tetrazolyl)borate ligands for **74** and **76**, respectively. In **74**, the proton on the ring core carbon atom of the tetrazolyl group appeared as a singlet at δ 8.61, while in **76** the methyl group resonated as a singlet at δ 2.29. The $^{13}\text{C}\{^1\text{H}\}$ NMR spectrum of **74** exhibited resonance at 148.12 ppm for the carbon atom of the tetrazolyl ring, and 136.78 ppm for the carbon atom of the cyano group. In **76**, the resonances corresponding to the carbon atoms of the tetrazolyl ring and the cyano group appeared at 156.88 ppm and 137.10 ppm, respectively, and the methyl group showed a resonance at 8.93 ppm in the $^{13}\text{C}\{^1\text{H}\}$ NMR spectra. The ^{11}B NMR exhibited triplet resonances at -26.73 ppm and -24.99 ppm for the BH_2 groups in **74** and **76**, respectively, with coupling constants of $^1J_{\text{B-H}} \approx 100$ Hz. The infrared spectra showed the characteristic BH_2 stretching frequencies between 2377 and 2425 cm^{-1} for both **74** and **76**, and the cyano group absorptions at 2215 and 2223 cm^{-1} for **74** and **76**, respectively.

5.2.2 Thermal and Energetic Properties. Complexes **74-77** have similar melting points in a narrow range of 218-224 $^\circ\text{C}$. TGA experiments under a nitrogen atmosphere between 50 and 500 $^\circ\text{C}$ with a heating rate of 5 $^\circ\text{C}/\text{min}$ were carried out to investigate the thermal properties of **74** and **76** (Figure 16). Complex **74** started to decompose at ~ 230 $^\circ\text{C}$, and **76** decomposed at temperatures higher than 290 $^\circ\text{C}$. The weight losses are 33.5% and 43.1% upon reaching 500 $^\circ\text{C}$ for **74** and **76**, respectively. There was no evidence of detonation during the melting point and TGA experiments. When small samples of **74-77** were used to do the preliminary safety tests, no detonation or deflagration occurred either in the hammer

and friction tests, or when sparked with a Tesla coil. In the flame tests of **74-77** with ~10 mg samples, bright orange yellow flames were observed and the samples expanded in volume to a white foaming solid which then collapsed into ashes when the combustion completed.

Figure 16. TGA traces for **74** and **76** from 50 to 500 °C at 5 min/°C.



5.2.3 Structural Aspects. X-ray crystal structure investigations were carried out for **74-77** to explore the geometries about the metal centers and the bonding modes of the cyano(tetrazolyl)borate ligands. Crystallographic data are summarized in Table 13, selected bond lengths and angles are listed in Tables 14-17, and perspective views are given in Figures 17-21.

Table 13. Crystal data and data collection parameters for **74-77**.

	74	75	76	77
Empirical formula	C ₂ H ₃ BN ₅ Na	C ₃ H ₇ BN ₅ NaO	C ₃ H ₅ BN ₅ Na	C ₅ H ₁₃ BN ₅ NaO ₂
FW	130.89	162.94	144.92	209.00
Space group	P1 bar	P1 bar	P2 ₁ /c	P2 ₁
a (Å)	6.2412(4)	6.1842(3)	8.7157(3)	8.6642(3)
b (Å)	7.0004(5)	7.3325(3)	9.8500(4)	6.8727(3)
c (Å)	7.3424(5)	8.9119(4)	8.0688(8)	9.3972(4)
β (°)	94.186(3)	99.592(2)	104.231(2)	105.977(2)
V (Å ³)	279.07(3)	380.90(3)	671.45(4)	538.22(4)
Z	2	2	4	2
T (K)	100(2)	100(2)	100(2)	100(2)
λ (Å)	0.71073	0.71073	0.71073	0.71073
ρ _{calc} (g cm ⁻³)	1.558	1.421	1.434	1.290
μ (mm ⁻¹)	0.176	0.153	0.154	0.131
R(<i>F</i>) (%)	3.17	3.39	3.17	4.08
R _w (<i>F</i>) (%)	8.29	9.15	8.57	10.30

$$R(F) = \frac{\sum ||F_o| - |F_c||}{\sum |F_o|}, R_w(F)^2 = \left[\frac{\sum w(F_o^2 - F_c^2)^2}{\sum w(F_o^2)^2} \right]^{1/2} \text{ for } I > 2\sigma(I).$$

A perspective view of **74** is shown in Figure 17. The sodium atoms are arranged in pairs and each sodium ion is five coordinate. The two sodium ions are bridged by two cyano(tetrazolyl)borate ligands, each through the N² and N³ nitrogen atoms of the tetrazolyl group, forming a Na₂N₄ six membered ring (see numbering scheme in eq 31). The ring is almost planar and the Na-N²-N³-Na' torsion angle is 5.91(7)°. Another two cyano(tetrazolyl)borate ligands bridge between the same two sodium ions each through the nitrogen atom of the cyano group, resulting in a Na₂N₂ four membered ring with the four atoms exactly on the same plane. The above mentioned two planes are perpendicular to each other through the two sodium ions with a N^{3'}-Na-Na'-N⁵ torsion angle of 89.27°. For the two sodium ions, each one is further coordinated to a κ¹-N⁴-cyano(tetrazolyl)borate ligand. The Na-Na distance is 3.2014(6) Å, and the Na-N bond lengths range between 2.4232(8) and 2.5679(8) Å. All of the nitrogen atoms in the ligands are involved in coordination to sodium ions except the N¹ atoms which form bonds to the boron atoms. The dinuclear units are connected into a three dimensional network.

The crystal structure of **75** also contains dinuclear units of sodium ions which are bridged by the oxygen atoms of two methanol ligands (Figure 18). The geometry around each sodium ion is roughly trigonal bipyramidal and is formed by the coordination to one κ¹-N², one κ¹-N⁴, and one κ¹-N⁵ cyano(tetrazolyl)borate ligands, together with the two μ₂-O methanol ligands (see numbering scheme in eq 31). The two Na-O bonds are *cis* to each other with an O-Na-O angle of 78.86(2)°. The Na-O bond lengths are 2.3853(7) and

2.4257(7) Å, respectively, and the Na-N bond lengths range from 2.4448(8) to 2.5209(8) Å. The Na-Na distance is 3.7160(7) Å. In the ligands, the B-N bonds are to the N¹ atoms of the tetrazolyl rings. Each cyano(tetrazolyl)borate ligand is coordinated to three sodium ions through the N², N⁴, and N⁵ atoms, thus the crystal structure is a complex three dimensional network.

A perspective view of **76** is depicted in Figure 19. Similar to **74**, two sodium ions are bridged by two μ_2 -N²,N³-cyano(tetrazolyl)borate ligands. The two sodium ions and four nitrogen atoms form a Na₂N₄ hexagon, and the six atoms are approximately planar with the Na1-N2B-N3B-Na1A torsion angle of 4.48(11)°. The planes of the two interconnected tetrazolyl rings deviate from the Na₂N₄ hexagon plane by 16-20°, since the N4C-N3C-N2C-Na1A torsion angle is 164.34(6)°, and the N1B-N2B-N3B-Na1A torsion angle is -159.80(5)°. The two interconnected tetrazolyl rings are approximately parallel to each other. Each of the two sodium ions is further coordinated to another κ^1 -N⁴-cyano(tetrazolyl)borate ligand which has its tetrazolyl ring roughly perpendicular to the Na₂N₄ hexagon. The Na-N bond lengths range from 2.3663(9) to 2.5143(9) Å. The Na-Na distance is 4.0920(7) Å. In this complex, all the nitrogen atoms are coordinated to sodium atoms except the N¹ atoms which bond to the boron atoms, and the crystal structure is a three dimensional coordination polymer.

A perspective view of **77** is shown in Figure 20. The arrangement around each sodium ion is approximately octahedral with four cyano(tetrazolyl)borate ligands and two

trans methanol ligands with the O-Na-O' angle of 174.37(6)°. Each methanol ligand forms bonds to two sodium ions through their oxygen atoms. Additionally, each cyano(tetrazolyl)borate ligand forms four N-Na bonds by bridging between two sodium ions with a μ_2 -N³,N⁴ coordination mode, and further coordinating to another two sodium ions in a μ_1 -N⁵ fashion. The Na-O bond lengths are 2.4202(15) and 2.4230(15) Å, respectively, and the Na-N bond lengths are in the range of 2.4666(15)-2.5466(16) Å. The distance between two sodium ions Na-Na' is 3.44059(16) Å. In addition, the crystal lattice contains solvated methanol molecules which are stabilized through O-H...O and O-H...N hydrogen bonds as shown in Figure 21. The hydrogen bonds are formed by the interactions of the hydrogen atoms of the methanol ligands with the oxygen atoms of the methanol solvates, and the hydrogen atoms of the methanol solvates with the nitrogen atoms on the tetrazolyl groups.

Figure 17. Perspective view of **74** with thermal ellipsoids at the 50% probability level.

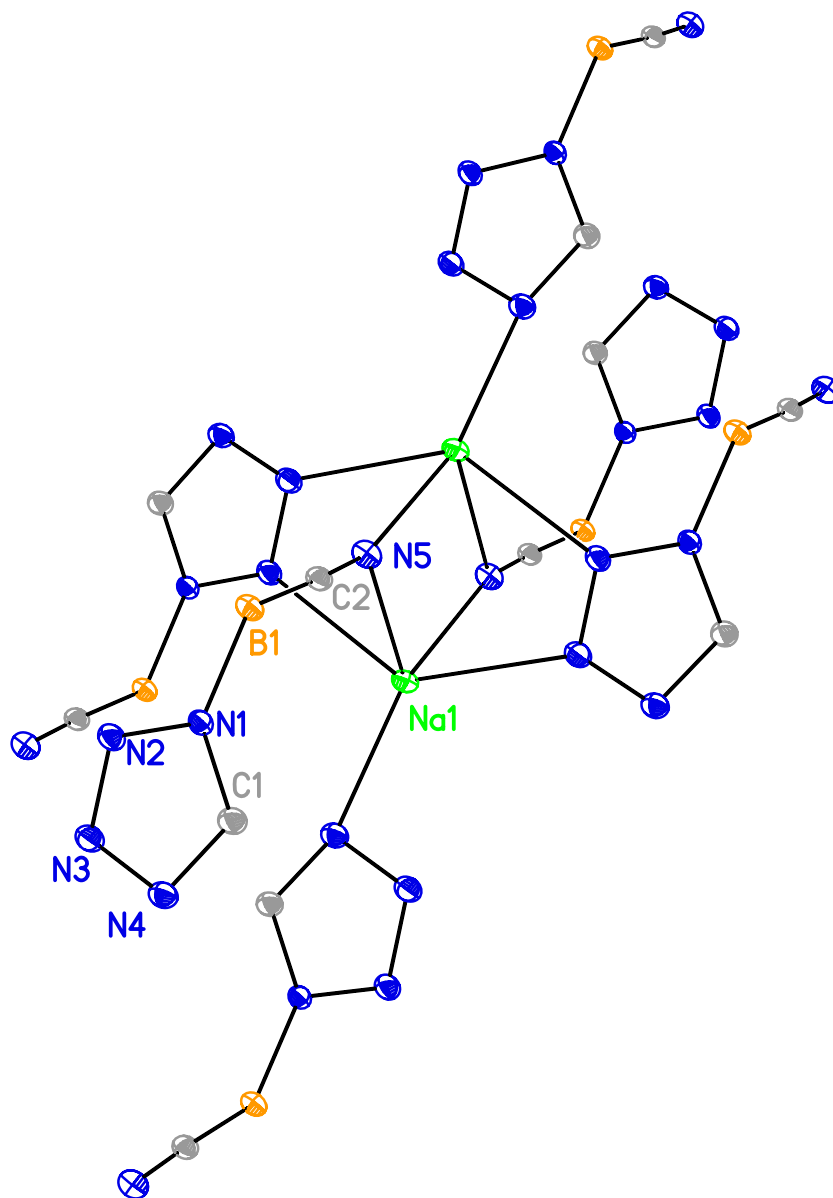


Table 14. Selected bond lengths (Å) and angles (°) for **74**.

Na(1)-N(5)	2.5318(8)	N(5)#2-Na(1)-N(5)	100.92(2)
Na(1)-N(2)#3	2.5541(8)	Na(1)#2-N(5)-Na(1)	79.08(2)
Na(1)-N(3)#4	2.5679(8)	C(2)-N(5)-Na(1)	119.59(6)
Na(1)-N(4)#1	2.4232(8)	C(2)-N(5)-Na(1)#2	161.16(6)
Na(1)-N(5)#2	2.4968(8)	C(2)-N(5)-Na(1)	119.59(6)
Na(1)-Na(1)#2	3.2014(6)	N(5)-C(2)-B(1)	177.02(8)
N(1)-B(1)	1.5592(10)	N(1)-B(1)-C(2)	109.79(6)
C(2)-B(1)	1.5930(12)	N(2)-N(1)-B(1)	121.48(6)
C(2)-N(5)	1.1510(11)	C(1)-N(1)-B(1)	131.74(7)
N(1)-C(1)	1.3354(10)		
N(4)-C(1)	1.3260(10)	Na(1)#3-N(2)-N(3)-Na(1)#6	5.91(7)
N(1)-N(2)	1.3431(9)	N(5)#2-Na(1)-N(5)-Na(1)#2	0.0
N(2)-N(3)	1.2994(9)	N(3)-Na(1)-Na(1)#1-N(5)#1	89.27
N(3)-N(4)	1.3546(10)		

Figure 18. Perspective view of 75 with thermal ellipsoids at the 50% probability level.

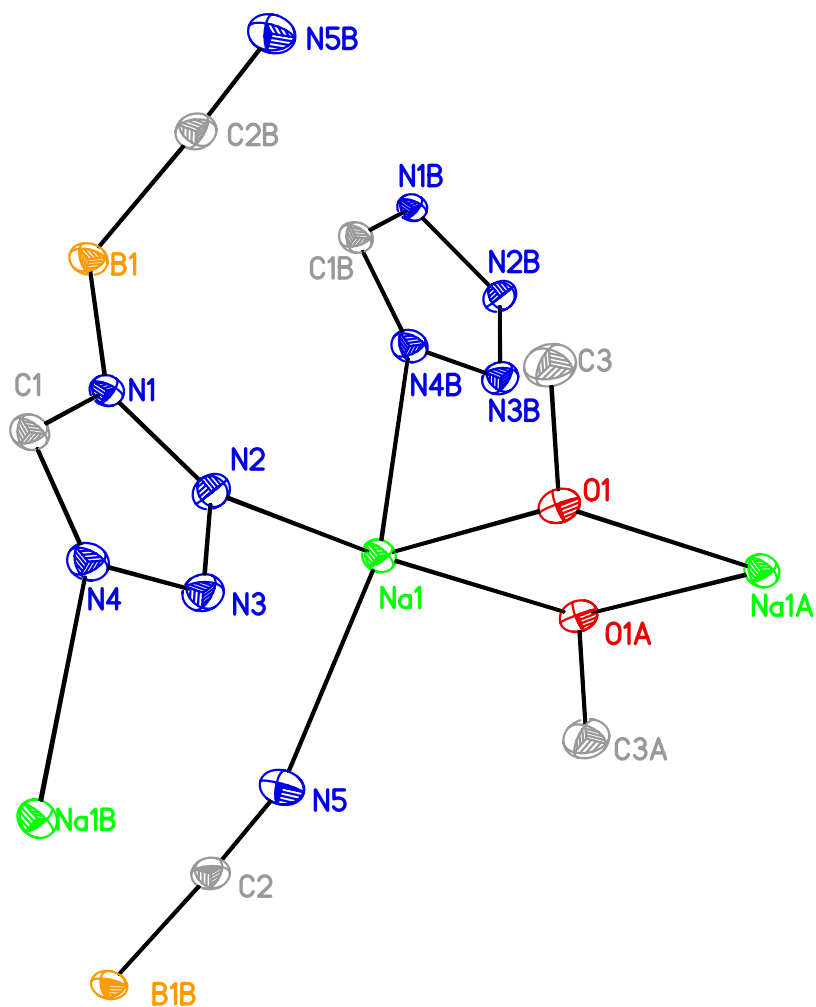


Table 15. Selected bond lengths (Å) and angles (°) for **75**.

Na(1)-N(2)	2.5044(8)	N(3)-N(2)-Na(1)	112.20(5)
Na(1)-N(5)	2.4448(8)	N(3)-N(4)-Na(1)#4	105.77(5)
Na(1)-N(4)#2	2.5209(8)	C(1)-N(4)-Na(1)#4	146.42(5)
Na(1)-O(1)	2.3853(7)	N(1)-N(2)-Na(1)	139.77(5)
Na(1)-O(1)#1	2.4257(7)	C(2)-N(5)-Na(1)	158.86(7)
Na(1)-Na(1)#1	3.7160(7)	C(3)-O(1)-Na(1)	115.20(5)
N(1)-B(1)	1.5639(11)	C(3)-O(1)-Na(1)#1	121.03(5)
B(1)-C(2)#6	1.5988(12)	Na(1)-O(1)-Na(1)#1	101.14(2)
N(5)-C(2)	1.1497(11)	N(1)-B(1)-C(2)#6	109.43(7)
N(1)-C(1)	1.3376(10)	N(2)-N(1)-B(1)	121.98(6)
N(4)-C(1)	1.3253(11)	C(1)-N(1)-B(1)	131.24(7)
N(1)-N(2)	1.3463(9)	N(5)-Na(1)-N(2)	89.33(3)
N(2)-N(3)	1.2997(10)	N(2)-Na(1)-N(4)#2	105.75(3)
N(3)-N(4)	1.3559(10)	N(5)-Na(1)-N(4)#2	144.82(3)
		O(1)-Na(1)-O(1)#1	78.86(2)
		O(1)-Na(1)-N(5)	117.36(3)
		O(1)-Na(1)-N(2)	82.62(2)
		O(1)-Na(1)-N(4)#2	96.31(2)

Figure 19. Perspective view of 76 with thermal ellipsoids at the 50% probability level.

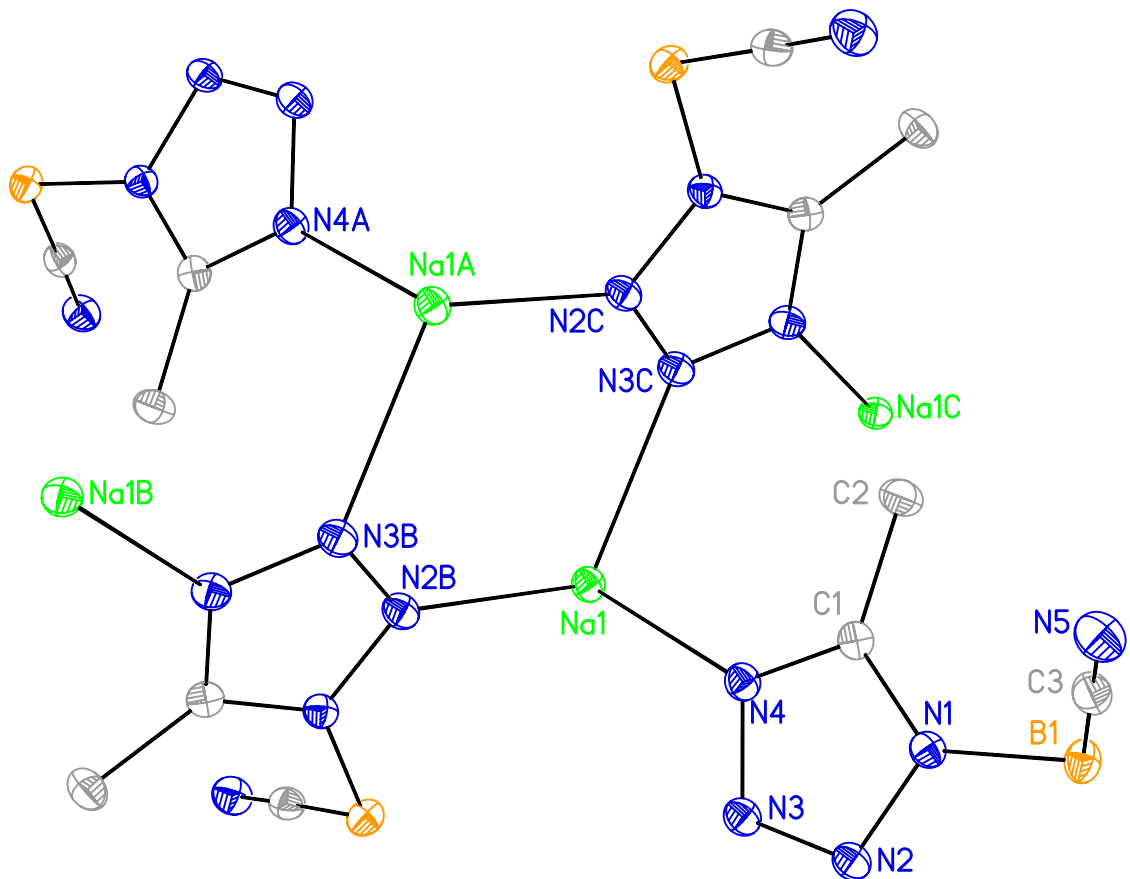


Table 16. Selected bond lengths (Å) and angles (°) for **76**.

Na(1)-N(4)	2.4645(9)	N(1)-B(1)-C(3)	109.06(7)
Na(1)-N(2)#3	2.5143(9)	N(5)-C(3)-B(1)	178.45(10)
Na(1)-N(3)#2	2.4742(9)	N(2)-N(1)-B(1)	122.37(7)
Na(1)-N(5)#1	2.3663(9)	C(1)-N(1)-B(1)	130.08(8)
Na(1)-Na(1)#5	4.0920(7)	N(3)-N(4)-Na(1)	118.32(5)
Na(1)-B(1)#4	2.9866(11)	C(1)-N(4)-Na(1)	134.79(6)
N(1)-B(1)	1.5622(12)	N(3)-N(2)-Na(1)#6	136.56(6)
C(3)-B(1)	1.5895(14)	N(2)-N(3)-Na(1)#7	111.96(6)
N(5)-C(3)	1.1449(13)	N(4)-Na(1)-N(2)#3	90.08(3)
N(1)-C(1)	1.3399(12)	N(4)-Na(1)-N(3)#2	96.27(3)
N(4)-C(1)	1.3288(11)	C(3)-N(5)-Na(1)#8	168.92(8)
N(1)-N(2)	1.3486(10)		
N(2)-N(3)	1.2986(11)	Na(1)#6-N(2)-N(3)-Na(1)#7	4.48(11)
N(3)-N(4)	1.3560(11)	Na(1)#6-N(2)-N(3)-N(4)	164.34(6)
		N(1)-N(2)-N(3)-N(1)#7	-159.80(5)

Figure 20. Perspective view of 77 with thermal ellipsoids at the 50% probability level.

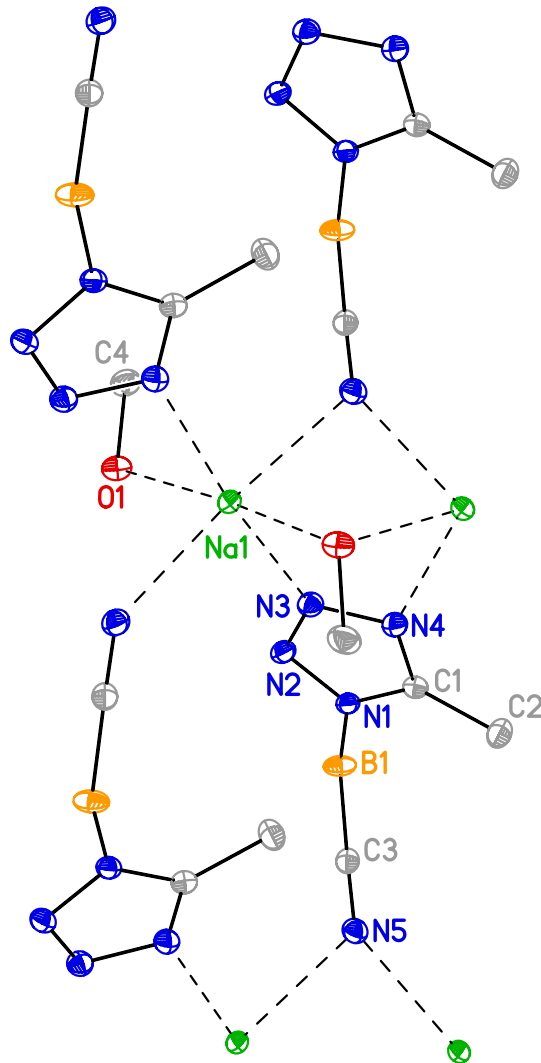
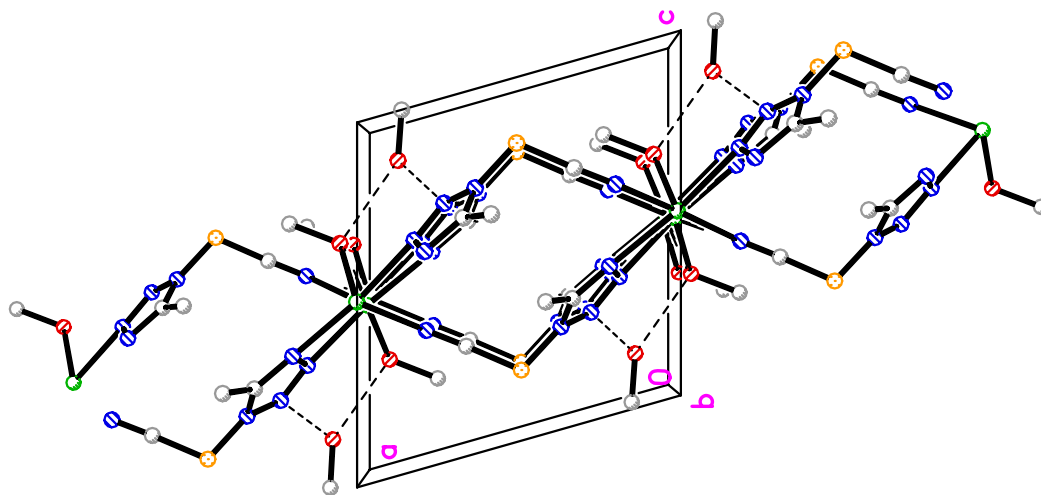


Table 17. Selected bond lengths (Å) and angles (°) for **77**.

Na(1)-N(3)	2.4984(15)	N(1)-B(1)-C(3)	108.21(12)
Na(1)-N(4)#2	2.4666(15)	N(5)-C(3)-B(1)	177.70(18)
Na(1)-N(5)#3	2.5148(16)	N(2)-N(1)-B(1)	122.70(16)
Na(1)-O(1)	2.4230(15)	C(1)-N(1)-B(1)	129.88(16)
Na(1)-O(1)#1	2.4202(15)	N(2)-N(3)-Na(1)	131.82(12)
Na(1)-Na(1)#1	3.44059(16)	N(4)-N(3)-Na(1)	116.36(11)
B(1)-N(1)	1.567(2)	C(4)-O(1)-Na(1)	112.80(11)
B(1)-C(3)	1.600(2)	C(3)-N(5)-Na(1)#5	146.14(15)
C(3)-N(5)	1.1441(19)	C(3)-N(5)-Na(1)#6	128.19(15)
N(1)-C(1)	1.333(2)	Na(1)#5-N(5)-Na(1)#6	85.65(4)
N(4)-C(1)	1.333(2)	Na(1)#2-O(1)-Na(1)	90.54(4)
N(1)-N(2)	1.344(2)	N(4)#2-Na(1)-N(3)	173.20(5)
N(2)-N(3)	1.2983(19)	N(4)#2-Na(1)-N(5)#3	92.98(5)
N(3)-N(4)	1.349(2)	N(3)-Na(1)-N(5)#3	93.70(5)
		N(5)#3-Na(1)-N(5)#4	173.98(6)
		N(4)#2-Na(1)-N(5)#4	88.76(5)
		O(1)-Na(1)-N(3)	94.52(5)
		O(1)#1-Na(1)-O(1)	174.37(6)

Figure 21. Hydrogen bonding interaction in the molecular packing of 77.



5.3 Discussion

As mentioned above, the reaction between NaNCBH_3 and tetrazoles was initially performed in 1:3 ratio. No tris(tetrazolyl)borate ligands were obtained from the reaction, and only one tetrazolyl group was attached to the boron atom as indicated by the characteristic BH_2 stretching frequencies around 2400 cm^{-1} in the infrared spectra and the triplet resonances in the ^{11}B NMR spectra. The reluctance to attach a second or a third tetrazolyl group is mostly caused by the electron deficiency of the boron center, which makes the B-H bonds too stable to be cleaved. Accordingly, LiMeBH_3 was used to react with tetrazoles for the preparation of tris(tetrazolyl)borate ligands. Since a methyl group is more electron donating than a cyano group, the use of LiMeBH_3 might facilitate more proton substitution by the tetrazoles. Unfortunately, based on spectroscopic characterization of the products after the reaction of LiMeBH_3 with tetrazole, again, only one tetrazolyl group was attached to the boron atom, since typical BH_2 resonances and absorptions were observed in the ^1H NMR and IR spectra, respectively. Therefore, no further experiments were explored for the LiMeBH_3 and tetrazole reaction.

Complexes **74-77** have been characterized by single crystal X-ray crystallographic studies. The crystal structure of **76** resembles a MOF, but no practical use could be realized as the cavity size of $\sim 2\text{ \AA}$ is too small to accommodate any small molecules. However, the unique structural features of complexes **74-77** still hold considerable interest as there are no structures of cyano(tetrazolyl)borate ligands reported in the literature.

Complexes **74-77** are not sensitive toward mechanic stimuli, friction, and sparks, but they burned rapidly with bright orange yellow flames when small samples of them were placed in a Bunsen burner flame. The volume increase of the sample in the flame tests suggests that there is considerable gas evolution during this process. Complex **74** is thermally stable up to 230 °C, and **76** does not decompose until temperatures above 290 °C. The higher degradation temperature of **76** than **74** is attributable to the electronic stabilization of the tetrazolyl group by the more electron donating methyl group than the hydrogen substituent. With high nitrogen contents, especially for **74** and **76** of 53.51 and 48.33%, respectively, these complexes may find use as energetic materials.

Complex **74** was previously prepared by Györi and coworkers through the reaction of Na(H₂B(CN)(NC)) with NaN₃ and NH₄Cl in refluxing acetonitrile and it was isolated in 55% yield.⁹³ This procedure is troublesome because the preparation of Na(H₂B(CN)(NC)) involves several steps using cyanodihydroborane as the starting material. In comparison, **74** was made through one single step in this work and obtained in 87.5% yield. In addition, Györi and coworkers did not provide structural characterization of **74**, and the X-ray crystal structure of **74** was described herein for the first time. Carboxyboron compounds have been reported to be active in biological and pharmacological studies,⁹⁴ and since tetrazole and carboxylic acid are bioequivalent,¹⁰ **74-77** may also possess some interesting biological properties.

5.4 Conclusions

Sodium cyano(tetrazolyl)borate complexes have been prepared and structurally characterized. These complexes have thermal decomposition temperatures higher than 230 °C and are insensitive toward shock, friction, and electrostatic discharge. They deflagrated and produced some white ash upon burning. These sodium complexes are potential nitrogen rich energetic materials and can be used as starting materials to prepare other metal complexes. Additionally, these compounds are potentially attractive in biological studies.

5.5 Experimental Section

General Considerations. All starting materials and products were air stable and reactions were performed under ambient conditions unless stated otherwise. A 3 wt. % solution of 1H-tetrazole in acetonitrile was purchased from Aldrich Chemical Company. The acetonitrile was removed under reduced pressure, and the 1H-tetrazole was used as a solid. 5-Methyl-1H-tetrazole was purchased from Aldrich Chemical Company and used as received. ^1H , $^{13}\text{C}\{^1\text{H}\}$ and ^{11}B NMR spectra were obtained at 500, 125, and 160 MHz, respectively. Chemical shifts for ^{11}B NMR were measured in ppm using $\text{BF}_3 \cdot \text{Et}_2\text{O}$ as external reference. Infrared spectra were obtained using Nujol as the medium. Elemental analyses were performed by Midwest Microlab, Indianapolis, IN. It was necessary to add V_2O_5 as a combustion enhancing agent to obtain acceptable carbon values. Melting points were obtained on a Thermo Scientific Mel-Temp 3.0 melting point apparatus and are

uncorrected. TGA experiments were conducted on a Perkin-Elmer Pyris 1 TGA system from 50 to 500 °C for **74** and **76** using nitrogen as the flow gas with a heating rate of 5 °C/min.

General procedure for the preparation of 74-77. A 100-mL Schlenk flask was charged with sodium cyanoborohydride, one equivalent of the specific tetrazole as a fine powder, a stir bar, and was equipped with a reflux condenser. The solid mixture was then heated under stirring to 120 °C, until the gas evolution stopped. The resultant white porous material was washed with 3 × 15 mL portions of anhydrous Et₂O to afford the powdery product. Complexes **74** and **76** were crystallized from concentrated methanol solutions at room temperature. Complexes **75** and **77** were crystallized by slow evaporation of dilute methanol solutions at ambient conditions.

Na(H₂B(CN)(HCN₄)) (74). Prepared from sodium cyanoborohydride (0.500 g, 7.96 mmol) and 1H-tetrazole (0.558 g, 7.96 mmol) to afford **74** in 87.5% yield as a white solid. Mp: 218-220 °C; IR (Nujol, cm⁻¹): $\tilde{\nu}$ = 3149 (s), 2423 (s), 2396 (m), 2377 (s), 2266 (w), 2238 (w), 2215 (s), 1758 (m), 1510 (w), 1406 (w), 1366 (s), 1302 (w), 1255 (s), 1208 (s), 1189 (w), 1152 (s), 1133 (s), 1107 (s), 1051 (s), 1001 (s), 980 (s), 882 (s), 858 (m), 792 (w), 775 (m), 737 (m), 703 (s), 658 (w), 647 (s); ¹H NMR (D₂O, 23 °C): δ = 8.61 (s, 1H, HCN₄), 2.47 (broad q, 2H, BH₂); ¹³C{¹H} NMR (D₂O, 23 °C): δ = 148.12 (s, HCN₄), 136.78 (broad s, BCN); ¹¹B NMR (D₂O, 23 °C): δ = -26.73 (t, J_{BH} = 101 Hz); elemental analysis calculated for C₂H₃N₅ BNa (%): C 18.35, H 2.31, N 53.51; found: C 18.34, H 2.28, N 53.32.

Na(H₂B(CN)(HCN₄))(CH₃OH) (75). A 25 mL methanol solution containing ~1.00 g of **74** was allowed to evaporate slowly to afford **75** as a colorless crystalline solid. Mp: 220-222 °C; IR (Nujol, cm⁻¹): $\tilde{\nu}$ = 3149 (s), 2423 (s), 2396 (m), 2377 (s), 2267 (w), 2238 (w), 2216 (s), 1758 (m), 1376 (s), 1366 (s), 1298 (w), 1255 (s), 1208 (s), 1189 (m), 1152 (s), 1134 (s), 1108 (s), 1052 (s), 1001 (s), 980 (s), 882 (s), 858 (m), 792 (w), 775 (m), 737 (m), 703 (s), 658 (w), 647 (s); ¹H NMR (D₂O, 23 °C): δ = 8.65 (s, 1H, HCN₄), 3.26 (s, CH₃OH), 2.52 (broad q, 2H, BH₂); ¹³C{¹H} NMR (D₂O, 23 °C): δ = 148.21 (s, HCN₄), 136.63 (broad s, BCN); ¹¹B NMR (D₂O, 23 °C): δ = -26.73 (t, J_{BH} = 101 Hz).

Na(H₂B(CN)(MeCN₄))(76). Prepared from sodium cyanoborohydride (0.500 g, 7.96 mmol) and 5-methyl-1H-tetrazole (0.669 g, 7.96 mmol) to afford **76** in 90.4% yield as a white solid. Mp: 220-222 °C; IR (Nujol, cm⁻¹): $\tilde{\nu}$ = 2425 (s), 2409 (s), 2223 (s), 1591 (w), 1508 (s), 1401 (m), 1304 (w), 1269 (s), 1205 (s), 1168 (s), 1129 (s), 1117 (s), 1054 (w), 1028 (w), 1002 (m), 973 (w), 891 (w), 864 (w), 851 (s), 787 (w), 732 (m), 698 (s), 660 (w), 648 (s); ¹H NMR (D₂O, 23 °C): δ = 2.35 (broad q, 2H, BH₂), 2.29 (s, 3H, CN₄CH₃); ¹³C{¹H} NMR (D₂O, 23 °C): δ = 156.88 (s, MeCN₄), 137.10 (broad s, BCN), 8.93 (s, CN₄CH₃); ¹¹B NMR (D₂O, 23 °C): δ = -24.99 (t, J_{BH} = 97 Hz); elemental analysis calculated for C₃H₅N₅BNa (%): C 24.87, H 3.48, N 48.33; found: C 25.14, N 3.55, N 47.90.

Na(H₂B(CN)(MeCN₄))(CH₃OH)·(CH₃OH) (77). A 25 mL methanol solution containing ~1.00 g of **76** was allowed to evaporate slowly to afford **77** as a colorless crystalline solid. Mp: 222-224 °C; IR (Nujol, cm⁻¹): $\tilde{\nu}$ = 2425 (s), 2409 (s), 2223 (s), 1591

(w), 1508 (s), 1401 (m), 1304 (w), 1269 (s), 1205 (s), 1168 (s), 1129 (s), 1117 (s), 1054 (w), 1028 (w), 1002 (m), 973 (w), 891 (w), 864 (w), 851 (s), 787 (w), 732 (m), 698 (s), 660 (w), 648 (s); ^1H NMR (D_2O , 23 °C): δ = 3.22 (s, CH_3OH), 2.39 (broad q, 2H, BH_2), 2.33 (s, 3H, CN_4CH_3); $^{13}\text{C}\{^1\text{H}\}$ NMR (D_2O , 23 °C): δ = 156.94 (s, MeCN_4), 136.78 (broad s, BCN), 8.99 (s, CN_4CH_3); ^{11}B NMR (D_2O , 23 °C): δ = -24.99 (t, $J_{\text{BH}} = 97$ Hz).

CHAPTER 6

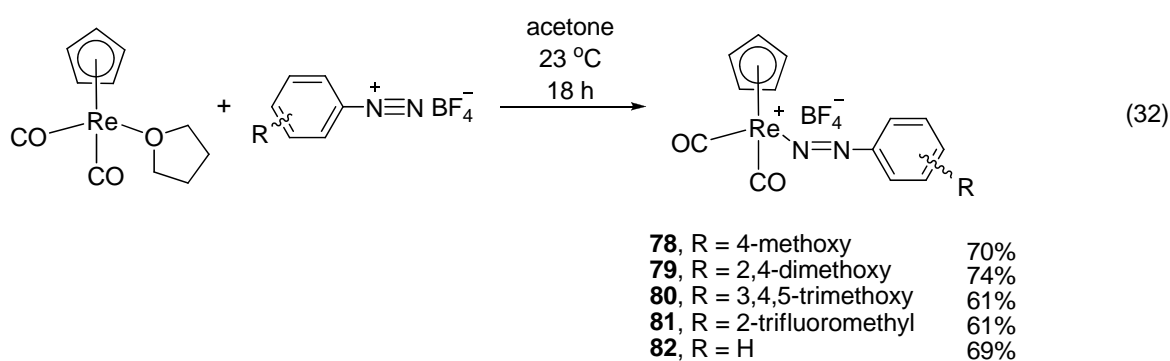
Attempted Synthesis of Rhenium(I) Aryl Pentazole Complexes

6.1 Introduction

As mentioned in Chapter 1, aryl pentazoles have been synthesized and characterized by X-ray diffraction studies.⁷³ However, the pentazolate ion (N_5^-) was only detected in the gas phase recently and it has not been observed in condensed phases.^{70b,71} Available data suggest that N_5^- or the protonated form (HN_5) only exist as fleeting intermediates in solution at low temperatures. To date, metal complexes containing pentazolate ligands or aryl pentazole ligands have not been reported. This chapter describes the attempted experiments for the stabilization of aryl pentazoles by coordinating them to electron-rich, low valent metal centers that are also kinetically inert with respect to ligand substitution reactions. If these syntheses are successful, the aryl pentazole complexes will possibly be stabilized through d- π backbonding between the filled d-orbitals on the metal center and the unfilled π -orbitals on the pentazole ring. Furthermore, aryl pentazole complexes are potential precursors for pentazolate complexes because the rich electron density on the metal center may contribute to the stability of the pentazolate ring. Therefore, by cleavage of the C-N bond between the aryl group and the pentazole moiety, pentazolate complexes might be prepared. In case the aryl pentazole complexes are stable enough to handle, their energetic properties will be investigated to see if they are suitable to be used as HEDMs.

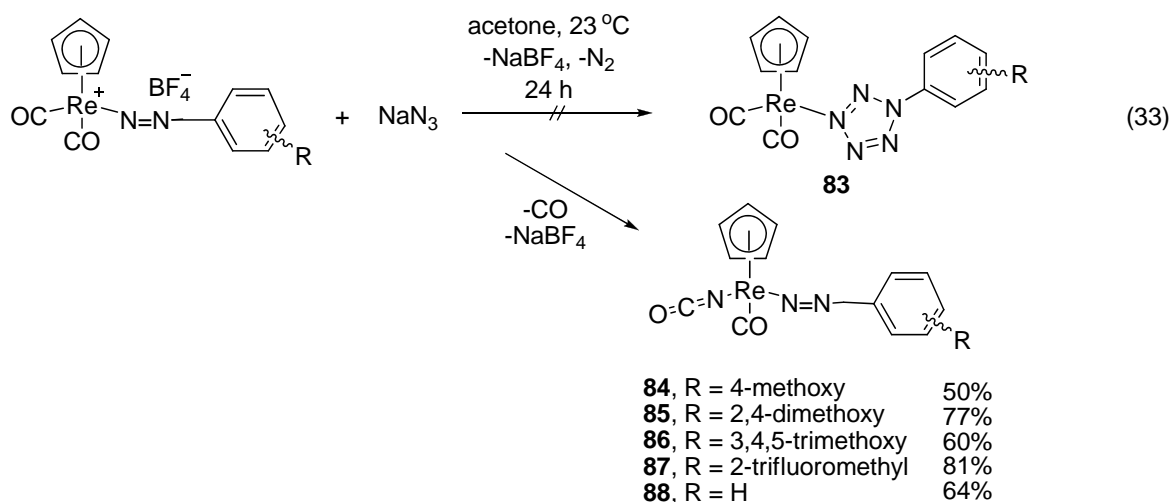
6.2 Results

6.2.1 Synthetic Aspects. Complexes **78-82** were prepared by the reaction of $(\eta^5\text{-C}_5\text{H}_5)\text{Re}(\text{CO})_2(\text{THF})$ with the specific aryl diazonium salt in acetone at ambient temperature in good yields (eq 32). The products are soluble in acetone, CH_2Cl_2 , and ethanol, but not soluble in Et_2O , hexane, and other aprotic organic solvents. Complexes **78-82** were crystallized by layering their concentrated acetone solutions with Et_2O . A single crystal of **78** was subjected to an X-ray crystal structural determination. The formation of **78-82** was confirmed by NMR and IR spectroscopy. In **78-82**, the Cp groups resonated as singlets at δ 6.55-6.67 in the ^1H NMR spectra and appeared at 95.21-95.57 ppm in the $^{13}\text{C}\{^1\text{H}\}$ NMR spectra when using acetone- d_6 as the solvent. The CO groups showed resonances in a small range between 186.41 and 190.01 ppm in the $^{13}\text{C}\{^1\text{H}\}$ NMR spectra. The infrared spectra of **78-82** exhibited strong CO group absorptions between 2082 and 1923 cm^{-1} and stretching frequencies of the diazenido $\text{N}=\text{N}$ groups from 1717 to 1756 cm^{-1} .



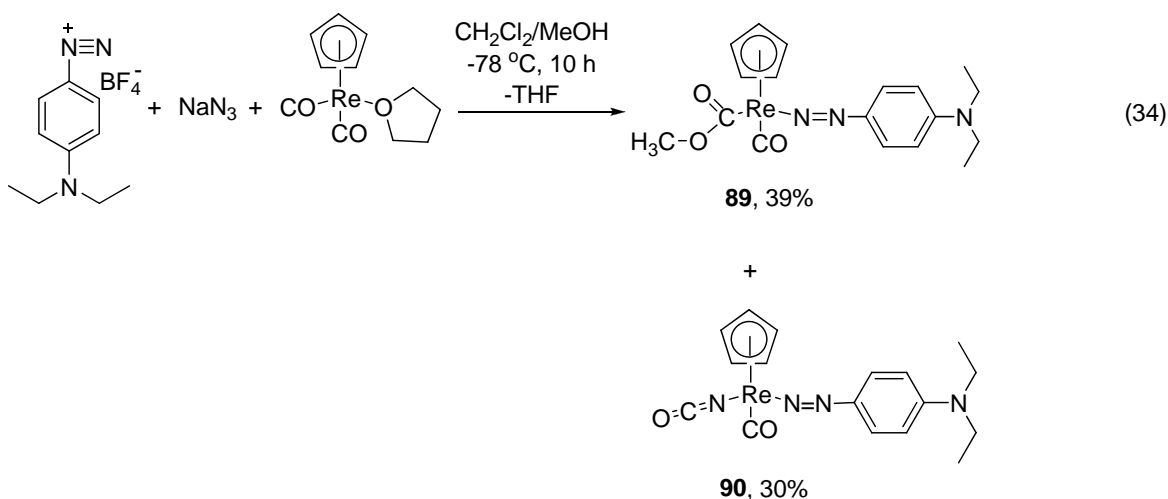
Treatment of **78-82** with NaN_3 was attempted to synthesize aryl pentazole complexes,

but a series of isocyanate complexes **84-88** was isolated as orange red crystalline solids instead of the expected aryl pentazole complex **83** (eq 33). In contrast to **78-82**, **84-88** are soluble in Et₂O and can be crystallized from concentrated ether solutions at -25 °C. The structural assignments for **84-88** were supported by spectral and X-ray crystallographic studies. In the ¹H NMR spectra of **84-88** in acetone-d₆, the Cp groups appeared as singlets in a narrow range of δ 6.06-6.21. In the ¹³C{¹H} NMR spectra, the Cp ligands resonated between 94.76-95.98 ppm, and the CO groups showed singlet resonances between 196.74 and 197.70 ppm. In **84-88**, the NCO groups exhibited absorptions at 2241-2249 cm⁻¹, the CO groups showed stretching frequencies between 1923 and 1953 cm⁻¹, and the diazenido N=N groups had absorptions in the range of 1939-1973 cm⁻¹ in the infrared spectra.



Treatment of (η⁵-C₅H₅)Re(CO)₂(THF), 4-Et₂NC₆H₄N₂BF₄, and NaN₃ in MeOH/CH₂Cl₂ at -78 °C was attempted as another approach to prepare an aryl pentazole complex. However, **89** and **90** were obtained rather than the desired product (eq 34).

Complex **89** precipitated as a golden yellow solid from concentrated toluene solution of the crude products containing both **89** and **90** at $-25\text{ }^{\circ}\text{C}$. After isolation of **89**, the toluene solution was evaporated to dryness under reduced pressure, and the resultant brown solid was crystallized in concentrated Et_2O solution at $-25\text{ }^{\circ}\text{C}$ to afford **90** as an orange red crystalline solid. Single crystals of **89** were obtained by slow diffusion of pentane into a concentrated solution of the golden yellow precipitate in CH_2Cl_2 at $0\text{ }^{\circ}\text{C}$. In the ^1H NMR spectra, the Cp group of **89** showed a sharp singlet resonance at δ 5.90, while the Cp group of **90** resonated at δ 6.04. In the infrared spectra of **89**, the strong absorption at 1914 cm^{-1} was assigned to the stretching frequency of the CO group, the absorption at 1663 cm^{-1} was assigned to the diazenido N=N group, and the absorption at 1613 cm^{-1} was assigned to the CO group in the methoxy carbonyl group. In **90**, the NCO group absorption appeared at 2233 cm^{-1} , the CO group at 2049 cm^{-1} , and the diazenido N=N group at 1659 cm^{-1} in the infrared spectra.



6.2.3 Structural Aspects. The X-ray crystal structures of **78**, **84-87**, and **89** were determined to establish the geometry about the potassium centers and the bonding modes of the ligands. Perspective views of **78**, **84**, and **89** are illustrated in Figures 22-24, experimental crystallographic parameters are listed in Table 18, and selected bond length and angles are given in Tables 19-21.

Table 18. Crystal data and data collection parameters for **78**, **84**, and **89**.

	78	84	89
Empirical formula	C ₁₄ H ₁₂ N ₂ BF ₄ O ₃ Re	C ₁₄ H ₁₂ N ₃ O ₃ Re	C ₁₈ H ₁₇ N ₃ O ₃ Re
FW	539.27	456.47	509.55
Space group	C2/c	P1 bar	P2 ₁ 2 ₁ 2 ₁
a (Å)	25.4845(10)	7.3499(4)	6.8491(4)
b (Å)	7.6496(3)	9.1194(5)	10.4531(5)
c (Å)	16.6216(6)	12.0516(7)	25.5399(13)
β (°)	97.154(3)	73.327(2)	90
V (Å ³)	3215.1(2)	703.84(7)	1828.51(17)
Z	8	2	4
T (K)	100(2)	100(2)	100(2)
λ (Å)	0.71073	0.71073	0.71073
ρ _{calc} (g cm ⁻³)	2.187	2.154	1.851
μ (mm ⁻¹)	7.619	8.645	6.666
R(F) (%)	0.0232	0.0404	0.0372
R _w (F) (%)	0.0530	0.0875	0.0712

$$R(F) = \frac{\sum ||F_o| - |F_c||}{\sum |F_o|}, R_w(F)^2 = \frac{[\sum w(F_o^2 - F_c^2)^2]}{\sum w(F_o^2)^2}]^{1/2} \text{ for } I > 2\sigma(I).$$

A perspective view of **78** is depicted in Figure 22. The rhenium containing part of **78** is cationic and is paired with a BF_4^- counter ion. The coordination environment around the rhenium atom is distorted tetrahedral formed by the centroid of one $\eta^5\text{-Cp}$ ligand, two CO ligands, and one diazenido ligand. The $\text{Re}(1)\text{-N}(1)$ bond length in **78** is 1.8345(19) Å and it falls between the Re-N bond lengths of 1.75(1) and 1.937(7) Å in $[\text{ReCl}_2(\text{NH}_3)(\text{N}_2\text{HC}_6\text{H}_5)(\text{P}(\text{CH}_3)_2\text{C}_6\text{H}_5)_2]\text{Br}$ and $(\eta^5\text{-C}_5\text{H}_5)\text{Re}(\text{CO})_2(p\text{-NN}(\text{CH}_3)\text{C}_6\text{H}_4\text{OMe})$, respectively.⁹⁵ The $\text{Re}(1)\text{-N}(1)\text{-N}(2)$ angle is almost linear with an angle of $175.30(17)^\circ$ which is similar to the Re-N-N angles in $[\text{ReCl}_2(\text{NH}_3)(\text{N}_2\text{HC}_6\text{H}_5)(\text{P}(\text{CH}_3)_2\text{C}_6\text{H}_5)_2]\text{Br}$ ($172(1)^\circ$) and $\text{ReCl}_2(\text{N}_2\text{C}_6\text{H}_5)(\text{P}(\text{CH}_3)_2\text{C}_6\text{H}_5)_3$ ($173(2)^\circ$).^{95a} The $\text{C}(1)\text{-N}(2)\text{-N}(1)$ bond angle of $122.62(19)^\circ$ is also close to the C-N-N angles of $119(2)^\circ$ in both $[\text{ReCl}_2(\text{NH}_3)(\text{N}_2\text{HC}_6\text{H}_5)(\text{P}(\text{CH}_3)_2\text{C}_6\text{H}_5)_2]\text{Br}$ and $\text{ReCl}_2(\text{N}_2\text{C}_6\text{H}_5)(\text{P}(\text{CH}_3)_2\text{C}_6\text{H}_5)_3$. The $\text{N}(1)\text{-N}(2)$ bond length is 1.197(2) Å, which is slightly shorter than the typical N-N double bond length of 1.23 Å and much longer than the N-N triple bond length of 1.10 Å. The $\text{Re}(1)\text{-C}(8)\text{-O}(2)$ angle is $178.2(2)^\circ$.

A perspective view of **84** is illustrated in Figure 23. The rhenium atom is coordinated to one $\eta^5\text{-Cp}$ ligand, one CO ligands, one diazenido ligand, and one NCO ligand through the nitrogen atom. The $\text{Re}(1)\text{-N}(1)$ bond length is 1.823(4) Å, the $\text{Re}(1)\text{-N}(1)\text{-N}(2)$ bond angle is $176.3(4)^\circ$, and the $\text{C}(7)\text{-N}(2)\text{-N}(1)$ bond angle is $123.6(4)^\circ$. The $\text{N}(1)\text{-N}(2)$ bond also has a double bond character with a length of 1.210(6) Å. The $\text{Re}(1)\text{-C}(8)\text{-O}(2)$ bond angle is $178.2(2)^\circ$ and the $\text{Re}(1)\text{-N}(3)\text{-C}(14)$ bond angle is $165.0(5)^\circ$. The $\text{N}(3)\text{-C}(14)$

distance is 1.168(6) Å and is between the bond lengths of C-N double bonds and C-N triple bonds (1.16-1.29 Å). The C(14)-O(3) bond length is 1.196(6) Å and represents a C-O double bond as the typical C=O bond length is 1.20 Å.

As shown in Figure 24, the crystal structure of **89** consists of a rhenium atom which has a distorted tetrahedral geometry provided by one CO ligand, one aryl diazenido ligand, and one methoxy carbonyl ligand. The Re(1)-N(1) and N(1)-N(2) bond lengths are 1.819(5) Å and 1.221(7) Å, respectively. The Re(1)-N(1)-N(2) and Re(1)-C(16)-O(1) are almost linear with bond angles of 177.9(5) and 175.8(6)°. The N(1)-N(2)-C(6) angle is 121.5(5)°. The Re(1)-C(17) distance is 2.115(6) Å. The Re(1)-C(17)-O(2) and Re(1)-C(17)-O(3) angles are 125.7(5) and 112.1(4)°, respectively, suggesting the C(17) atom is sp² hybridized. The bond length of 1.158(7) Å for C(16)-O(1) is between the bond lengths of C-O double and triple bonds (1.13-1.20 Å), while the C(17)-O(2) distance of 1.198(7) Å indicates that it has a C-O double bond character.

Figure 22. Perspective view of **78** with thermal ellipsoids at the 50% probability level.

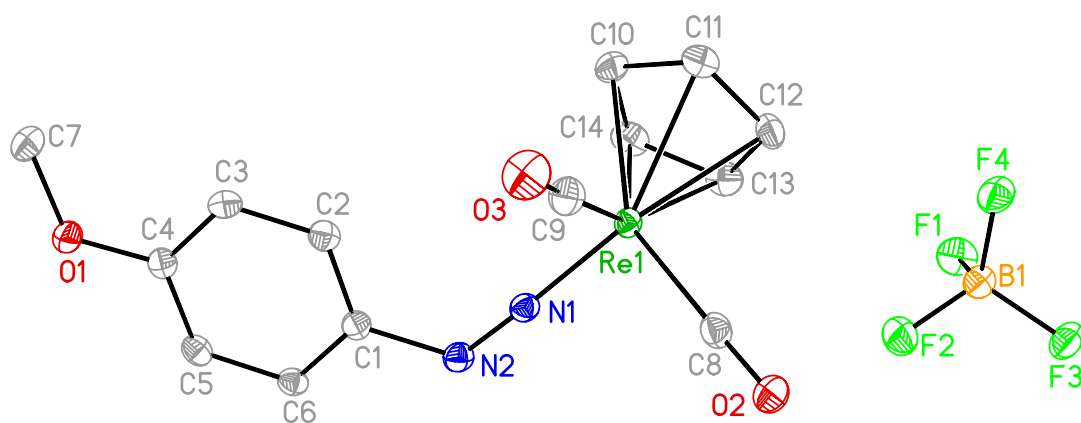


Table 19. Selected bond lengths (Å) and angles (°) for **78**.

Re(1)-N(1)	1.8345(19)	N(1)-Re(1)-C(9)	93.11(10)
Re(1)-C(8)	1.971(2)	N(1)-Re(1)-C(8)	96.71(9)
Re(1)-C(9)	1.953(3)	C(9)-Re(1)-C(8)	85.63(10)
Re(1)-C(11)	2.304(2)	N(2)-N(1)-Re(1)	175.30(17)
N(1)-N(2)	1.197(2)	O(2)-C(8)-Re(1)	178.2(2)
N(2)-C(1)	1.431(3)	N(1)-N(2)-C(1)	122.62(19)
C(8)-O(2)	1.131(3)		

Figure 23. Perspective view of **84** with thermal ellipsoids at the 50% probability level.

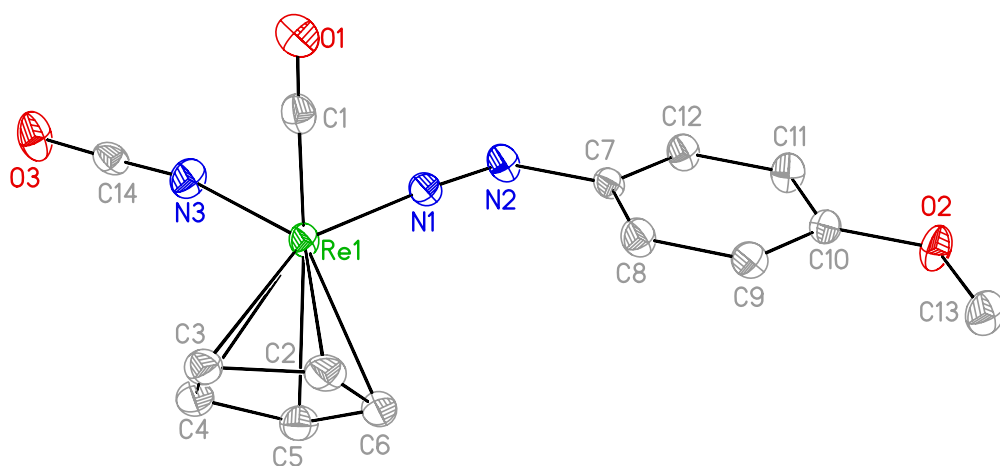


Table 20. Selected bond lengths (Å) and angles (°) for **84**.

Re(1)-N(1)	1.823(4)	N(1)-Re(1)-N(3)	102.22(18)
Re(1)-N(3)	2.056(4)	N(1)-Re(1)-C(1)	91.2(2)
Re(1)-C(1)	1.897(6)	C(1)-Re(1)-N(3)	92.9(2)
Re(1)-C(5)	2.345(5)	N(2)-N(1)-Re(1)	176.3(4)
N(1)-N(2)	1.210(6)	C(14)-N(3)-Re(1)	165.0(5)
N(3)-C(14)	1.168(6)	O(1)-C(1)-Re(1)	175.4(5)
C(14)-O(3)	1.196(6)	N(1)-N(2)-C(7)	123.6(4)
C(1)-O(1)	1.155(7)	N(3)-C(14)-O(3)	178.3(6)
N(2)-C(7)	1.429(6)		

Figure 24. Perspective view of **89** with thermal ellipsoids at the 50% probability level.

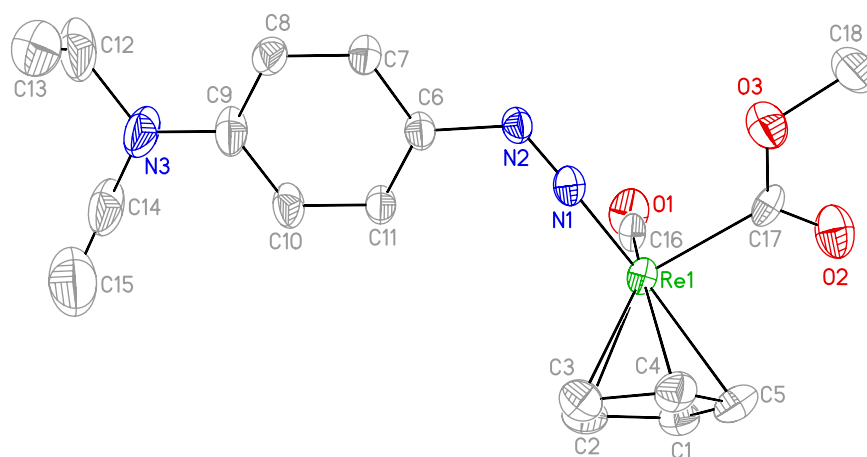


Table 21. Selected bond lengths (Å) and angles (°) for **89**.

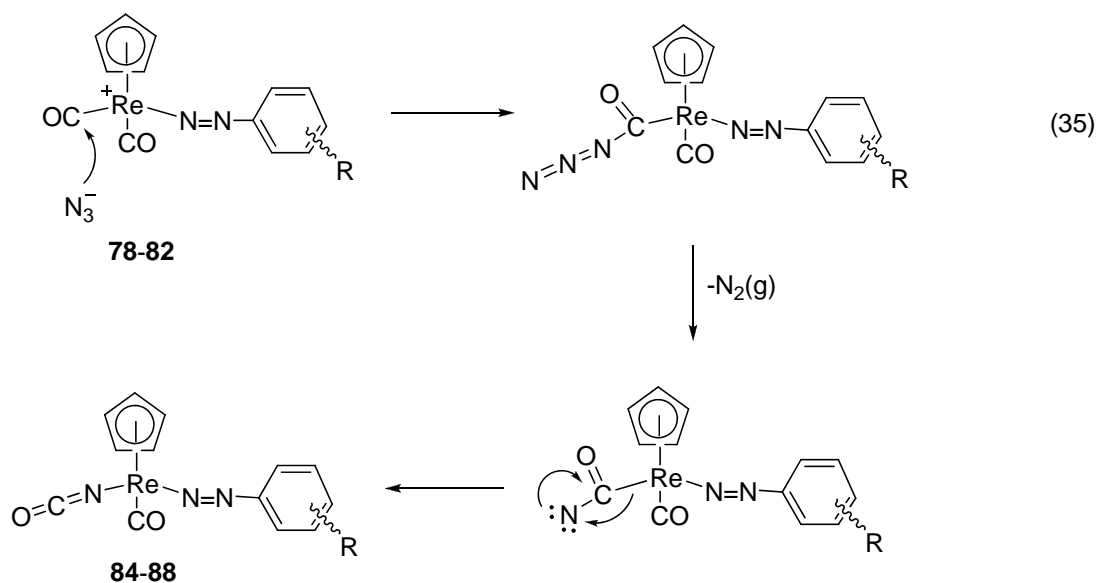
Re(1)-N(1)	1.819(5)	N(1)-Re(1)-C(16)	92.6(3)
Re(1)-C(16)	1.894(6)	N(1)-Re(1)-C(17)	98.5(2)
Re(1)-C(17)	2.115(6)	C(16)-Re(1)-C(17)	83.8(2)
Re(1)-C(1)	2.305(7)	N(2)-N(1)-Re(1)	177.9(5)
N(1)-N(2)	1.221(7)	O(1)-C(16)-Re(1)	175.8(6)
N(2)-C(6)	1.418(7)	O(2)-C(17)-Re(1)	125.7(5)
C(16)-O(1)	1.158(7)	O(3)-C(17)-Re(1)	112.1(4)
C(17)-O(2)	1.198(7)	N(1)-N(2)-C(6)	121.5(5)

6.3 Discussion

Aryl pentazoles synthesized by [3+2] cycloaddition of aryl diazonium salts with NaN_3 decompose at or below room temperature through the loss of dinitrogen, to afford aryl azides.⁷⁴ Electron-donating substituents on the 4-position of the aryl groups help stabilizing the aryl pentazoles with respect to nitrogen loss, whereas electron-withdrawing substituents on the 4-position will destabilize the aryl pentazole.^{9a,72b} Therefore, it might be possible to prepare metal pentazole complexes by the [3+2] cycloaddition of a metal coordinated diazonium cation and sodium azide. Sutton has reported the synthesis and properties of some rhenium(I) complexes containing coordinated aryl diazonium ligands.^{95b} Rhenium(I) is kinetically inert and has energetically accessible filled d-orbitals and thus is a good initial choice for a metal center to stabilize an aryl pentazole ligand. Additionally, since aryl pentazoles are most stable to dinitrogen loss when the aryl group has a strong electron donating substituent in the 2- or 4- position, rhenium(I) might also stabilize an aryl pentazole ligand through donation of d-electron density to the electron poor N_5^- ring.

Therefore, aryldiazenido complexes $[(\eta^5\text{-C}_5\text{H}_5)\text{Re}(\text{CO})_2(\text{N}_2\text{Ar})][\text{BF}_4]$ (**78-82**) were prepared according to Sutton's procedures,^{95b} and were isolated as red orange crystalline solids (eq 32). These complexes were chosen to assess the effects on the formation of the expected aryl pentazole complexes of a range of electron-donating and electron-withdrawing aryl groups. It was hoped that treatment of **78-82** with sodium azide would lead to formation of the aryl pentazole complexes. Instead, a combination of infrared spectroscopy,

NMR spectroscopy, and X-ray crystallography demonstrated that a series of isocyanate complexes $(\eta^5\text{-C}_5\text{H}_5)\text{Re}(\text{CO})(\text{NCO})(\text{N}_2\text{Ar})$ (**84-88**) formed as the products. Infrared spectroscopy and X-ray crystal structures of **78** and **84** provided clear insight into these transformations. For example, **78** showed two carbonyl stretches at 2076 and 2012 cm^{-1} and the nitrogen-nitrogen stretch at 1725 cm^{-1} . Complex **84** showed one carbonyl stretch at 1929 cm^{-1} and no BF_4^- absorption bands, suggesting loss of one carbonyl ligand and formation of a neutral complex. The N=N stretch of the diazonium ligand appeared at 1673 cm^{-1} , and isocyanate NCO stretch was also observed at 2244 cm^{-1} . The mechanism of these transformations most probably involves the initial nucleophilic attack of the azide ion at one of the coordinated carbonyl carbon atoms, forming an acyl azide intermediate. The acyl azide then undergoes a Curtius type rearrangement by losing one dinitrogen molecule, forming an acyl nitrene species, which then quickly rearranges by migration of the $\text{CpRe}(\text{CO})(\text{N}_2\text{C}_6\text{H}_5\text{R})$ moiety, forming the isocyanate complex (eq 35).⁹⁶



As shown above, the attempted [3+2] cycloaddition reactions between azide ion and the rhenium-coordinated diazonium ions did not lead to the expected aryl pentazole complexes. These studies suggest that the orbitals that would normally be used to achieve the [3+2] cycloaddition transition state are used up by the d_{π} - p_{π} backbonding between the rhenium ion and the N-N fragment of the diazonium ligand. Consequently, the rate of [3+2] cycloaddition becomes much slower than the rate of isocyanate ligand formation. We have been unable to observe the desired [3+2] cycloaddition reaction even with diazonium ions containing extremely electron-donating substituents (e.g., 2,4-dimethoxyphenyl diazonium).

Another attempted method was employed to synthesize rhenium(I) aryl pentazole complexes. It was hoped that the labile THF ligand in $\text{CpRe}(\text{CO})_2(\text{THF})$ could be replaced by an aryl pentazole ligand. $\text{CpRe}(\text{CO})_2(\text{THF})$ was treated with organic aryl pentazole made *in situ* or by an one pot reaction as illustrated in eq 34. Acetone was initially used as

solvent; however, the reaction produced the isocyanate complex as the major product. Since MeOH/CH₂Cl₂ mixture has been reported to have the best performance as solvent in making organic aryl pentazole with respect to yield and stability,^{9a} this solvent system was used in the one pot reaction. The ¹H NMR spectroscopy indicated that a mixture of two complexes was obtained as the reaction products, including the isocyanate complex and another unidentified compound. This compound was selectively precipitated as a golden yellow solid from toluene solution at -25 °C, and then recrystallized by slow diffusion of pentane into a dichloromethane solution at -10 °C. However, the X-ray structure revealed that it was a methoxycarbonyl complex (**89**), which has been reported previously. The formation of **89** can be achieved by direct reaction of $[(\eta^5\text{-C}_5\text{H}_5)\text{Re}(\text{CO})_2(\text{N}_2\text{C}_6\text{H}_5\text{NEt}_2)][\text{BF}_4]$ with equimolar quantity of sodium methoxide in methanol.⁹⁶

6.4 Conclusions

The attempted [3+2] cycloaddition of rhenium aryldiazenido complexes $[(\eta^5\text{-C}_5\text{H}_5)\text{Re}(\text{CO})_2(\text{N}_2\text{Ar})][\text{BF}_4]$ (**78-82**) with sodium azide afforded the corresponding isocyanate complexes $(\eta^5\text{-C}_5\text{H}_5)\text{Re}(\text{CO})(\text{NCO})(\text{N}_2\text{Ar})$ (**84-88**). One pot reaction of $\text{CpRe}(\text{CO})_2(\text{THF})$ and $\text{Et}_2\text{NC}_6\text{H}_5\text{N}_5$ made *in situ* afforded a mixture of two products including the methoxycarbonyl complex $(\eta^5\text{-C}_5\text{H}_5)\text{Re}(\text{CO})(\text{COOCH}_3)(\text{N}_2\text{C}_6\text{H}_5\text{NEt}_2)$ (**89**) and the isocyanate complex $(\eta^5\text{-C}_5\text{H}_5)\text{Re}(\text{CO})(\text{NCO})(\text{N}_2\text{C}_6\text{H}_5\text{NEt}_2)$ (**90**). The formation of the complexes is supported by spectroscopic and X-ray crystallographic studies. The attempted reactions did not proceed to the desired aryl pentazole complexes.

6.5 Experimental Section

General Considerations. All reactions were performed under argon using standard glovebox and Schlenk line techniques. THF was freshly distilled from sodium benzophenone ketyl under nitrogen. Aryl diazonium tetrafluoroborates,⁹⁷ $\text{CpRe}(\text{CO})_3$,⁹⁸ and $\text{CpRe}(\text{CO})_2(\text{THF})$ ^{95b} were synthesized according to literature procedures. ^1H and $^{13}\text{C}\{^1\text{H}\}$ NMR spectra were obtained at 300, 400, and 75, and 100 MHz Varian instruments, respectively, in acetone- d_6 . Infrared spectra were obtained using Nujol as the medium. Elemental analyses were performed by Midwest Microlab, Indianapolis, IN. Melting points were obtained on a Thermo Scientific Mel-Temp 3.0 melting point apparatus and are uncorrected.

$[(\eta^5\text{-C}_5\text{H}_5)\text{Re}(\text{CO})_2(4\text{-N}_2\text{C}_6\text{H}_4\text{OCH}_3)][\text{BF}_4]$ (78). A 100 mL Schlenk flask was charged with $(\eta^5\text{-C}_5\text{H}_5)\text{Re}(\text{CO})_2(\text{THF})$ (0.100 g, 0.264 mmol), 20 mL anhydrous acetone, and a stir bar. To the stirred brownish yellow solution at 23 °C, solid 4- $\text{CH}_3\text{OC}_6\text{H}_4\text{N}_2\text{BF}_4$ (0.059 g, 0.27 mmol) was slowly added and the reaction mixture turned brownish red. The mixture was stirred at ambient temperature for 18 h and then filtered through a 2-cm pad of Celite on a coarse glass frit. The clear filtrate was concentrated to ~5 mL and layered with 30 mL Et_2O to afford **78** in 70% yield as a brownish red crystalline solid. Mp: 154-155 °C (decompose); IR (Nujol, cm^{-1}): $\tilde{\nu} = 2076$ (s), 2030 (s), 2012 (s), 1725 (s), 1588 (m), 1310 (m), 1260 (m), 1151 (w), 1101 (m), 1058 (s), 1025 (m), 965 (w), 842 (w); ^1H NMR (acetone- d_6 , 23 °C): $\delta = 7.56$ (d, $J = 9.0$ Hz, 2H, $\text{N}_2\text{C}(\text{CH})_2(\text{CH})_2\text{COCH}_3$), 7.19 (d, $J = 9.3$ Hz, 2H,

$\text{N}_2\text{C}(\text{CH})_2(\text{CH})_2\text{COCH}_3$), 6.63 (s, 5H, C_5H_5), 3.92 (s, 3H, OCH_3); $^{13}\text{C}\{^1\text{H}\}$ NMR (acetone- d_6 , 23 °C): δ = 188.25 (s, CO), 164.60 (s, 4- CH_3OCCH), 126.81 (s, N_2CCH), 116.95 (s, N_2CCHCH), 116.04 (s, N_2CCH), 96.23 (s, C_5H_5), 56.46 (OCH_3).

$[(\eta^5\text{-C}_5\text{H}_5)\text{Re}(\text{CO})_2(2,4\text{-N}_2\text{C}_6\text{H}_3(\text{OCH}_3)_2)][\text{BF}_4]$ (79). In a fashion similar to the preparation of **78**, treatment of $(\eta^5\text{-C}_5\text{H}_5)\text{Re}(\text{CO})_2(\text{THF})$ (0.100 g, 0.264 mmol) with 2,4- $(\text{CH}_3\text{O})_2\text{C}_6\text{H}_3\text{N}_2\text{BF}_4$ (0.059 g, 0.27 mmol) afforded **79** in 74% yield as a red orange crystalline solid. Mp: 167-169 °C (decompose); IR (Nujol, cm^{-1}): $\tilde{\nu}$ = 2057 (s), 2001 (s), 1741 (s), 1598 (m), 1577 (w), 1300 (s), 1260 (m), 1215(m), 1155 (m), 1110 (m), 1065 (s), 1027 (s), 967 (w), 936 (w), 919 (w), 892 (w), 864 (w), 843 (m), 808 (w), 770 (w); ^1H NMR (acetone- d_6 , 23 °C): δ = 7.35 (d, $^3\text{J} = 9.3$ Hz, 1H, N_2CCH), 6.80 (d, $^4\text{J} = 2.4$ Hz, 1H, 2- CH_3OCCH), 6.72 (doublet of doublet, $^3\text{J} = 9.3$ Hz, $^4\text{J} = 2.4$ Hz, 1H, N_2CCHCH), 6.55 (s, 5H, C_5H_5), 4.03 (s, 3H, 4- OCH_3), 3.94 (s, 3H, 2- OCH_3); $^{13}\text{C}\{^1\text{H}\}$ NMR (acetone- d_6 , 23 °C): δ = 190.01 (s, CO), 166.47 (s, 2- CH_3OCCH), 161.93 (s, 4- CH_3OCCH), 128.10 (s, N_2CCH), 108.51 (s, N_2CCHCH), 102.74 (s, N_2CCH), 100.52 (s, 2- CH_3OCCH), 95.56 (s, C_5H_5), 57.06 (s, 2- OCH_3), 56.74 (s, 4- OCH_3); elemental analysis calculated for $\text{C}_{15}\text{H}_{14}\text{N}_2\text{O}_4\text{ReBF}_4$ (%): C 32.21, H 2.52, N 5.01; found: C 31.10, H 2.42, N 4.65.

$[(\eta^5\text{-C}_5\text{H}_5)\text{Re}(\text{CO})_2(3,4,5\text{-N}_2\text{C}_6\text{H}_2(\text{OCH}_3)_3)][\text{BF}_4]$ (80). In a fashion similar to the preparation of **78**, treatment of $(\eta^5\text{-C}_5\text{H}_5)\text{Re}(\text{CO})_2(\text{THF})$ (0.100 g, 0.264 mmol) with 3,4,5- $(\text{CH}_3\text{O})_3\text{C}_6\text{H}_3\text{N}_2\text{BF}_4$ (0.059 g, 0.27 mmol) afforded **80** in 61% yield as a red orange crystalline solid. Mp: 194-196 °C (decompose); IR (Nujol, cm^{-1}): $\tilde{\nu}$ = 2066 (s), 2002 (s),

1731 (s), 1590 (s), 1568 (m), 1310 (m), 1229 (s), 1130 (m), 1068 (s), 1028 (s), 892 (w), 840 (m), 803 (w), 771 (w); ^1H NMR (acetone- d_6 , 23 °C): δ = 6.82 (s, 2H, C_6H_2) 6.67 (s, 5H, C_5H_5), 3.89 (s, 6H, 3,5-(OCH_3) $_2$), 3.81 (s, 3H, 4- OCH_3); $^{13}\text{C}\{^1\text{H}\}$ NMR (acetone- d_6 , 23 °C): δ = 187.72 (s, CO), 155.01 (s, 3,5-(OCH_3) $_2$), 143.51 (s, 4- OCH_3), 119.45 (s, N_2CCH), 102.23 (s, $\text{N}_2\text{C}(\text{CH})_2$), 96.57 (s, C_5H_5), 61.28 (s, 4- OCH_3), 56.95 (s, 3,5-(OCH_3) $_2$).

$[(\eta^5\text{-C}_5\text{H}_5)\text{Re}(\text{CO})_2(2\text{-N}_2\text{C}_6\text{H}_4\text{CF}_3)]\text{[BF}_4\text{]} (81)$. In a fashion similar to the preparation of **78**, treatment of $(\eta^5\text{-C}_5\text{H}_5)\text{Re}(\text{CO})_2(\text{THF})$ (0.100 g, 0.264 mmol) with 2- $\text{CF}_3\text{C}_6\text{H}_3\text{N}_2\text{BF}_4$ (0.059 g, 0.27 mmol) afforded **81** in 61% yield as a red orange crystalline solid. Mp: 142-144 °C (decompose); IR (Nujol, cm^{-1}): $\tilde{\nu}$ = 2082 (s), 2047 (m), 2004 (s), 1717 (s), 1597 (m), 1577 (m), 1315 (s), 1271 (m), 1186 (m), 1153 (s), 1143 (s), 1078 (s), 1051 (s), 1034 (s), 968 (w), 891 (w), 847 (w), 781 (w), 766 (m); ^1H NMR (acetone- d_6 , 23 °C): δ = 8.32-7.75 (m, 4H, C_6H_4), 6.74 (s, 5H, C_5H_5); $^{13}\text{C}\{^1\text{H}\}$ NMR (acetone- d_6 , 23 °C): δ = 186.41 (s, CO), 135.71 (s, N_2CCHCH), 133.60 (s, N_2CCH), 128.40 (s, CF_3CCH), 128.32 (s, CF_3CCHCH), 125.46 (s, CF_3CCH), 124.12 (s, CF_3), 121.32 (s, N_2CCH), 97.21 (s, C_5H_5).

$[(\eta^5\text{-C}_5\text{H}_5)\text{Re}(\text{CO})_2(\text{N}_2\text{C}_6\text{H}_5)]\text{[BF}_4\text{]} (82)$. In a fashion similar to the preparation of **78**, treatment of $(\eta^5\text{-C}_5\text{H}_5)\text{Re}(\text{CO})_2(\text{THF})$ (0.100 g, 0.264 mmol) with $\text{C}_6\text{H}_5\text{N}_2\text{BF}_4$ (0.051 g, 0.27 mmol) afforded **82** in 69% yield as a red orange crystalline solid. IR (Nujol, cm^{-1}): $\tilde{\nu}$ = 2071 (s), 2011 (s), 1923 (s), 1756 (s), 1711 (m), 1588 (s), 1574 (m), 1304 (w), 1261 (s), 1094 (s), 1024 (s), 935 (m), 866 (m), 802 (s), 761 (m), 682 (m); ^1H NMR (acetone- d_6 , 23 °C): δ = 7.70-7.58 (m, C_6H_5), 6.67 (s, 5H, C_5H_5); $^{13}\text{C}\{^1\text{H}\}$ NMR (acetone- d_6 , 23 °C): δ = 187.48 (s,

CO), 133.95 (s, N₂CCHCH), 131.55 (s, N₂CCH), 124.74 (s, N₂CCHCHCH), 119.24 (s, N₂CCH), 96.52 (s, C₅H₅).

(η^5 -C₅H₅)Re(CO)(NCO)(4-N₂C₆H₄OCH₃) (84). A 100 mL Schlenk flask was charged with **78** (0.100 g, 0.264 mmol), 20 mL anhydrous acetone, and a stir bar. To the stirred brownish yellow solution at 23 °C, solid NaN₃ (0.059 g, 0.27 mmol) was slowly added and the reaction mixture turned orange red immediately. The mixture was stirred at ambient temperature for 24 h and then dried under reduced pressure. The resultant orange red solid was dissolved in 40 mL Et₂O and the solution was filtered through a 2-cm pad of Celite on a coarse glass frit. The clear orange red filtrate was concentrated to ~10 mL and kept at -25 °C to afford **84** in 50% yield as an orange red crystalline solid. Mp: 133-135 °C (decompose); IR (Nujol, cm⁻¹): $\tilde{\nu}$ = 2244 (s), 1929 (s), 1673 (s), 1591 (w), 1304 (m), 1259 (m), 1154 (w), 1021 (w); ¹H NMR (acetone-d₆, 23 °C): δ = 7.20 (d, J = 9.0 Hz, 2H, N₂C(CH)₂(CH)₂COCH₃), 7.07 (d, J = 9.0 Hz, 2H, N₂C(CH)₂(CH)₂COCH₃), 6.10 (s, 5H, C₅H₅), 3.85 (s, 3H, OCH₃); ¹³C {¹H} NMR (acetone-d₆, 23 °C): δ = 197.12 (s, CO), 161.58 (s, N₂CCH), 137.45 (s, NCO), 127.54 (s, CH₃OCCH), 123.83 (s, N₂CCH), 115.90 (s, CH₃OC(CH)₂), 95.05 (s, C₅H₅), 56.02 (s, 4-OCH₃); elemental analysis calculated for C₁₄H₁₂N₃O₃Re (%): C 36.84, H 2.65, N 9.21; found: C 36.99, H 2.76, N 9.10.

(η^5 -C₅H₅)Re(CO)(NCO)(2,4-N₂C₆H₃(OCH₃)₂) (85). In a fashion similar to the preparation of **84**, treatment of **79** (0.100 g, 0.264 mmol) with NaN₃ (0.059 g, 0.27 mmol) afforded **85** in 77% yield as an orange red crystalline solid. Mp: 159-161 °C (decompose);

IR (Nujol, cm^{-1}): $\tilde{\nu} = 2244$ (s), 1923 (s), 1673 (s), 1596 (m), 1345 (w), 1319 (w), 1284 (m), 1257 (m), 1213 (m), 1163 (m), 1114 (w), 1099 (w), 1028 (m), 966 (w), 891 (w), 770 (w); ^1H NMR (acetone- d_6 , 23 $^\circ\text{C}$): $\delta = 7.28$ -6.04 (m, C_6H_3), 6.06 (s, 5H, C_5H_5), 3.87 (s, 3H, 4- OCH_3), 3.86 (s, 3H, 2- OCH_3); $^{13}\text{C}\{^1\text{H}\}$ NMR (acetone- d_6 , 23 $^\circ\text{C}$): $\delta = 197.70$ (s, CO), 162.81 (s, 2- CH_3OCCH), 155.23 (s, 4- CH_3OCCH), 137.00 (s, NCO), 123.00 (s, N_2CCH), 107.04 (s, N_2CCHCH), 100.15 (s, 2- CH_3OCCH), 99.43 (s, N_2CCH), 94.76 (s, C_5H_5), 56.31 (s, 2- OCH_3), 56.07 (s, 4- OCH_3); elemental analysis calculated for $\text{C}_{15}\text{H}_{14}\text{N}_3\text{O}_4\text{Re}$ (%): C 37.03, H 2.90, N 8.64; found: C 38.73, H 2.99, N 8.64.

($\eta^5\text{-C}_5\text{H}_5$)Re(CO)(NCO)(3,4,5- $\text{N}_2\text{C}_6\text{H}_2(\text{OCH}_3)_3$) (86). In a fashion similar to the preparation of **84**, treatment of **80** (0.100 g, 0.264 mmol) with NaN_3 (0.059 g, 0.27 mmol) afforded **86** in 61% yield as an orange red crystalline solid. Mp: 171-173 $^\circ\text{C}$ (decompose); IR (Nujol, cm^{-1}): $\tilde{\nu} = 2249$ (s), 1925 (s), 1648 (s), 1592 (s), 1572 (s), 1307 (m), 1227 (s), 1169 (w), 1132 (s), 1000 (m), 969 (m), 891 (w), 820 (m); ^1H NMR (acetone- d_6 , 23 $^\circ\text{C}$): $\delta = 6.58$ (s, 2H, C_6H_2) 6.14 (s, 5H, C_5H_5), 3.83 (s, 6H, 3,5- $(\text{OCH}_3)_2$), 3.74 (s, 3H, 4- OCH_3); $^{13}\text{C}\{^1\text{H}\}$ NMR (acetone- d_6 , 23 $^\circ\text{C}$): $\delta = 196.85$ (s, CO), 154.90 (s, 3,5- $(\text{OCH}_3)_2\text{C}$), 139.94 (s, 4- $(\text{OCH}_3)\text{C}$), 137.56 (s, NCO), 130.95 (s, N_2CCH), 100.02 (s, $\text{N}_2\text{C}(\text{CH})_2$), 95.35 (s, C_5H_5), 60.97 (s, 4- OCH_3), 56.46 (s, 3,5- $(\text{OCH}_3)_2$).

($\eta^5\text{-C}_5\text{H}_5$)Re(CO)(NCO)(2- $\text{N}_2\text{C}_6\text{H}_4\text{CF}_3$) (87). In a fashion similar to the preparation of **84**, treatment of **81** (0.100 g, 0.264 mmol) with NaN_3 (0.059 g, 0.27 mmol) afforded **87** in 61% yield as an orange red crystalline solid. Mp: 137.5-138.5 $^\circ\text{C}$

(decompose); IR (Nujol, cm^{-1}): $\tilde{\nu} = 2246$ (s), 1953 (s), 1639 (s), 1577 (m), 1317 (s), 1132 (m), 1109 (w), 1032 (w), 965 (w), 847 (w), 775 (m); ^1H NMR (acetone- d_6 , 23 $^\circ\text{C}$): $\delta = 7.85$ -7.47 (m, 4H, C_6H_4), 6.21 (s, 5H, C_5H_5); $^{13}\text{C}\{^1\text{H}\}$ NMR (acetone- d_6 , 23 $^\circ\text{C}$): $\delta = 196.74$ (s, CO), 137.82 (s, NCO), 134.75 (s, N_2CCHCH), 133.98 (s, N_2CCH), 129.54 (s, CF_3CCHCH), 127.74 (q, $^2\text{J}_{\text{C-F}} = 24$ Hz, CF_3CCH), 125.73 (s, CF_3CCH), 123.51 (q, $^1\text{J}_{\text{C-F}} = 128.1$ Hz, CF_3), 122.18 (s, N_2CCH), 95.98 (s, C_5H_5); elemental analysis calculated for $\text{C}_{14}\text{H}_9\text{N}_3\text{F}_3\text{O}_2\text{Re}$ (%): C 34.01, H 1.83, N 8.50; found: C 34.27, H 1.79, N 8.55.

($\eta^5\text{-C}_5\text{H}_5$)Re(CO)(NCO)($\text{N}_2\text{C}_6\text{H}_5$) (88). In a fashion similar to the preparation of **84**, treatment of **82** (0.100 g, 0.264 mmol) with NaN_3 (0.059 g, 0.27 mmol) afforded **88** in 69% yield as an orange red crystalline solid. Mp: 107-108 $^\circ\text{C}$ (decompose); IR (Nujol, cm^{-1}): $\tilde{\nu} = 2241$ (s), 1933 (s), 1649 (s), 1587 (m), 1571 (m), 1305 (w), 1155 (w), 1073 (w), 1009 (w), 966 (m), 837 (m), 763 (m); ^1H NMR (acetone- d_6 , 23 $^\circ\text{C}$): $\delta = 7.55$ -7.26 (m, C_6H_5), 6.14 (s, 5H, C_5H_5); $^{13}\text{C}\{^1\text{H}\}$ NMR (acetone- d_6 , 23 $^\circ\text{C}$): $\delta = 197.04$ (s, CO), 137.55 (s, NCO), 135.99 (s, N_2CCH), 130.68 (s, N_2CCHCH), 130.14 (s, N_2CCH), 122.37 (s, $\text{N}_2\text{CCHCHCH}$), 95.35 (s, C_5H_5).

($\eta^5\text{-C}_5\text{H}_5$)Re(CO)(COOMe)(4- $\text{N}_2\text{C}_6\text{H}_4\text{NEt}_2$) (89). A 100 mL Schlenk flask was charged with 4-Et $_2\text{NC}_6\text{H}_4\text{N}_2\text{BF}_4$ (0.100 g, 0.380 mmol), NaN_3 (0.027 g, 0.42 mmol), ($\eta^5\text{-C}_5\text{H}_5$)Re(CO) $_2$ (THF) (0.144 g, 0.380 mmol), and a stir bar. MeOH and CH_2Cl_2 were chilled in flasks to -78 $^\circ\text{C}$ by an acetone/dry ice bath. To the solid reactants mixture at -78 $^\circ\text{C}$, 10 mL pre-cooled MeOH and 20 mL pre-cooled CH_2Cl_2 were injected. The

greenish yellow reaction mixture was stirred at $-78\text{ }^{\circ}\text{C}$ for 10 h and then allowed to warm to ambient temperature. The volatile components were removed from the reaction mixture under reduced pressure. The resultant brown solid was dissolved in 40 mL Et_2O and the solution was filtered through a 2-cm pad of Celite on a coarse glass frit. The brown filtrate was dried under reduced pressure and the resultant brown solid was dissolved in 10 mL toluene. The solution was concentrated to ~ 3 mL and kept at $-25\text{ }^{\circ}\text{C}$ to afford **89** in 50% yield as an golden yellow solid. IR (Nujol, cm^{-1}): $\tilde{\nu} = 1914$ (s), 1663 (s), 1613 (s), 1595 (s), 1561 (m), 1510(s), 1407 (m), 1304 (m), 1273 (m), 1262 (m), 1216 (w), 1196 (w), 1140 (m), 1094 (m), 1077 (w), 1064 (m), 1041 (s), 815 (s), 772 (w); ^1H NMR (acetone- d_6 , $23\text{ }^{\circ}\text{C}$): $\delta = 7.28\text{-}6.73$ (m, C_6H_4), 5.90 (s, 5H, C_5H_5), 3.49 (s, 3H, COOCH_3), 3.46 (q, $J = 7.1$ Hz, 4H, $\text{N}(\text{CH}_2\text{CH}_3)_2$), 1.15 (t, $J = 6.9$ Hz, 6H, $\text{N}(\text{CH}_2\text{CH}_3)_2$).

($\eta^5\text{-C}_5\text{H}_5$)Re(CO)(NCO)(4- $\text{N}_2\text{C}_6\text{H}_4\text{NEt}_2$) (90). In the preparation of **89**, after isolation of the golden yellow crystalline **89**, the mother liquor was dried under vacuum. The resulted brown red solid was dissolved in 20 mL Et_2O and concentrated to ~ 5 mL. The solution was kept at $-25\text{ }^{\circ}\text{C}$ to afford **90** in 30 % yield as an orange red crystalline solid. Mp: $148\text{-}149\text{ }^{\circ}\text{C}$ (decompose); IR (Nujol, cm^{-1}): $\tilde{\nu} = 2233$ (s), 2049 (s), 1659 (s), 1588 (s), 1561 (m), 1508 (s), 1404 (m), 1308 (w), 1270 (s), 1207 (m), 1195 (w), 1158 (w), 1134 (m), 1094 (w), 1075 (w), 1009 (w), 815 (s), 681 (w); ^1H NMR (acetone- d_6 , $23\text{ }^{\circ}\text{C}$): $\delta = 7.05\text{-}6.76$ (m, C_6H_4), 6.04 (s, 5H, C_5H_5), 3.47 (q, $J = 7.2$ Hz, 4H, $\text{N}(\text{CH}_2\text{CH}_3)_2$), 1.15 (t, $J = 7.2$ Hz, 6H, $\text{N}(\text{CH}_2\text{CH}_3)_2$); $^{13}\text{C}\{^1\text{H}\}$ NMR (acetone- d_6 , $23\text{ }^{\circ}\text{C}$): $\delta = 197.58$ (s, CO), 149.59 (s, Et_2NCCH),

137.19 (s, NCO), 123.91 (s, N₂CCH), 120.14 (s, N₂CCH), 112.79 (s, Et₂NCCH), 94.50 (s, C₅H₅), 45.00 (s, N(CH₂CH₃)₂), 12.81 (s, N(CH₂CH₃)₂).

CHAPTER 7

CONCLUSION

New energetic materials are under continuous exploration to satisfy the growing demands of industrial and military applications. Although the achievement of higher energy contents of energetic materials is a general goal to optimize a material for a specific task, the safety properties, such as toxicity and sensitivities to classical stimuli, are also very important, since too many of them may cause various unwanted effects in the processes of manufacture, transportation, and usage. Consequently, materials with better explosive performance and/or reasonable insensitivities are highly desired. The goal is to create relatively safe materials with large amounts of stored chemical energy that can be delivered to the particular target. Recently, nitrogen-rich compounds have been studied as a new class of energetic materials which rely on their large positive heats of formation for energy liberation. These compounds are superior to existing energetic materials because they can produce bigger explosions by liberating more gaseous products which are mainly non-toxic elemental nitrogen. This thesis has focused on the synthesis and characterization of new high nitrogen metal complexes containing tetrazolate, poly(tetrazolyl)borate, and aryl pentazolate ligands for potential application as energetic materials.

Metal tetrazolates usually possess good thermal stabilities and insensitivities to mechanical stimuli and electrical discharge owing to the aromaticity of the five-membered heterocyclic tetrazolate groups. Heavier alkaline earth metal tetrazolates have been investigated by spectral and analytical methods. The complexes were prepared both in their

anhydrous form and as aqua ligand containing crystals. The coordination strength of water molecules to the metal ions increase in the order $\text{Ba}^{2+} < \text{Sr}^{2+} < \text{Ca}^{2+}$, which is in accordance with the increasing Lewis acidities of the metal ions. The complexes are thermally stable up to 325 °C, and are insensitive toward shock, friction, and electrostatic discharge. The calcium and strontium complexes have potential use as propellants or secondary energetic materials, while the barium complexes may behave as primary energetic materials. The high physical and thermal stability makes these group 2 metal tetrazolates good candidates for colorants in pyrotechnic mixtures. In particular, the strontium tetrazolate pentahydrate is a promising red color generating agent.

In the construction of new nitrogen-rich energetic metal complexes, it is more efficient to achieve high nitrogen contents by using poly(tetrazolyl)borates instead of tetrazolate ligands because poly(tetrazolyl)borates can release more nitrogen gas per negative charge than the tetrazolate ligands. A range of potassium complexes containing bis(tetrazolyl)borate ligands and their 18-crown-6 adducts have been synthesized and characterized. In the solid state, the potassium bis(tetrazolyl)borates exhibit three dimensional polymeric structures, while the 18-crown-6 adducts exist either as a one dimensional polymer or as a molecular monomer. With small functional groups on the core carbon atom of the tetrazolyl rings, the boron-nitrogen bonds form to the nitrogen atoms proximal to the carbon atom and the ligands adopt bridging coordination modes to the $[\text{K}(18\text{-crown-6})]^+$ fragments, whereas with larger substituents the boron-nitrogen bonds are

to the nitrogen atoms distal to the core carbon and the ligands take on κ^3 -N,N',H-chelating coordination modes. The new complexes are air stable and have thermal decomposition temperatures higher than 210 °C as evidenced by TGA. They are insensitive toward impact, friction, and spark, but deflagrate when burned in a Bunsen burner flame. These potassium bis(tetrazolyl)borate complexes are potential secondary energetic materials and they can serve as starting materials to make other metal bis(tetrazolyl)borate complexes.

In order to transfer the bis(tetrazolyl)borate ligands to metal ions with higher charges, a series of group 2 metal bis(5-methyltetrazolyl)borate complexes has been synthesized. The new complexes are fully characterized by spectral, analytical, and X-ray spectroscopic methods. They are insensitive toward impact, friction, and electrostatic discharge, but deflagrate more violently in the flame tests compared with the potassium complex of the same ligand. These group 2 metal complexes are thermally stable up to 230 °C as indicated by TGA and have potential for as secondary energetic materials or as colorants in pyrotechnic formulations.

A series of sodium cyano(tetrazolyl)borate complexes has been synthesized and structurally characterized. The complexes were isolated as crystals with methanol ligands/solvates and solvent-free crystals. The methanol molecules are lost rapidly at ambient temperature from the crystals once they are separated from the solution. With high nitrogen contents and thermal decomposition temperatures higher than 230 °C, these sodium complexes are potential nitrogen-rich energetic materials and can be used as starting

materials to prepare other metal complexes.

Attempted experiments have been carried out to stabilize the aryl pentazole ligands by an electron-rich, chemically inert metal center. A range of rhenium(I) isocyanate complexes has been prepared from the reaction of the corresponding rhenium(I) aryldiazenido complexes with sodium azide. A mixture of two products including the isocyanate complex $(\eta^5\text{-C}_5\text{H}_5)\text{Re}(\text{CO})(\text{NCO})(\text{N}_2\text{C}_6\text{H}_5\text{NEt}_2)$ and a methoxycarbonyl complex $(\eta^5\text{-C}_5\text{H}_5)\text{Re}(\text{CO})(\text{COOCH}_3)(\text{N}_2\text{C}_6\text{H}_5\text{NEt}_2)$ has been isolated from the reaction of $\text{CpRe}(\text{CO})_2(\text{THF})$ with $\text{Et}_2\text{NC}_6\text{H}_5\text{N}_5$ made *in situ*. The [3+2] cycloaddition reactions between azide ion and the rhenium-coordinated diazonium ions do not proceed to the desired aryl pentazole complexes and the attempted preparation of rhenium aryl pentazole complexes failed.

REFERENCES

1. (a) Olah, G. A.; Squire, D. R. *Chemistry of Energetic Materials*; Academic Press, Inc.: San Diego, California, 1991. (b) Nielsen, A. T. *Nitro Compounds: Recent Advances in Synthesis and Chemistry*; VCH: New York, NY, 1990. (c) Brill, T. B. *Decomposition, Combustion, and Detonation Chemistry of Energetic Materials*; Materials Research Society: Pittsburgh, PA, 1996.
2. Akhavan, J. *The Chemistry of Explosives*. 2nd ed.; RSC: Cambridge, UK, 2004.
3. (a) Huynh, M. H. V.; Coburn, M. D.; Meyer, T. J.; Wetzler, M. *PNAS* **2006**, *103*, 10322-10327. (b) Huynh, M. H. V.; Hiskey, M. A.; Meyer, T. J.; Wetzler, M. *PNAS* **2006**, *103*, 5409-5412.
4. (a) Patinkin, S. H.; Horwitz, J. P.; Lieber, E. *J. Am. Chem. Soc.* **1955**, *77*, 562-567. (b) Mei, G. C.; Pickett, J. W. *Propellants Explos. Pyrotech.* **1998**, *23*, 172-178.
5. (a) Xue, H.; Twamley, B.; Shreeve, J. M. *Inorg. Chem.* **2005**, *44*, 7009-7013. (b) Xue, H.; Gao, Y.; Twamley, B.; Shreeve, J. M. *Chem. Mater.* **2005**, *17*, 191-198.
6. (a) Klapötke, T. M.; Mayer, P.; Sabaté, C. M.; Welch, J. M.; Wiegand, N. *Inorg. Chem.* **2008**, *47*, 6014-6027. (b) Karaghiosoff, K.; Klapötke, T. M.; Mayer, P.; Sabaté, C. M.; Penger, A.; Welch, J. M. *Inorg. Chem.* **2008**, *47*, 1007-1019. (c) Ye, C.; Gao, H.; Shreeve, J. M. *J. Fluorine Chem.* **2007**, *128*, 1410-1415.
7. Klapötke, T. M. *High Energy Density Materials*; Springer: Berlin, 2007.
8. (a) Singh, R. P.; D. Verma, R.; Meshri, D. T.; Shreeve, J. M. *Angew. Chem. Int. Ed.* **2006**,

- 45, 3584-3601. (b) Steinhauser, G.; Klapötke, T. M. *Angew. Chem. Int. Ed.* **2008**, *47*, 3330-3347.
9. (a) Butler, R. N. *Comprehensive Heterocyclic Chemistry II*; Pergamon Press: Oxford, 1996. (b) Gaponik, P. N.; Voitekhovich, S. V.; Ivashkevich, O. A. *Russ. J. Chem. Rev.* **2006**, *75*, 507-539. (c) Momose, Y.; Maekawa, T.; Odaka, H.; Ikeda, H.; Sohda, T. *Chem. Pharm. Bull.* **2002**, *50*, 100-111.
10. (a) Mckie, H. A.; Friedland, S.; Hof, F. *Org. Lett.* **2008**, *10*, 4653-4655. (b) Herr, R. J. *Bioorg. Med. Chem.* **2002**, *10*, 3379-3393. (c) Singh, H.; Chawla, A. S.; Kapoor, V. K.; Paul, D.; Malhotra, R. K. *Prog. Med. Chem.* **1980**, *17*, 151-183.
11. (a) Joo, Y. H.; Shreeve, J. M. *Eur. J. Inorg. Chem.* **2009**, 3573-3578. (b) Ostrovskii, V. A.; Pevzner, M. S.; Kofmna, T. P.; Shcherbinin, M. B.; Tselinskii, I. V. *Targets Heterocycl. Syst.* **1999**, *3*, 467-526.
12. v. Braun, J.; Keller, W. *Ber. Dtsch. Chem. Ges.* **1932**, *65*, 1677-1680.
13. (a) Koguro, K.; Oga, T.; Mitsui, S.; Orita, R. *Synthesis* **1998**, *30*, 910-914. (b) Garbrecht, W. L.; Herbst, R. M. *J. Org. Chem.* **1953**, *18*, 1003-1013.
14. (a) Demko, Z. P.; Sharpless, K. B. *J. Org. Chem.* **2001**, *66*, 7945-7950. (b) Himo, F.; Demko, Z. P.; Noodleman, L.; Sharpless, K. B. *J. Am. Chem. Soc.* **2002**, *124*, 12210-12216. (c) Himo, F.; Demko, Z. P.; Noodleman, L.; Sharpless, K. B. *J. Am. Chem. Soc.* **2003**, *125*, 9983-9987.
15. Myznikov, L. V.; Roh, J.; Artamonova, T. V.; Hrabalek, A.; Koldobskii, G. I. *Russ. J.*

Org. Chem. **2007**, *43*, 765-767.

16. Rostamizadeh, S.; Ghaieni, H.; Aryan, R.; Amani, A. *Chin. Chem. Lett.* **2009**, *20*, 1311-1314.
17. Kantam, M. L.; Kumar, K. B. S.; Sridhar, C. *Adv. Synth. Catal.* **2005**, *347*, 1212-1214.
18. Kantam, M. L.; Balasubrahmanyam, V.; Kumar, K. B. S. *Synth. Commun.* **2006**, *36*, 1809-1814.
19. Kantam, M. L.; Kumar, K. B. S.; Raja, K. P. *J. Mol. Catal. A: Chem.* **2006**, *247*, 186-188.
20. Venkateshwarlu, G.; Premalatha, A.; Rajanna, K. C.; Saiprakash, P. K. *Synth. Commun.* **2009**, *39*, 4479-4485.
21. He, J.; Li, B.; Chen, F.; Z., X.; Yin, G. *J. Mol. Catal. A: Chem.* **2009**, *304*, 135-138.
22. Venkateshwarlu, G.; Rajanna, K. C.; Saiprakash, P. K. *Synth. Commun.* **2009**, *39*, 426-432.
23. Nasrollahzadeh, M.; Bayat, Y.; Habibi, D.; Moshae, S. *Tetrahedron Lett.* **2009**, *50*, 4435-4438.
24. Das, B.; Reddy, C. R.; Kumar, D. N.; Krishnaiah, M.; Narender, R. *synlett.* **2010**, *21*, 391-394.
25. Roh, J.; Artamonova, T. V.; Vávrová, K.; Koldobskii, G. I.; Hrabálek, A. *Synthesis* **2009**, *41*, 2175-2178.
26. Aureggi, V.; Sedelmeier, G. *Angew. Chem. Int. Ed.* **2007**, *46*, 8440-8444.

27. Amantini, D.; Beleggia, R.; Fringuelli, F.; Pizzo, F.; Vaccaro, L. *J. Org. Chem.* **2004**, *69*, 2896-2898.
28. (a) Jin, T.; Kitahara, F.; Kamijo, S.; Yamamoto, Y. *Tetrahedron Lett.* **2008**, *49*, 2824-2827. (b) Jin, T.; Kitahara, F.; Kamijo, S.; Yamamoto, Y. *Chem. Asian J.* **2008**, *3*, 1575-1580.
29. Bonnamour, J.; Bolm, C. *Chem. Eur. J.* **2009**, *15*, 4543-4545.
30. (a) Ernst, W.; Klapötke, T. M.; Stierstorfer, J. *Z. Anorg. Allg. Chem.* **2007**, *633*, 879-887. (b) Klapötke, T. M.; Stein, M.; Stierstorfer, J. *Z. Anorg. Allg. Chem.* **2008**, *634*, 1711-1723.
31. Arp, H. P. H.; Decken, A.; Passmore, J.; Wood, D. J. *Inorg. Chem.* **2000**, *39*, 1840-1848.
32. (a) Klapötke, T. M.; Sabaté, C. M.; Welch, J. M. *Dalton Trans.* **2008**, 6372-6380. (b) Klapötke, T. M.; Sabaté, C. M.; Welch, J. M. *Eur. J. Inorg. Chem.* **2009**, 769-776. (c) Klapötke, T. M.; Stierstorfer, J. *J. Am. Chem. Soc.* **2009**, *131*, 1122-1134.
33. (a) Zheng, L. L.; Li, H. X.; Leng, J. D.; Wang, J.; Tong, M. L. *Eur. J. Inorg. Chem.* **2008**, 213-217. (b) Zhang, X. M.; Jiang, T.; Wu, H. S.; Zeng, M. H. *Inorg. Chem.* **2009**, *48*, 4536-4541. (c) Pachfule, P.; Das, R.; Poddar, P.; Banerjee, R. *Cryst. Growth Des.* **2010**, *10*, 2475-2478.
34. (a) Fu, D. W.; Dai, J.; Ge, J. Z.; Ye, H. Y.; Qu, Z. R. *Inorg. Chem. Commun.* **2010**, *13*, 282-285. (b) Zhong, D. C.; Lin, J. B.; Lu, W. G.; Jiang, L.; Lu, T. B. *Inorg. Chem.* **2009**,

- 48, 8656-8658. (c) Liu, D. S.; Sui, Y.; Huang, C. C.; Pan, T. H.; Huang, X. H.; Chen, J. Z.; You, X. Z. *Inorg. Chem. Commun.* **2010**, *13*, 762-765. (d) Tong, X. L.; Wang, D. Z.; Hu, T. L.; Song, W. C.; Tao, Y.; Bu, X. H. *Cryst. Growth Des.* **2009**, *9*, 2280-2286. (e) Hu, T.; Liu, L.; Lv, X.; Chen, X.; He, H.; Dai, F.; Zhang, G.; Sun, D. *Polyhedron* **2010**, *29*, 296-302. (f) Wang, X. W.; Chen, J. Z.; Liu, J. H. *Cryst. Growth Des.* **2007**, *7*, 1227-1229. (g) Fu, D. W.; Ge, J. Z.; Dai, J.; Ye, H. Y.; Qu, Z. R. *Inorg. Chem. Commun.* **2009**, *12*, 994-997. (h) Fu, D. W.; Ge, J. Z.; Zhang, Y.; Ye, H. Y. *Z. Anorg. Allg. Chem.* **2009**, *635*, 2631-2635.
35. Kobrsi, I.; Zheng, W.; Knox, J., E.; Heeg, M. J.; Schlegel, H. B.; Winter, C. H. *Inorg. Chem.* **2006**, *45*, 8700-8710.
36. Poturovic, S.; Lu, D.; Heeg, M. J.; Winter, C. H. *Polyhedron* **2008**, *27*, 3280-3286.
37. Fried, L. E.; Manaa, M. R.; Pagoria, P. F.; Simpson, R. L. *Annu. Rev. Mater. Sci.* **2001**, *31*, 291-321.
38. Klapötke, T. M.; Radies, H.; Stierstorfer, J. *Z. Naturforsch.* **2007**, *62b*, 1343-1352.
39. Hammerl, A.; Holl, G.; Kaiser, M.; Klapötke, T. M.; Piotrowski, H. *Z. Anorg. Allg. Chem.* **2003**, *629*, 2117-2121.
40. (a) Hammerl, A.; Holl, G.; Klapötke, T. M.; Mayer, P.; Nöth, H.; Piotrowski, H.; Warchhold, M. *Eur. J. Inorg. Chem.* **2002**, 834-845. (b) Klapötke, T. M.; Sabaté, C. M. *Z. Anorg. Allg. Chem.* **2007**, *633*, 2671-2677.
41. Klapötke, T. M.; Sabaté, C. M.; Rasp, M. *Dalton Trans.* **2009**, 1825-1834.

42. Kobrsi, I.; Knox, J. E.; Heeg, M. J.; Schlegel, H. B.; Winter, C. H. *Inorg. Chem.* **2005**, *44*, 4894-4896.
43. Karaghiosof, K.; Klapötke, T. M.; Sabaté, C. M. *Eur. J. Inorg. Chem.* **2009**, 238-250.
44. Klapötke, T. M.; Stierstorfer, J.; Tarantik, K. R.; Thoma, I. D. *Z. Anorg. Allg. Chem.* **2008**, *634*, 2777-2784.
45. Klapötke, T. M.; Sabaté, C. M. *Dalton Trans.* **2009**, 1835-1841.
46. Friedrich, M.; Gálvez-Ruiz, J. C.; Klapötke, T. M.; Mayer, P.; Weber, B.; Weigand, J. J. *Inorg. Chem.* **2005**, *44*, 8044-8052.
47. (a) Geisberger, G.; Klapötke, T. M.; Stierstorfer, J. *Eur. J. Inorg. Chem.* **2007**, 4743-4750. (b) Klapötke, T. M.; Stierstorfer, J.; Weber, B. *Inorg. Chim. Acta* **2009**, *362*, 2311-2320.
48. Tao, G. H.; Twamley, B.; Shreeve, J. M. *Inorg. Chem.* **2009**, *48*, 9918-9923.
49. Karaghiosoff, K.; Klapötke, T. M.; Sabaté, C. M. *Chem. Eur. J.* **2009**, *15*, 1164-1176.
50. Bronisz, R. *Inorg. Chim. Acta* **2002**, *340*, 215-220.
51. Lin, J. M.; Guan, Y. F.; Dong, W. *Acta Cryst.* **2008**, *E64*, m238.
52. (a) Jia, Q. X.; Qian, X. B.; Wu, H. H.; Wang, Q. L.; Gao, E. Q. *Inorg. Chim. Acta* **2009**, *362*, 2213-2216. (b) Lin, J. M.; Guan, Y. F.; Dong, W. *Acta Cryst.* **2007**, *E63*, m3017. (c) Zhang, J. G.; Li, Z. M.; Zang, Y.; Zhang, T. L.; Shu, Y. J.; Yang, L.; Power, P. P. *J. Hazard. Mater.* **2010**, *178*, 1094-1099. (d) Lin, J. M.; Huang, B. S.; Guan, Y. F.; Liu, Z. Q.; Wang, D. Y.; Dong, W. *Cryst. Eng. Commun.* **2009**, *11*, 329-336.

53. (a) Poganiuch, P.; Decurtins, S.; Gütlich, P. *J. Am. Chem. Soc.* **1990**, *112*, 3270-3278. (b) Guan, Y. F.; Zhou, A. J.; Wang, D. Y.; Wang, J.; Dong, W. *J. Mol. Struct.* **2009**, *938*, 150-155.
54. (a) Steinhauser, G.; Giester, G.; Leopold, N.; Wagner, C.; Villa, M.; Musilek, A. *Helv. Chim. Acta* **2010**, *93*, 183-202. (b) Steinhauser, G.; Giester, G.; Leopold, N.; Wagner, C.; Villa, M. *Helv. Chim. Acta* **2009**, *92*, 2038-2051. (c) Steinhauser, G.; Giester, G.; Wagner, C.; Leopold, N.; Sterba, J. H.; Lendl, B.; Bichler, M. *Helv. Chim. Acta* **2009**, *92*, 1371-1384.
55. Eulgen, P. J.; Klein, A.; Maggiorosa, N.; Naumann, D.; Pohl, R. W. H. *Chem. Eur. J.* **2008**, *14*, 3727-3736.
56. Gálvez-Ruiz, J. C.; Holl, G.; Karaghiosoff, K.; Klapötke, T. M.; Lohnwitz, K.; Mayer, P.; Noth, H.; Polborn, K.; Rohbogner, C. J.; Suter, M.; Weigand, J. J. *Inorg. Chem.* **2005**, *44*, 4237-4253.
57. (a) Neutz, J.; Grosshardt, O.; Schäufele, S.; Schuppler, H.; Schweikert, W. *Propellants Explos. Pyrotech.* **2003**, *28*, 181-188. (b) Tao, G. H.; Guo, Y.; Joo, Y. H.; Twamley, B.; Shreeve, J. M. *J. Mater. Chem.* **2008**, *18*, 5524-5530. (c) Wang, R.; Guo, Y.; Zheng, Z.; Shreeve, J. M. *Chem. Commun.* **2009**, 2697-2699. (d) Wang, R.; Guo, Y.; Zeng, Z.; Twamley, B.; Shreeve, J. M. *Chem. Eur. J.* **2009**, *15*, 2625-2634.
58. (a) Joo, Y. H.; Shreeve, J. M. *Chem. Eur. J.* **2009**, *15*, 3198-3203. (b) Xue, H.; Gao, H.; Twamley, B.; Shreeve, J. M. *Chem. Mater.* **2007**, *19*, 1731-1739. (c) Xue, H.; Gao, Y.;

- Twamley, B.; Shreeve, J. M. *Inorg. Chem.* **2005**, *44*, 5068-5072. (d) Ye, C.; Xiao, J. C.; Twamley, B.; Shreeve, J. M. *Chem. Commun.* **2005**, 2750-2752. (e) Klapötke, T. M.; Sabaté, C. M.; Welch, J. M. *Z. Anorg. Allg. Chem.* **2008**, *634*, 857-866. (f) Klapötke, T. M.; Karaghiosoff, K.; Mayer, P.; Penger, A.; Welch, J. M. *Propellants Explos. Pyrotech.* **2006**, *31*, 188-195.
59. Crawford, M. J.; Karaghiosoff, K.; Klapötke, T. M.; Martin, F. A. *Inorg. Chem.* **2009**, *48*, 1731-1743.
60. Hammerl, A.; Klapötke, T. M.; Nöth, H.; Warchhold, M. *Inorg. Chem.* **2001**, *40*, 3570-3575.
61. (a) Trofimenko, S. *Scorpionates: The Coordination Chemistry of Polypyrazolylborate Ligands*; Imperial College Press: London, 1999. (b) Prananto, Y. P.; Turner, D. R.; Duriska, M. B.; Lu, J.; Batten, S. R. *Inorg. Chim. Acta* **2009**, *362*, 4646-4650. (c) Chávez-Gil, T.; Cedeño, D. L.; Hamaker, C. G.; Vega, M.; Rodriguez, J. *J. Mol. Struct.* **2008**, *888*, 168-172. (d) Loroño-Gonzalez, D. J. *Acta Crystallogr., Sect. C: Cryst. Struct. Commun.* **2008**, *C64*, m228-m232. (e) Reger, D. L.; Pender, M. J.; Caulder, D. L.; Reger, L. B.; Rheingold, A. L.; Liable-Sands, L. M. *J. Organomet. Chem.* **1996**, *512*, 91-96. (f) Dias, H. V. R.; Gorden, J. D. *Inorg. Chem.* **1996**, *35*, 318-324.
62. (a) Pettinari, C.; Cingolani, A.; Lobbia, G. G.; Marchetti, F.; Martini, D.; Pellei, M.; Pettinari, R.; Santini, C. *Polyhedron* **2004**, *23*, 451-469. (b) Saly, M. J.; Heeg, M. J.; Winter, C. H. *Inorg. Chem.* **2009**, *48*, 5303-5312. (c) Dias, H. V. R.; Fianchini, M.

- Comments Inorg. Chem.* **2007**, *28*, 73-92. (d) Blagg, R. J.; Adams, C. J.; Clarmant, J. P. H.; Connelly, N. G.; Haddow, M. F.; Hamilton, A.; Knight, J.; Orpen, A. G.; Ridgeway, B. M. *Dalton Trans.* **2009**, 8724-8736. (e) Kou, X.; Wu, J.; Cundari, T. R.; Dias, H. V. R. *Dalton Trans.* **2009**, 915-917. (f) Marzano, C.; Pellei, M.; Alidori, S.; Brossa, A.; Lobbia, G. G.; Tisato, F.; Santini, C. *J. Inorg. Biochem.* **2006**, *100*, 299-304. (g) Slugovc, C.; Padilla-Martinez, I.; Sirol, S.; Carmona, E. *Coord. Chem. Rev.* **2001**, *213*, 129-157.
63. Janiak, C.; Esser, L. *Z. Naturforsch. B* **1993**, *48*, 394-396.
64. (a) Janiak, C.; Scharmann, T. G.; Brzenzinka, K. W.; Reich, P. *Chem. Ber.* **1995**, *128*, 323-328. (b) Janiak, C.; Scharmann, T. G.; Günther, W.; Girgsdies, F.; Hemling, H.; Hinrichs, W.; Lentz, D. *Chem. Eur. J.* **1995**, *1*, 637-644. (c) Janiak, C. *J. Chem. Soc., Chem. Commun.* **1994**, 545-547.
65. (a) Janiak, C.; Scharmann, T. G.; Green, J. C.; Parkin, R. P. G.; Kolm, M. J.; Riedel, E.; Mickler, W.; Elguero, J.; Claramunt, R. M.; Sanz, D. *Chem. Eur. J.* **1996**, *2*, 992-1000. (b) Janiak, C.; Scharmann, T. G. *Polyhedron* **2003**, *22*, 1123-1133.
66. Groshens, T. J. *J. Coord. Chem.* **2010**, *63*, 1882-1892.
67. Wang, Y. L.; Cao, R.; Bi, W. H. *Polyhedron* **2005**, *24*, 585-591.
68. (a) Alvarez, H. M.; Tran, T. B.; Richter, M. A.; Alyounes, D. M.; Rabinovich, D. *Inorg. Chem.* **2003**, *42*, 2109-2114. (b) Alvarez, H. M.; Krawiec, M.; Donovan-merkert, B. T.; Fouzi, M.; Rabinovich, D. *Inorg. Chem.* **2001**, *40*, 5736-5737.
69. (a) Tsipis, A. C.; Chaviara, A. T. *Inorg. Chem.* **2004**, *43*, 1273-1286. (b) Hammerl, A.;

- Klapötke, T. M.; Schwerdtfeger, P. *Chem. Eur. J.* **2003**, *9*, 5511-5519. (c) Straka, M. *Inorg. Chem.* **2003**, *42*, 8241-8249.
70. (a) Christe, K. O.; Wilson, W. W.; Sheehy, J. A.; Boatz, J. A. *Angew. Chem. Int. Ed.* **1999**, *38*, 2004-2009. (b) Vij, A.; Pavlovich, J. G.; Wilson, W. W.; Vij, V.; Christe, K. O. *Angew. Chem. Int. Ed.* **2002**, *41*, 3051-3054. (c) Butler, R. N.; Fox, A.; Collier, S.; Burke, L. A. *Perkin Trans. 2* **1998**, 2243-2247.
71. Östmark, H.; Wallin, S.; Brinck, T.; Carlqvist, P.; Claridge, R.; Hedlund, E.; Yudina, L. *Chem. Phys. Lett.* **2003**, *379*, 539-546.
72. (a) Huisgen, R.; Ugi, I. *Angew. Chem.* **1956**, *68*, 705-706. (b) Ugi, I. *Comprehensive Heterocyclic Chemistry*; Pergamon Press: Oxford, 1996.
73. (a) Wallis, J. D.; Dunitz, J. D. *J. Chem. Soc., Chem. Commun.* **1983**, 910-911. (b) Bieseimer, F.; Müller, U.; Massa, W. Z. *Z. Anorg. Allg. Chem.* **2002**, *628*, 1933-1934.
74. Carlqvist, P.; Östmark, H.; Brinck, T. *J. Phys. Chem. A* **2004**, *108*, 7463-7467.
75. Benin, V.; Kaszynski, P.; Radziszewski, J. G. *J. Org. Chem.* **2002**, *67*, 1354-1358.
76. Butler, R. N.; Stephens, J. C.; Burke, L. A. *Chem. Commun.* **2003**, 1016-1017.
77. Schroer, T.; Haiges, R.; Schneider, S.; Christe, K. O. *Chem. Commun.* **2005**, 1607-1609.
78. (a) Guo, Y.; Tao, G. H.; Zeng, Z.; Gao, H.; Parrish, D. A.; Shreeve, J. M. *Chem. Eur. J.* **2010**, *16*, 3753-3762. (b) Tao, G. H.; Guo, Y.; Parrish, D. A.; Shreeve, J. M. *J. Mater. Chem.* **2010**, *10*, 2999-3005. (c) Chavez, D. E.; Tappan, B. C.; Mason, B. A. *Propellants Explos. Pyrotech.* **2009**, *34*, 475-479.

79. Giles, J. *Nature* **2004**, *427*, 580-581.
80. Xue, H.; Y. Gao; Twamley, B.; Shreeve, J. M. *Inorg. Chem.* **2004**, *43*, 7972-7977.
81. Klapötke, T. M. *Propellants Explos. Pyrotech.* **2010**, *35*, 213-219.
82. (a) Eberspächer, M.; Klapötke, T. M.; Sabaté, C. M. *New J. Chem.* **2009**, *33*, 517-527.
(b) Singh, G.; Prajapati, R.; Frohlich, R. *J. Hazard. Mater.* **2005**, *118*, 75-78.
83. (a) Lopez, C.; Claramunt, R. M.; Sanz, D.; Foces Foces, C.; Cano, F. H.; Faure, R.; Cayon, E.; Elguero, J. *J. Inorg. Chim. Acta* **1990**, *176*, 195-204. (b) Northcutt, T. O.; Lachicotte, R. J.; Jones, W. D. *Organometallics* **1998**, *17*, 5148-5152. (c) Bucher, U. E.; Currao, A.; Nesper, R.; Rügger, H.; Venanzi, L. M.; Younger, E. *Inorg. Chem.* **1995**, *34*, 66-74.
84. Webster, C. E.; Hall, M. B. *Inorg. Chim. Acta* **2002**, *330*, 268-282.
85. (a) Trofimenko, S. *J. Am. Chem. Soc.* **1967**, *89*, 3170-3177. (b) Trofimenko, S. *J. Am. Chem. Soc.* **1967**, *89*, 6288-6294. (c) Trofimenko, S. *Chem. Rev.* **1993**, *93*, 943-980.
86. Bondi, A. *J. Phys. Chem.* **1964**, *68*, 441-451.
87. Ruiz, J. C. G.; Nöth, H.; Warchhold, M. *Eur. J. Inorg. Chem.* **2008**, 251-266.
88. Xu, Y.; Zhao, F.; Zhang, Y.; Gu, Y.; Liu, T.; Cui, J. *Int. J. Quantum Chem.* **2010**, *110*, 1235-1244.
89. Zeng, Z.; Twamley, B.; Shreeve, J. M. *Organometallics* **2007**, *26*, 1782-1787.
90. (a) Santini, C.; Pellei, M.; Alidori, S.; Lobbia, G. G.; Benetollo, F. *Inorg. Chim. Acta* **2007**, *360*, 2121-2127. (b) Pellei, M.; Benetollo, F.; Lobbia, G. G.; Alidori, S.; Santini,

C. Inorg. Chem. **2005**, *44*, 846-848.

91. Lu, D.; Winter, C. H. *Inorg. Chem.* **2010**, *49*, 5795-5797.
92. Jones, H. C. *Principles of Inorganic Chemistry*; Macmillan: London, 1906.
93. Györi, B.; Berente, Z.; Lázár, I. *Polyhedron* **1998**, *17*, 3175-3180.
94. Spielvogel, B. F. *Phosphorus Sulfur* **1994**, *87*, 267-276.
95. (a) Mason, R.; Thomas, K. M.; Zubieta, J. A.; Douglas, P. G.; Galbraith, A. R.; Shaw, B. *L. J. Am. Chem. Soc.* **1974**, *96*, 260-262. (b) Barrientos-Penna, C. F.; Einstein, F. W. B.; Jones, T.; Sutton, D. *Inorg. Chem.* **1982**, *21*, 2578-2585.
96. Barrientos-Penna, C. F.; Klahn-Oliva, A. H.; Sutton, D. *Organometallics* **1985**, *4*, 367-373.
97. Roe, A. *Organic Reactions*; John Wiley & Sons: New York, 1957.
98. (a) Green, M. L. H.; Wilkinson, G. *J. Chem. Soc.* **1958**, 4314-4317. (b) Agbossou, F.; O'Connor, E.; Garner, C. M.; Méndez, N. Q.; Fernández, J. M.; Patton, A. T.; Ramsden, J. A.; A., G. J. *Inorg. Synth.* **1992**, *29*, 211-225.

ABSTRACT**SYNTHESIS AND CHARACTERIZATION OF METAL COMPLEXES
CONTAINING TETRAZOLATE, POLY(TETRAZOLYL)BORATE, AND ARYL
PENTAZOLE LIGANDS AS HIGH ENERGY DENSITY MATERIALS**

by

DONGMEI LU

December 2010

Advisor: Dr. Charles H. Winter**Major:** Chemistry (Inorganic)**Degree:** Doctor of Philosophy

Heavier alkaline earth metal tetrazolates have been prepared as crystals containing aqua ligands and as anhydrous powders, and have been characterized by spectral and analytical methods. Potassium bis(tetrazolyl)borate complexes $K(BH_2(RCN_4)_2)(H_2O)_n$ ($R = H, Me, NMe_2, \text{ and } NiPr_2$) and their 18-crown-6 adducts have been synthesized. In the solid state, complexes where $R = H$ and Me have B-N bonds to the nitrogen atoms proximal to the tetrazolyl ring core carbon atom, whereas those with $R = NMe_2$ and $NiPr_2$ possess isomeric B-N bonds to the nitrogen atoms distal to the core carbon. With small R groups, the bis(tetrazolyl)borate ligands adopt bridging μ_2 coordination modes to the [18-crown-6]⁺ fragments, while with larger R groups, they adopt chelating κ^3-N,N',H coordination modes in the 18-crown-6 adducts. Bis(5-methyltetrazolyl)borate complexes of lithium and heavier alkaline earth metals have been prepared. The new group 2 metal complexes have been

structurally characterized. Crystals of sodium cyano(tetrazolyl)borate complexes with or without methanol ligands have been prepared. The methanol ligands are lost rapidly from crystals of $\text{Na}(\text{H}_2\text{B}(\text{CN})(\text{HCN}_4))(\text{CH}_3\text{OH})$ and $\text{Na}(\text{H}_2\text{B}(\text{CN})(\text{MeCN}_4))(\text{CH}_3\text{OH}) \cdot (\text{CH}_3\text{OH})$ at 23°C once they are isolated from the solutions.

All of the new complexes mentioned above are air stable and thermally stable between 210°C and 325°C . They are insensitive toward impact, friction, and electrostatic discharge. The new complexes have potential use as propellants or secondary energetic materials; the barium tetrazolates may behave as primary energetic materials. The group 2 metal complexes are good candidates for colorants in pyrotechnic compositions. The potassium and sodium complexes can serve as starting materials to make other high nitrogen content bis(tetrazolyl)borate and cyano(tetrazolyl)borate complexes, respectively.

A series of rhenium isocyanate complexes $(\eta^5\text{-C}_5\text{H}_5)\text{Re}(\text{CO})(\text{NCO})(\text{N}_2\text{Ar})$ has been obtained by treatment of the specific rhenium aryldiazenido complexes $[(\eta^5\text{-C}_5\text{H}_5)\text{Re}(\text{CO})_2(\text{N}_2\text{Ar})][\text{BF}_4]$ (Ar = 4-methoxyphenyl, 2,4-dimethoxyphenyl, 3,4,5-trimethoxyphenyl, 2-trifluoromethylphenyl, and phenyl) with sodium azide. Treatment of $\text{CpRe}(\text{CO})_2(\text{THF})$ with $\text{Et}_2\text{NC}_6\text{H}_5\text{N}_5$ made *in situ* affords the isocyanate complex $(\eta^5\text{-C}_5\text{H}_5)\text{Re}(\text{CO})(\text{NCO})(\text{N}_2\text{C}_6\text{H}_5\text{NEt}_2)$ and the methoxycarbonyl complex $(\eta^5\text{-C}_5\text{H}_5)\text{Re}(\text{CO})(\text{COOCH}_3)(\text{N}_2\text{C}_6\text{H}_5\text{NEt}_2)$. The attempted preparation of rhenium aryl pentazole complexes does not proceed to form the desired products.

AUTOBIOGRAPHICAL STATEMENT

DONGMEI LU

Education Ph.D., Inorganic Chemistry, Wayne State University, Detroit, MI
2006-2010; Advisor: Professor Charles H. Winter

M.S., Organic Chemistry, Dalian University of Technology, Dalian, China
2002-2005; Advisor: Professor Jingyang Jiang

B.S., Chemical Engineering, Dalian University of Technology, Dalian, China
1996-2001 Minor: English

Publications

Poturovic, S.; Lu, D.; M. J. Heeg; Winter C. H. "Synthesis and Structural Characterization of Heavier Group 1 Methyl Tetrazolate Complexes: New Bridging Coordination Modes of the Tetrazolate Ligand." *Polyhedron* **2008**, *27*, 3280-3286.

Lu, D.; Winter, C. H. "Complexes of the [K(18-Crown-6)]⁺ Fragment with Bis(tetrazolyl)borate Ligands: Unexpected Boron-Nitrogen Bond Isomerism and Associated Enforcement of κ^3 -N,N',H-Ligand Chelation." *Inorg. Chem.* **2010**, *49*, 5795-5797.

Lu, D.; Poturovic, S.; Heeg, M. J.; Winter, C. H. "Synthesis and Characterization of Heavier Alkaline Earth Metal Tetrazolate Complexes as Energetic Materials" *Manuscript in preparation*.

Lu, D.; Heeg, M. J.; Winter, C. H. "Synthesis and Characterization of Group 1 and 2 Bis(tetrazolyl)borate Complexes as Energetic Materials." *Manuscript in preparation*.

Lu, D.; Heeg, M. J.; Winter, C. H. "Synthesis and Characterization of Sodium Cyano(tetrazolyl)borate Complexes." *Manuscript in preparation*.

Presentations

Lu, D.; Heeg, M. J.; Winter, C. H. "Synthesis of Dihydrobis(tetrazolyl)borate Ligands and Their Coordination to the [K(18-Crown-6)]⁺ Fragment: Unexpected Isomeric Structures." 239th ACS National Meeting, San Francisco, March 21-25, 2010.

Lu, D.; Heeg, M. J.; Winter, C. H. "Synthesis and Characterization of Group 1 and 2 Bis(tetrazolyl)borate Complexes as Energetic Materials." Eleventh Annual Chemistry Graduate Research Symposium, Wayne State University, October 3, 2009.